

HEAT AND VAPOUR TRANSFER
PROPERTIES OF KNITTED FABRICS



THE UNIVERSITY LIBRARY
LEEDS

LEEDS
UNIVERSITY
LIBRARY

DEPARTMENT
OF TEXTILE
EBL THRESES BLY

BOUND BY
HOLLINGWORTH & MOSS
LEEDS



3010601462293

FOR
LIBRARY USE
ONLY

		3
19		
0		
CANCEL		



CLOTHWORKERS' LIBRARY
UNIVERSITY OF LEEDS

HEAT AND VAPOUR TRANSFER PROPERTIES OF KNITTED FABRICS

by

Graham J. Blyth

Submitted in accordance with the requirements for the degree of
Doctor of Philosophy

University of Leeds

Department of Textile Industries

September 1984.

THESES

CLASS MARK
T.20617

ABSTRACT

The design and construction of an instrument for the measurement of the simultaneous flow of heat and vapour is described. This instrument is used to measure the relative contributions of heat and vapour in maintaining steady-state flow. The results indicate the importance of vapour flow and stationary air layers.

Steady-state thermal resistance measurements are made on a series of knitted fabrics using a two plate instrument set for different separations. The dependence of thermal insulation on volume fraction and the importance of radiation transfer within the fabric are discussed.

A model is produced to allow the solution of the equations describing the transient flow of heat through one and two layer systems. The results are compared to a range of experimental values. The relationship between the energy change in the fabric sample and the energy change as perceived by the hot-plate is considered. The results show that approximately half of the energy change is supplied by or to the hotplate and that the periods of transient response extend for up to one hour.

The energy involved in the absorption and desorption of water by the fibres is shown to be of prime importance in determining the fabric response to changing environments.

ACKNOWLEDGEMENTS

I would like to thank the International Wool Secretariat for funding this research.

I would also like to thank the Department of Textile Industries for giving me access to their facilities.

I wish to express my gratitude to my friends and colleagues at Leeds for making my time as a Research Student very enjoyable.

LIST OF SYMBOLS

a	Thermal Diffusivity	β	Coefficient of Thermal Expansion
A	Area	e	Emissivity
C	Heat Capacity	μ	Viscosity
d	Thickness	ν	Kinematic Viscosity
D	Diffusion Coefficient	ρ	Density
E	Energy	σ	Boltzmann's Constant
F	Radiation Factor		
h	Heat Transfer Coefficient		
i_m	Moisture Impermeability Index	SUBSCRIPTS	
k	Conductivity	a	Air, Ambient
K	Conductance	d	Fabric
l	Characteristic Dimension	e	Evaporation
m	mass	f	Fibre
M	Fabric Weight	h	Heat
P	Pressure	s	Surface
q	Heat Flux	t	Total
q_v	Rate of Heat Evolution		
Q_v	Differential Heat of Sorption		
r	Regain	DIMENSIONLESS NUMBERS	
R	Thermal Resistance	Gr	Grashof Number
t	Time	Nu	Nusselt Number
T	Temperature	Pr	Prandtl Number
v	Volume Fraction	Re	Reynolds Number
W	Vapour Resistance		

Table of Contents

THE MEASUREMENT OF CLOTHING COMFORT.....	1
1.1 INTRODUCTION.....	1
1.2 HEAT TRANSFER.....	3
1.2.1 CONDUCTION.....	3
1.2.2 CONVECTION.....	4
1.2.3 RADIATION.....	5
1.2.4 TOTAL HEAT FLOW.....	6
1.2.5 RESULTS OF DRY HEAT TRANSFER THROUGH FABRIC.....	7
1.2.6 DRY HEAT TRANSFER IN CLOTHING (MULTI-LAYER) SYSTEMS.....	8
1.3 MOISTURE TRANSFER.....	10
1.3.1 VAPOUR TRANSFER.....	10
1.3.2 VAPOUR TRANSFER IN MULTI-LAYER FABRICS.....	12
1.3.3 MEASUREMENT TECHNIQUES.....	14
1.3.4 MULTIPLE LAYER TECHNIQUE.....	14
1.3.5 CONTROL DISH.....	15
1.3.6 VOLUMETRIC METHOD.....	15
1.3.7 OTHER SYSTEMS.....	16
1.3.8 LIQUID WATER TRANSPORT.....	17
1.4 SIMULTANEOUS HEAT AND VAPOUR FLOW.....	18
1.4.1 DISTRIBUTION OF MOISTURE IN CLOTHING.....	21
1.4.2 THE BUFFERING EFFECT OF CLOTHING.....	23
1.5 SUBJECTIVE ASSESSMENT OF CLOTHING PROPERTIES.....	26
1.5.1 INDICES OF CLOTHING COMFORT.....	26
1.5.2 PHYSIOLOGY OF CLOTHING.....	30
1.6 CLOTHING SYSTEMS.....	32
1.7 THE AIM OF THE PRESENT WORK.....	33
AN INSTRUMENT FOR THE SIMULTANEOUS MEASUREMENT OF HEAT AND VAPOUR....	34
2.1 DESIGN CRITERIA.....	34
2.2 PLATE CONSTRUCTION.....	36
2.3 HEATER CONTROL.....	42
2.3.1 MODES OF CONTROL.....	42
2.4 CIRCUIT DESIGN.....	45
2.4.1 PROPORTIONAL CONTROL SECTION.....	47
2.4.2 PULSE GENERATION SECTION.....	50
2.4.3 OUTPUT DRIVER SECTION.....	54
2.4.4 INTEGRATOR SECTION.....	56
2.4.5 POWER SUPPLIES.....	58
2.4.6 COMBINED OPERATION OF PLATE CONTROL CIRCUITRY.....	59
2.4.7 GUARD RING HEATER CONTROL.....	64
2.5 LIQUID SUPPLY SYSTEM.....	66
2.5.1 CONSTRUCTION.....	68
2.5.2 LIQUID SUPPLY CIRCUITRY.....	71
2.6 RECORDING FACILITIES.....	72

THE MEASUREMENT OF FABRIC THICKNESS.....	74
3.1 INTRODUCTION.....	74
3.2 TEST METHODS AND RESULTS.....	75
3.2.1 THE RELATIONSHIP BETWEEN THICKNESS AND PRESSURE.....	75
3.3 TEST INSTRUMENT.....	78
3.4 EXPERIMENTAL.....	79
3.4.1 LOW PRESSURE.....	80
3.4.2 EXTENDED PRESSURE RANGE.....	85
DRY HEAT TRANSFER THROUGH FIBROUS ASSEMBLIES.....	90
4.1 HEAT CONDUCTION.....	90
4.1.1 CONDUCTION OF HEAT IN FIBROUS MATERIALS.....	93
4.2 RADIATION.....	99
4.2.1 RADIANT EXCHANGE WITHIN FIBROUS MATERIALS.....	101
4.3 CONVECTION.....	104
4.3.1 PROPERTIES OF FLUIDS.....	104
4.3.2 CONVECTION FROM FABRIC SURFACES.....	107
4.4 COMBINED HEAT TRANSFER IN FIBROUS ASSEMBLIES.....	110
4.5 EXPERIMENTAL TECHNIQUES IN STEADY STATE DRY HEAT TRANSFER.....	114
4.5.1 CONSTANT TEMPERATURE.....	114
4.5.2 RATE OF COOLING AND RATE OF HEATING.....	116
4.5.3 THERMAL RESISTANCE REFERENCES.....	117
4.6 EXPERIMENTAL.....	118
4.6.1 DESCRIPTION OF THE APPARATUS.....	120
4.6.2 TEMPERATURE CONTROL.....	122
4.7 THERMAL INSULATION RESULTS.....	124
4.7.1 TOG-METER.....	124
4.7.2 GUARDED HOT PLATE.....	139
STEADY STATE HEAT AND VAPOUR FLOW.....	146
5.1 EXPERIMENTAL PROCEDURE.....	146
5.2 RESULTS.....	147
5.2.1 AIR GAPS, NATURAL CONVECTION.....	147
5.2.2 MINIMAL AIR GAP, FORCED CONVECTION.....	148
5.3 DISCUSSION OF RESULTS.....	150
5.3.1 THERMAL RESISTANCE RESULTS.....	150
5.3.2 VAPOUR RESISTANCE RESULTS.....	152
TRANSIENT CONDUCTION.....	163
6.1 INTRODUCTION.....	163
6.2 BOUNDARY CONDITIONS.....	166
6.3 SOLUTION PROCEDURE.....	167
6.4 SINGLE LAYER CONVECTIVE SURFACES.....	168
6.5 TWO LAYERS, CONVECTIVE BOUNDARIES.....	174

MEASUREMENT OF TRANSIENT ENERGY CHANGES.....182
 7.1 ENERGY DEBT.....182
 7.1.1 EXPERIMENTAL PROCEDURE AND RESULTS.....182
 7.2 ENERGY CONTENT CHANGES.....185
 7.3 TRANSIENT CALCULATIONS.....191

CONCLUSION.....202

CHAPTER 1

THE MEASUREMENT OF CLOTHING COMFORT

1.1 INTRODUCTION

Mass and energy exchanges between the body and its environment are the essential elements of the physiology of clothing. While attributes such as fit, stretch and surface contact are important, it is the ability of the clothing to establish a satisfactory level of energy exchange which is the most important aspect of clothing comfort.

Body, clothing and environment all contribute to the level of energy exchange. The metabolic activity of the body and the temperature, relative humidity, air movement and radiation of the environment interact through the fabric layers. The clothing provides a resistance to the flow of heat, vapour and liquid water and can act as a buffer against sudden changes by absorbing and desorbing both heat and vapour. Any discussion of the comfort qualities of a particular item or system of clothing only has relevance in terms of the body and environmental conditions. Thus comfort is not a property of clothing but rather a relationship between the clothing and the role it must play as an interface.

There are two general approaches to the assessment of clothing performance. The first involves the use of human subjects and the direct assessment of the physiological response to the work load, clothing and environment. Such testing is very difficult and time

consuming though of great value in designing garments for extreme conditions in particular. The difficulties relate to the large number of variables and psychophysiological factors which depend on the individual subjects.

The second approach is to minimise the number of variables and test the insulating properties of the fabrics. Properties such as thermal insulation and vapour and air permeability can be measured. Relating such properties to the comfort or performance of a fabric in a garment under differing body and environmental conditions can be difficult.

The aim of this work is to consider the relationships between some of the properties which are regarded as important in determining the performance of a fabric. This is achieved by objective measurements of the response of fabric samples to different test arrangements under controlled environmental conditions.

The basic fabric properties of interest in any study of clothing comfort are the thermal insulation and the vapour resistance. In addition to these fabric properties are the environmental conditions which can influence them. The most important of these environmental factors is wind. The penetration of moving air into or through an insulating fabric layer can greatly change its performance.

1.2 HEAT TRANSFER

For most clothing applications the fabric can be regarded as an infinite plane and the transfer of heat and vapour can be considered as occurring only in the direction perpendicular to the plane. Contributions to the total heat transfer come from the three different modes of heat transfer, namely:

conduction, convection and radiation

1.2.1 CONDUCTION

The conductance of a fabric is generally expressed in the form:

$$K = \frac{q}{(T_1 - T_2)} \quad 1.1$$

where K = conductance ($W/m^2 \text{ degC}$)

q = heat flux (W/m^2)

T_1, T_2 = Temperature at either face of the fabric.

The conductance is a property of the fabric as a whole. To take into account the thickness of the fabric layer the thermal conductivity, k , is used:

$$k = \frac{q}{(T_1 - T_2)/d} \quad 1.2$$

or $k = K d$

Where k = conductivity ($W/m \text{ degC}$)

d = fabric thickness (m)

The thermal resistance, R , is the inverse of conductance and can be written as:

$$R = 1/K = d/k \quad 1.3$$

These formulae are approximately correct where the variation of temperature is small. However, in cases where the temperatures may vary greatly it is necessary to allow for the temperature dependence of these quantities. Empirically it has been found that the relationship is of the form:

$$k = k_0 (1 + b (T - T_0)) \quad 1.4$$

where k = conductivity at temperature T

k_0 = " " " " T_0

b = constant

For most clothing applications the temperature variation is not great enough to cause significant changes in conductivities.

1.2.2 CONVECTION

Convection is the process by which heat is transferred due to the bulk motion of the surrounding fluid (gas or liquid). As in the case of conduction, the heat flux is proportional to the temperature difference between the fluid, T_a , and the surface, T_s :

$$q = h_c (T_s - T_a) \quad 1.5$$

The heat transfer co-efficient, h_c , will be dependent on the shape and size of the surface as well as the pattern of flow and the fluid

velocity, temperature and physical properties.

Convection occurs in clothing in two forms which are referred to as forced and free (or natural) convection. The former covers the commonly encountered effect of wind, whether due to movement of the air or the movement of the object through the air. Free convection, on the other hand, is due to the creation of a density gradient in the air surrounding the object as a result of the condition of the object. This gradient is a function of the temperature and vapour pressure differences which may surround, in the case of most interest, a clothed person. This will be discussed in more detail later in this chapter.

1.2.3 RADIATION

The transfer of heat in the form of radiation can be approximated by the relationship:

$$q = \sigma F (T_s^4 - T_a^4) \quad 1.6$$

where σ = the Stefan-Boltzmann constant

F = view factor

If the difference between T_a and T_s is small compared to the magnitude of T_a then a further approximation can be made to yield the result:

$$q = h_r (T_s - T_a) \quad 1.7$$

where $h_r = \sigma F 4 T_s^3$

For black body radiation between large, parallel surfaces at room temperature the heat flux can be written as:

$$q = 6.3 (T_s - T_a) \quad 1.8$$

With this formula temperatures can be measured in either degC or degK without necessitating any conversion factors.

1.2.4 TOTAL HEAT FLOW

Considering the combined effect of the conduction, convection and radiation components will yield a formula for the combined heat flux:

$$q = \frac{(T_1 - T_a)}{d/k + 1/(h_r + h_c)} \quad 1.9$$

where T_1 = Temperature at inner fabric surface.

The aim of any research into the physical properties underlying the comfort of clothing must be based on the evaluation of the terms in the heat transfer equation and their relationship to the parameters which specify the fabric. Ultimately such research would lead to the possibility of accurately predicting the performance of a garment or of designing to meet a set of performance requirements. Several of the physical methods employed in clothing physiology are described in Chapter 4.

1.2.5 RESULTS OF DRY HEAT TRANSFER THROUGH FABRIC

For the transfer of dry heat through fabric layers in a still environment it is generally agreed that the fabric thickness is the controlling factor (1,2,3,4,5,6). A relationship of the form:

$$R = r d \quad 1.10$$

where R = thermal resistance ($m^2 \text{ degC/W}$)

d = fabric thickness (m)

$r = 1/k$ = thermal resistivity ($m \text{ degC/W}$)

has been indicated in the literature, r having a value of about 23 degC m/W (1,5,8) or:

$$R = 23 d \quad 1.11$$

This relationship implies that the thermal transfer properties of a fabric under dry, still conditions can be attributed solely to the air that is trapped within the structure and independent of the fibre type. If, however, the fabric is compressed sufficiently the conductivity will increase (or the resistivity will decrease) quite substantially and the fibre properties become more important. The conductivity will, of course, decrease again when the compression is removed. The magnitude of the decrease in conductivity depending on the resilience of the fabric.

These results refer mainly to the conductive mode of heat transfer. The radiative component of heat transfer within a fabric does not depend upon fabric thickness but depends upon fabric bulk density. The

lower the bulk density, the greater is the heat transfer by radiation, whereas the reverse is the case for the conductive mode of heat transfer. The total heat transfer is the sum of each of these two modes and it has been shown that fabrics of bulk density in the range 20-200 kg/m³ offer the highest heat insulation.

1.2.6 DRY HEAT TRANSFER IN CLOTHING (MULTI-LAYER) SYSTEMS

Fabric parameters affecting heat transfer were described earlier. When multi-layer assemblies are considered there are additional parameters to consider. These are the surface film layers and air layers between fabrics. The resistance of a multi-layered system, R_t , can be expressed as:

$$R_t = R_s + \sum R_f + \sum R_a \quad 1.12$$

where R_s = Surface resistance at clothing environment interface

$\sum R_f$ = Sum of the resistances of fabric layers

$\sum R_a$ = Sum of the resistances of air layers

The surface resistance of the fabric is composed of parallel convective and radiative components:

$$R_s = 1/(h_c + h_r) \quad 1.13$$

The convection component in the absence of wind has been shown by Spencer-Smith(9) to be well represented by the relationship:

$$h_c = 24.9 \, l^{-0.25} (3.83 \times 10^3 (T_s - T_a))^{0.25} \quad 1.14$$

for a horizontal surface and

$$h_c = 17.4 l^{-0.25} (3.83 \times 10^3 (T_s - T_a))^{0.25} \quad 1.15$$

for a vertical surface,

where l = is the length of the surface (m).

Provided that the air gaps within the system, are not greater than 0.5 cm each and hence do not allow significant natural convection, the resistance of the air gaps is given by:

$$\sum R_a = \sum \frac{l}{k_a/d_a + 1/h_r} \quad 1.16$$

where k_a is the thermal conductivity of air and d_a is the thickness of the air gap. This gives a total system resistance of:

$$R = \frac{1}{h_r + h_c} + 23 \sum d + \sum \frac{1}{k_a/d_a + h_r} \quad 1.17$$

1.3 MOISTURE TRANSFER

1.3.1 VAPOUR TRANSFER

The flow of water vapour through fabric layers can be regarded as a diffusion process. As such, it can be described in terms of the relationships derived from Fick's Law:

$$\frac{\Delta m}{\Delta t} = - D A \frac{\Delta c}{\Delta x} \times 10^4 \quad 1.18$$

where Δm = mass transferred (g)

Δt = time taken for transfer (s)

D = diffusion coefficient

$\frac{\Delta c}{\Delta x}$ = concentration gradient

As in the case of heat flow, it is only necessary to consider the flow as being perpendicular to the fabric surface and hence one-dimensional. Using the formula for the "ideal gas" it is possible to express the change of concentration, $\Delta c(\text{g/cm}^3)$, in terms of the partial pressure change, ΔP :

$$\Delta c = 2.17 \cdot 10^{-6} \frac{\Delta P}{T} \quad 1.19$$

Substitution of this equation into Eq.1.18 gives:

$$\frac{\Delta m}{\Delta t} = - \frac{D A 2.17 \cdot 10^{-2} \Delta P}{T \Delta x} \quad 1.20$$

From this it is possible to specify a water vapour permeability, V , such that:

$$\frac{\Delta m}{\Delta t} = V A \frac{\Delta P}{\Delta x} \quad 1.21$$

$$\text{where } V = - 2.17 \times 10^{-2} D/T \quad 1.22$$

Hence the water vapour resistance is given by:

$$W = \frac{\Delta x}{V} = - \frac{T \Delta x}{D \cdot 2.17 \cdot 10^{-2}} \left(\left(\text{N/m}^2 \right) / \left(\text{g/sm}^2 \right) \right) \quad 1.23$$

Frequently the vapour permeance will be expressed in terms of an equivalent thickness of still air.

The total resistance to vapour flow will also depend on the surface resistance of the outer fabric layer and the air gaps between the fabric layers and between the inner fabric layer and the source of water vapour.

$$W_t = W_a + W_d + W_s \quad 1.24$$

where t = total

a = air gaps

f = fabric

s = surface

Within the air gaps the vapour flow will be a function of both diffusion and, where the thickness of the gap is great enough, convection as well. At the outer surface the flow is governed by the convection currents set up by the density gradient which in this case is due to water molecules being lighter than the average weight of the molecules making up the air.

A large number of methods have been developed to assess the vapour permeability or resistance of fabrics. A common feature of all is the assessment of water transferred through the fabric under the influence of a known vapour pressure drop.

1.3.2 VAPOUR TRANSFER IN MULTI-LAYER FABRICS

Under equilibrium conditions it is generally assumed that the physical properties of the fibre, with the exception of its density, have very little influence on the vapour transfer through fabric layers. As in the case of heat transfer there are three components which affect vapour transfer, namely resistance associated with the fabric layers, the air layers and a surface layer:

$$W_t = W_s + \sum W_d + \sum W_a \quad 1.25$$

where W_t = total resistance

W_s = surface resistance

$\sum W_d$ = resistance of fabric layers

$\sum W_a$ = resistance of air layers

Several models have been developed to predict the resistance of fabric layers to flow of water vapour based on results from a variety of measurement techniques. Two formulations are shown below:

$$W_d = \frac{v_f}{(100 - v_f)} (0.9 + 0.034 v_f) d + 0.5 \quad 1.26$$

in units of equivalent thickness of still air (mm) (10) and (11):

$$W_d = \frac{M (W_f - 1) \times 10^{-4}}{\rho_f} + d \text{ (cm still air)} \quad 1.27$$

where M = fabric weight (g/m^2)

ρ_f = fibre density

W_f = fibre vapour resistance

By assuming the fibre resistance to be ten times that of air this second relationship can be simplified to give:

$$W_d = \frac{M \times 9 \times 10^{-4}}{\rho_f} + d \quad 1.28$$

The resistance of air gaps within the system, provided that they are not so large as to promote natural convection, can simply be expressed as their thickness if the units in use refer to equivalent layers of still air as above:

$$W_a = d_a \quad 1.29$$

The transfer of water vapour from the surface of the fabric is governed by natural convection in the absence of wind. This is analagous to the heat transfer with the density gradient now a function of the changing vapour pressure rather than temperature and can be equated to:

$$W_s = 9.1 \cdot 10^{0.25} (P_s - P_a)^{-0.25} \quad 1.30$$

The total vapour transfer would thus be given by:

$$W_t = \frac{9.1 \cdot 10^{0.25}}{(P_s - P_a)} + \frac{M \cdot 9 \times 10^{-4}}{\rho_f} + \sum d + \sum d_a \quad 1.31$$

1.3.3 MEASUREMENT TECHNIQUES

A large number of methods have been used to assess the vapour permeability or resistance of fabrics. A common feature of all is the measurement of water transferred through the fabric under the influence of a known vapour pressure difference.

1.3.4 MULTIPLE LAYER TECHNIQUE

Generally this method employs three dishes containing water which are covered by one, two and three layers of the fabric to be tested (11,12). From measurements of dm/dt (weighing the dish at various times) and a knowledge of the surface area, A , and the vapour pressure P_{sat} (P_{sat} is the saturation vapour pressure (i.e. 100% R.H. for water at the temperature used)) the resistance to vapour flow can be plotted against the number of layers of fabric. The resistance of individual fabric layers is given by the slope of the line plotted while the intercept at zero fabric layers is due to the air gap between the water layer and fabric assembly and some contribution of the fabric surface characteristics. If the thickness of the air gap is known its resistance can be obtained from published data and hence the fabric surface effect will be given by:

$$W_s = W_t - n W_d - W_a \quad 1.32$$

where n = number of layers of fabric.

Naturally with this system it is important to ensure consistent contact between the fabric layers or the air gaps between them will become significant and lead to non-reproducible results.

1.3.5 CONTROL DISH

This method is essentially an extension of the previous one. Six dishes are used - three with sample fabrics and three as controls(10,11). The control dishes have a porous reference material covering while the sample dishes have the fabric under test and the same reference material. The three pairs of dishes employ different air gaps and the test specimen is calibrated in terms of equivalent still air resistance against the reference dish that would give the same rate of vapour flow.

This is achieved by plotting the resistance against air gap for the control dishes and then comparing the values obtained with the test specimens. A result for a test specimen will equal the resistance of some equivalent control and hence the difference between the air gaps in the test and the equivalent control will equal the vapour resistance of the test fabric. The vapour losses are assessed by weighing. Other features are similar to the Multiple Layer Technique.

Other variations on these two methods exist. Different solutions can be used to give different vapour pressures and sometimes the losses are assessed by single layers and given only as weight loss per unit time with no differentiation of components involved in the transfer.

1.3.6 VOLUMETRIC METHOD

A porous cylindrical container is used with its surface covered by a film which is permeable to water vapour but not liquid water(13). The container is sealed and supplied with water from a horizontal capillary. The movement of the meniscus shows the volume of water

being transferred as vapour. The cylinder is then covered with the test fabric and the rate of water loss again measured.

From the known vapour pressures, area and vapour flow rates the resistance of the fabric to vapour transmission can be readily assessed. This method does suffer from the uncertainty of the values of the two surface resistances. Only if their values are identical will the resulting difference be the resistance of the fabric W_d .

1.3.7 OTHER SYSTEMS

Other less commonly used systems have been employed. Partition cells have proved successful particularly for transient diffusion through the systems but are often difficult and slow to use. The use of guarded hot plates to assess the amount of vapour flow via the heat of vapourisation of water has been attempted though generally in the absence of a temperature gradient. Possibly one of the most accurate systems uses infra-red absorption to measure the water vapour pressures on either side of the samples. This system is especially useful at low vapour pressures(9).

As in the case of dry heat transfer, there are difficulties both in achieving meaningful and reproducible results and in interpreting those results in terms of the comfort characteristics required for clothing.

In systems where the vapour loss is measured by weighing the dish, the air gap between liquid and fabric surfaces also changes which introduces serious error. Such errors are compounded when, as in the control dish method, air gaps also have to be measured and compared.

The multiple layer technique carries with it the problem of contact between the fabric layers. Such contact has to be consistent and uniform. Even uniform air gaps will effectively introduce an error into the measurement of the fabric properties.

The volumetric methods seem to offer the greatest chance for an accurate assessment of vapour resistance, provided the characteristics of the surface air film are precisely known. A resistance value found by this method will include both the fabric and the fabric surface air film resistance. Analogously to the multiple layer technique it would be possible to differentiate between the two components though the contact between fabric layers would still present a problem.

1.3.8 LIQUID WATER TRANSPORT

The transportation of liquid water through a fabric can occur due to any combination of three major mechanisms. The most important of these is due to capillary action. Transfer can also take place along the fibre surfaces or through the fibres themselves by absorption at one face and desorption at another.

The transport of liquid water from the skin to the outer fabric surface by capillary flow depends on the continuity, length and orientation of the capillaries within the fabric. The greater the number and the longer the capillaries the more liquid that will be removed from the skin for a given fibre type. Hence "straight" fibres which run parallel to one another thus introducing many long capillaries are likely to promote liquid flow. Yarn construction becomes an important variable because of this feature.

All three transfer mechanisms depend very greatly on the fabric/skin contact. Where there are significant numbers of protruding surface fibres the moisture uptake will be impaired even though the fibres and yarn construction may be conducive to liquid water transfer. The surface characteristics of the fibres are also important. In particular, the wettability or hydrophobicity of the surface is involved in all forms of liquid transport. Hydrophobic fibres can be modified in finishing to give surface properties which can allow liquid flow.

The importance of liquid transport has become more recognised in recent times. However in terms of the comfort of the wearer and his thermal balance, it is of uncertain value. If a fabric removes liquid water from the skin then the energy associated with its evaporation is not supplied entirely by the body and the desired effect of the perspiration as a coolant is lessened. Hence the body will produce more sweat and the comfort could well be reduced.

1.4 SIMULTANEOUS HEAT AND VAPOUR FLOW

The flow of heat and vapour from the skin are the major components affecting the energy exchange needed to maintain the body in the narrow temperature band required for comfort and survival. Under some circumstances the heat loss through respiration can dominate but this only applies to extreme conditions.

The total flow of energy from the body is the sum of the dry heat flow and the product of the vapour flow and the latent heat of vaporisation of water. Generally it has been assumed that these two components are

independent and governed only by the temperature and vapour pressure gradients respectively for a given clothing system. However, it has been shown(14) that the total energy transfer cannot be precisely described with the aid of data from separate experiments on dry heat flow and water vapour transfer. The driving force for heat transfer is the temperature gradient and for moisture transfer it is the vapour pressure gradient. Where both gradients exist simultaneously the associated density gradients will be added and the energy loss due to convection will not be a simple sum of individual heat and vapour losses.

One estimate for the combined heat and vapour transfer due to natural convection(9) gives:

$$q_e = C_1 (P_s - P_a) (\rho_a - \rho_s) \quad 1.33$$

$$q_h = C_2 (T_s - T_a) (\rho_s - \rho_a) \quad 1.34$$

$$\text{where } (\rho_a - \rho_s) = [(3.83 \times 10^{-3} (T_s - T_a) + (4.20 \times 10^{-6} (P_s - P_a))^{0.25}] \quad 1.35$$

and q_e, q_h = energy flux due to evaporation and heat
 ρ_s, ρ_a = air density at surface and ambient

Using these formulae expected values of energy flow for one square metre of fabric have been calculated (Table 1.1) for a range of temperatures and pressure differences over a horizontal sample. (Vertical samples are expected to give 0.7 of these values). Similar effects can also occur within air gaps which are of sufficient thickness(0.75 - 1.0 cm min.) for convection to become important.

The calculations for simultaneous heat and vapour flow are based on

		Temperature difference (degC)				
		0	5	10	15	20
Pressure difference (Kpa)	0		46.3	110.2	182.9	262
	0.5	12.3	69.3	137.2	212.6	294
	1.0	29.2	93.1	170.7	243	327
	2.0	68.2	143.6	221.8	304	390
	3.0	115.7	197.0	280.7	368	459

Table 1.1

Total energy flux due to natural convection.(9)
 $W m^{-2}$

equilibrium conditions and on the assumption that the temperature gradient does not influence the vapour flow within the fabric and that the regain and vapour pressure gradient do not influence heat flow within the fabric. Without suitable experimental evidence the validity of these assumptions and other features of fabric under conditions approaching those in wear cannot be properly assessed.

When a garment assembly is subject to a change in thermal load, either as a result of a change in atmospheric conditions or a change in work load and hence energy output from the body, then the fabric layers will undergo changes in temperature and regain. These changes in the energy stores within the fibres increase the importance of some fibre properties which could essentially be ignored in the steady-state transfer as previously considered. In particular the specific heat, the heat of absorption and desorption and the change of regain with relative humidity will introduce heat sources and heat sinks into the insulating layer and influence the reaction to change of the garment assembly.

Generally mathematical solutions to the equations involved in transient conditions are complex and difficult to apply.

1.4.1 DISTRIBUTION OF MOISTURE IN CLOTHING

Since heat and moisture flow continuously from the skin through clothing to the environment, a gradient of temperature and vapour pressure exists from the skin to the ambient air.

Data published by Rees(15) on two environmental situations, one a

temperate environment (21 degC, 50% R.H.) and the other a cold environment (-15 degC, 90% R.H.), offer good examples in elucidating moisture distribution. The temperature and moisture distribution in the clothing for the two environments were shown. In the temperate case the saturation moisture curve was, at all points within the clothing system, greater than the actual vapour pressure curve. For the cold environment however, the actual and saturation vapour pressure curves cross at a point 2 mm away from the skin so the R.H. at this point and beyond liquid water is present. The two curves recross each other some 5 mm away from the skin. Since the slope of the actual vapour pressure-thickness plot depends upon the vapour permeability of the clothing and on the ambient conditions it is possible for the second crossover to occur within the clothing system. Beyond this second crossover point there would be no condensation.

Some of the liquid water in the wet layers may wick back to the inner warmer layers where it can be reevaporated at the expense of its latent heat and later recondense in the water layers giving up its latent heat further away from the skin. This cycling causes additional heat loss from the body.

The above example of water condensation in a very cold environment is not an isolated case but can occur at relatively high ambient temperature as well.

1.4.2 THE BUFFERING EFFECT OF CLOTHING.

The absorption of moisture by textiles is an exothermic process and the amount of heat evolved depends upon the type of fibre, the amount of moisture already present in the fibre, the amount of further moisture absorbed and finally the state of the moisture (i.e. vapour or liquid) which is absorbed.

The difference between the amount of heat evolved when the same quantity of moisture in vapour and liquid form is absorbed is the latent heat of vaporisation which is 2.44 kJ/g of vapour. Thus a much greater quantity of heat is evolved when vapour rather than liquid water is transferred to fibre.

Secondly the absorption of water by the fibre involves inter-molecular bonds which bind the water in the fibre and would evolve more heat than when the same amount of vapour is condensed on the fibre surface. This additional energy would vary with the amount of moisture already present in the fibre.

The amount of heat evolved in completely wetting the fibre from the dry state can be found from published values (Table 1.2) (16).

In clothing systems, the amount of actual heat evolved, dQ , can be calculated from the change in regain, $d\alpha$, using:

$$dQ = M d\alpha Q_v \quad 1.36$$

where M = mass of dry textile

Q_v = differential heat of absorption

Regain	Heat of complete wetting(J/g of wool)	Heat of absorption of liquid water(J/g of water)
0	100.9	854
2	85.0	754
5	64.5	624
7	52.8	540
10	38.1	431
15	20.5	276
20	10.0	142
25	4.1	100
30	1.1	42
33	0.0	33

Table 1.2

As an example, for a person moving from a room at 20 degC and 40% R.H. to outdoors at 10 degC and 90% R.H., a kg of wool garment will liberate 348 kJ of heat which is as much as a human body produces in one hour. A similar weight of cotton garment under the same conditions will liberate about 209 kJ.

The effect of wool fibres in delaying the reduction of temperature through clothing is well demonstrated by the work of Cassie(17) and shows that the time required to establish a temperature change with wool is some twenty times longer than that would be required for synthetic fibres.

Similar effects of a strong buffering action by wool were demonstrated by David(18) who carried out direct tests on wool suiting and found that the heat loss through the fabric was reduced by about 12% immediately falling to 3% after 20 minutes.

In the above two cases, a sudden increase in heat insulation was demonstrated when a wearer moved from warm, dry environment (indoors) to cold damp one (outdoors). The buffering action also occurs at the onset of perspiration and was demonstrated by Spencer-Smith(19).

In actual wear situations clothing is more often subjected to transient rather than steady state conditions and, for this reason, any possible advantage of hygroscopic material to physiological comfort is not observed in laboratory tests under steady state conditions.

1.5 SUBJECTIVE ASSESSMENT OF CLOTHING PROPERTIES

1.5.1 INDICES OF CLOTHING COMFORT

Physiological studies by Vokac(20) and others have shown that, when a man is at rest or engaged in light activity, the relative humidity at the skin surface is about 35%, appreciably lower than the ambient humidity of 50-60%. The vapour transfer from skin to environment still occurs because of vapour pressure differences resulting from temperature differences. If water vapour cannot escape sufficiently quickly through the clothing assembly, then the relative humidity of the skin would rise to 100%, liquid moisture would be formed by condensation of water vapour and the sensation of discomfort accentuated. The need for fabrics used in the form of garments to allow the transmission of water vapour is universally appreciated.

The misunderstanding of associating ability to transfer moisture with fabric air permeability is widespread. Air and vapour pass through clothing systems in different ways. Air permeability is dependent almost entirely on the structure of the fabric and is practically independent of the type of fibre used. The measurement of air permeability uses bulk air movement and can lead to fibre rearrangement within the fabric. Vapour permeability is essentially a diffusion process and can show important differences between fibre types.

The insensible perspiration emitted by the body will pass through air spaces in the clothing and through the fabric. The rate at which water vapour passes through the fibre depends on the nature of the fibre. With hydrophobic fibres the rate is very slow whereas with hydrophilic

fibres it is relatively fast.

When clothing is worn to provide thermal insulation, it imposes an unavoidable and unwanted water vapour resistance between the body and the environment. Generally, the higher the thermal insulation, R , the higher is the vapour resistance W .

$$W = f R \quad 1.37$$

Clearly, it is desirable that the value of f be as low as possible. There is a definite lower limit to the attainable value of f . The ideal material is still air and if radiant heat losses are eliminated, the f value is 2.5. If radiant heat losses are not eliminated, the f value of still air would not be a constant but increase with increase in W .

A similar way of expressing this as a ratio is the more commonly used Woodcock's Moisture Permeability Index(22) where:

$$i_m = 0.45 R/W \quad 1.38$$

The coefficient 0.45 is the ratio of the vapour to heat resistances of still air so that i_m is expressing the efficiency of the garment relative to an air gap of the same thickness. Since the thermal resistance of a fabric is always less than that of the equivalent still air layer while the vapour resistance of the fabric is always higher than the air gap then the permeability index, i_m , must always have a value less than 1.

From the physiological point of view it is generally considered that

the moisture permeability should be as high as possible within the limitations imposed by the desired thermal insulation. Thus, the higher the value of i_m the more comfortable the fabric. Systems for different end uses obviously impose different limitations on the designer so different types of garment cover different ranges of desired values for i_m . The range of i_m for various end uses is suggested by Mecheels (Table 1.3) (23).

The movement of air within the clothing can remove significant quantities of vapour from the clothing and it is suggested by Mecheels(24) that considerable moisture can be lost through vapour impermeable clothing by proper design of garment ventilation.

As resistance to the passage of moisture also increases with increased fabric thickness the fibre comparisons are best carried out for a range of fabric constructions by the use of vapour resistance per unit thermal insulation, such as f values, or by comparing clothing heat and vapour resistances with those for air using the Permeability Index, i_m . The data for f values are shown in Table 1.4 (21).

The i_m ratio has become widely used. The higher the value the more comfortable is the fabric. The ratio of i_m to fabric resistance which is in fact a function of the reciprocal of the vapour resistance is shown by Gilling(25) to be inversely related to the rise in mean body temperature. This demonstrates the importance of considering both the heat and vapour transfer processes.

Suits, Dresses, Overgarments	0.15	0.35
Shirts	0.20	0.45
Underwear	0.25	0.50
Fleeces	0.35	0.55
Upholstery	0.25	0.45
Furs	0.45	0.70
Quilted covers, Sleeping bags	0.50	0.90

Table 1.3

Suggested ranges for moisture impermiability index(23)

Vests			
Cotton interlock			5.7
Wool interlock			5.0
Shirts			
Cotton poplin	8.2	15.0
Wool			6.9
Nylon			22.0
Coatings			
P.U. coated wool/nylon			117
P.U. coated nylon			558
P.V.C. coated cotton			2950

Table 1.4

Measured f Values(21)

1.5.2 PHYSIOLOGY OF CLOTHING.

Moisture transport in clothing can occur both in the liquid and in the vapour phase. The difference is an important one. If water evaporates at the skin and passes as a vapour through a fabric the pores of the fabric remain free and this enables the movement of air within these pores to be maintained. If on the other hand, moisture is transported in the liquid phase by wicking and only evaporates on reaching the air layer at the fabric surface, comfort is reduced in two ways. The sensation of wetness is perceived by the skin so that the garment feels clammy. In addition, the water filled fabric pores no longer hold dead air pockets so that the heat insulating ability of the fabric is lost and the wearer feels cold.

Whether the vapour generated at the skin condenses in the clothing system depends not only on the temperature and humidity differences between the skin and the environment but also on the vapour permeability of the clothing. If more vapour is secreted than can be transferred through the clothing condensation results. The former depends upon the level of activity and the metabolic heat production. Invariably in active sport, the rate of secretion of vapour would exceed the rate of removal of moisture even in the most vapour permeable of all clothing.

Wear trials(20) of a woven and knitted scandinavian cross-country ski dress with identical underwear showed that 1/2 of the sweat produced did not evaporate during the experiments and remained trapped in the clothing.

The contribution of ventilation to vapour resistance was measured by

Mecheels(24) who found that:

$$W_v = 0.51 \times R_v \quad 1.39$$

v = ventilation contribution

Thus, from the knowledge of heat and vapour transfers, the range of environments and body activities for given clothing system can be calculated.

For a resting subject the minimum and maximum comfortable ambient temperatures, $T_{a,\min}$ and $T_{a,\max}$ (24) are:

$$T_{a,\min} = 32 - R \left[\frac{M + H_r}{A} - \frac{0.06}{R_e} (35.7 - P_a) \right] \quad 1.40$$

$$T_{a,\max} = 36 - R \left[\frac{M - H_r}{A} - \frac{0.06}{R_e} (44.6 - P_a) \right] \quad 1.41$$

where H_r = rate of heat loss by respiration

M = metabolic heat production (350 W)

R_e = heat equivalent of vapour resistance

(including ventilation contribution)

The figures for maximum temperature were compiled for suits with the same dry heat resistance but different moisture permeability. The suit with high vapour permeability gave a value of 27.9 degC. compared to low moisture permeability suit of 25.2 degC. In subjective evaluation of comfort these two clothing systems will show differences only when the wear trials are conducted between 25.2 and 27.9 degC air temperatures and these computations become essential to the design of wear trials.

Givoni and Goldman(26) have considered the relationship between clothing systems and heart rate and rectal temperature for various climatic and work activities. Such work is considered very important to clothing physiology calculations which are shown to offer a very good prediction for survival.

Larsen(27) detailed theoretical and experimental studies of the movement of heat, water vapour and liquid water through clothing systems.

1.6 CLOTHING SYSTEMS.

The transfer of energy through fabric and fabric layers described in previous sections becomes highly complicated when clothing systems are considered. This is due to differences in the layers, the skin area covered, the movement of air layers due to body movement, and by different microclimates in different skin areas.

It frequently happens in fabric and garment design that as certain desirable features are imparted to clothing, other less desirable characteristics result. Thus, if a fabric is made more waterproof, its vapour resistance is increased.

Because of these associations a ratio of positive to negative attributes are an indication of physiological comfort. Examples of these are warmth to weight ratios. Fabrics of optimum warmth to weight obviously do not offer protection against wind and rain and are generally more suitable for underwear. The performance of any one garment assembly is therefore to be judged in the context of a whole

clothing assembly appropriate to the climatic conditions of wear.

It is assumed (6) that about a quarter of the heat produced in the body would be lost by respiration and the remainder must be lost as sensible or insensible perspiration and heat. Except in very adverse cold environments, this heat and vapour is lost from the skin.

The total heat insulation between the skin and the environment is due to the insulation of the fabric layers, the air layers and fabric surface film layers. In assigning a clothing assembly an insulation value, difficulty arises if different parts of the body are covered with variable layers of clothing and some parts may not be clothed at all. In such situations, clothing may be assigned an insulation value using a simplified, segmental average, approach.

1.7 THE AIM OF THE PRESENT WORK.

The aim of this work is to investigate the heat and vapour transfer properties of a range of knitted fabrics. The techniques employed all involve the direct measurement of the fabric response to temperature and vapour pressure gradients.

Three main areas of interest are the thermal resistance at different applied pressures, the simultaneous flow of heat and vapour and the transient response to changing conditions. All three of these areas are of considerable importance with regards the performance of a fabric as an insulator.

Samples chosen for the experimental work are described in Appendix 1.

CHAPTER 2

AN INSTRUMENT FOR THE SIMULTANEOUS MEASUREMENT OF HEAT AND VAPOUR
FLOW THROUGH FABRICS

2.1 DESIGN CRITERIA

The development of an instrument to measure the simultaneous flow of heat and vapour through fabrics is of primary importance to the understanding of the overall energy balance between the human body and the environment. For the purposes of this work and for future investigations it was considered that the following features were essential.

The first and most obvious attribute of the envisaged instrument was that it must be capable of separating the contributions of heat flow and evaporation. If the fabric properties are to be fully ascertained it is essential that these two forms of energy transfer and the interaction between them can be reliably estimated. By only measuring the total energy flow the available information would be insufficient to adequately investigate the importance of the various system parameters or to consider the interaction between the two energy transfer mechanisms.

When considering any clothing system it is impossible to ignore the influence of entrapped stationary air layers. In order to simulate this feature of garments as insulation it is desirable to incorporate a facility for the introduction of an air layer of variable thickness

into the simulated clothing system. Such an air gap will effect the relative importance of evaporation and heat flow in maintaining the thermal balance of the system as a whole. Also the contributions of radiation, convection and conduction within the air layer are governed by quite different functions of its thickness.

It is normal in this field to concentrate on steady-state energy transfer. While this can provide a very considerable amount of information about the sample of fabric, it would be advantageous to have the facility to also record its transient response to the differing environments. This implies the need for a very sensitive temperature control system to ensure that the test conditions are not changed significantly when a fabric sample is first placed on the apparatus. The alternative is to construct a monitoring system to keep track of the test conditions and allow for any variations in the subsequent calculations of sample properties.

In addition to an instantaneous read out of heat and vapour transfer for the assessment of transient response, it is desirable to incorporate an averaging or integrating system for improved accuracy in long term steady-state experiments. Such an integrating system would also enable a ready calculation of the total energy consumed during a period of transient response. This would effectively be a record of the area under the power versus time trace.

2.2 PLATE CONSTRUCTION

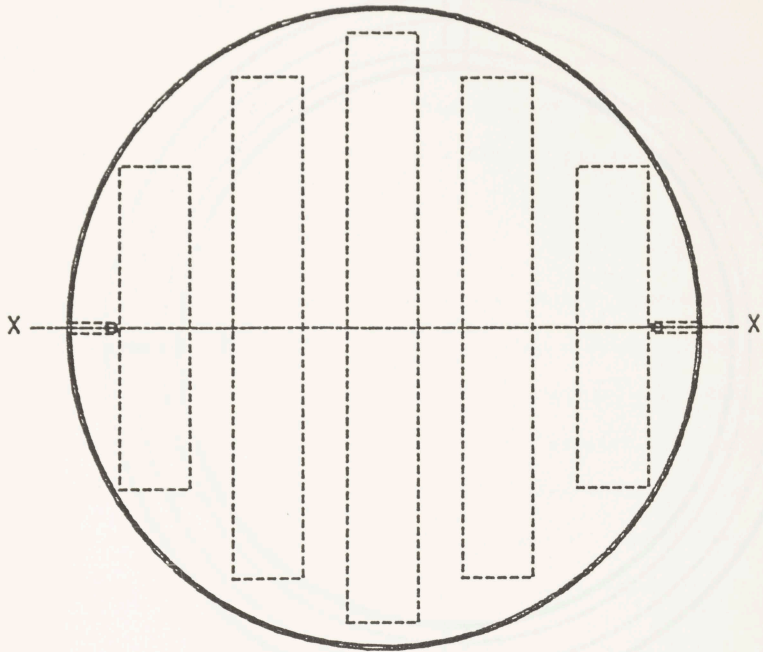
The guarded hot plate system was designed with four major components.

- 1/ Heated centre plate forming the test area.
- 2/ Independently heated guard ring.
- 3/ Insulating base with levelling facilities.
- 4/ Framework for fabric support.

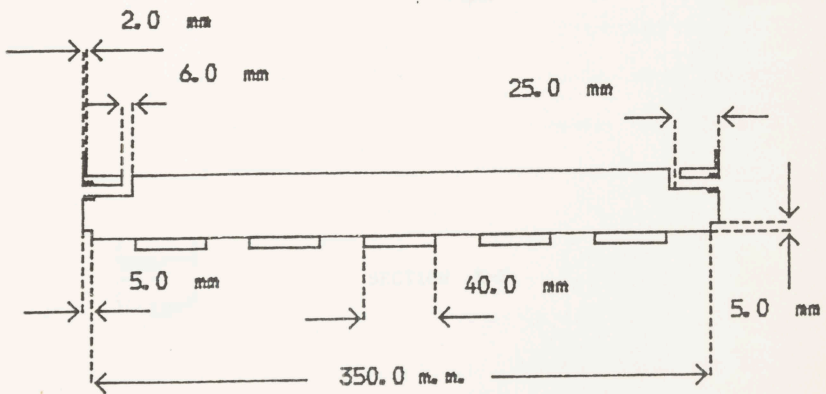
The centre plate was circular with an area of 0.1 square metre. It had a 2 mm thick cylindrical wall around the outer edge. This wall enables the plate to hold liquid up to a depth of 1.0 cm. Holes were drilled into the side and top of the plate (Fig.2.1) to facilitate the supply and maintenance of a level of liquid on the plate. The side hole was threaded to accept a steel tube which emerged through the guard ring and insulating base where it could be connected to the liquid supply system.

Five heater elements were mounted on the lower surface of the plate. These elements were chosen to give a uniform heat flux over the entire surface when a parallel connection to an electrical power supply was used.

The guard ring was concentric with the plate, and of course required both an inner and an outer wall for the containment of liquid (Fig.2.2). When in situ the side of the plate and the inner side of the ring were separated by 1 mm. The ring also had drilled and threaded holes in the top and side for the steel tube supplying its liquid. In addition there were horizontal slots cut into the lower face of the ring to admit the tubes carrying the liquid supply to the plate.



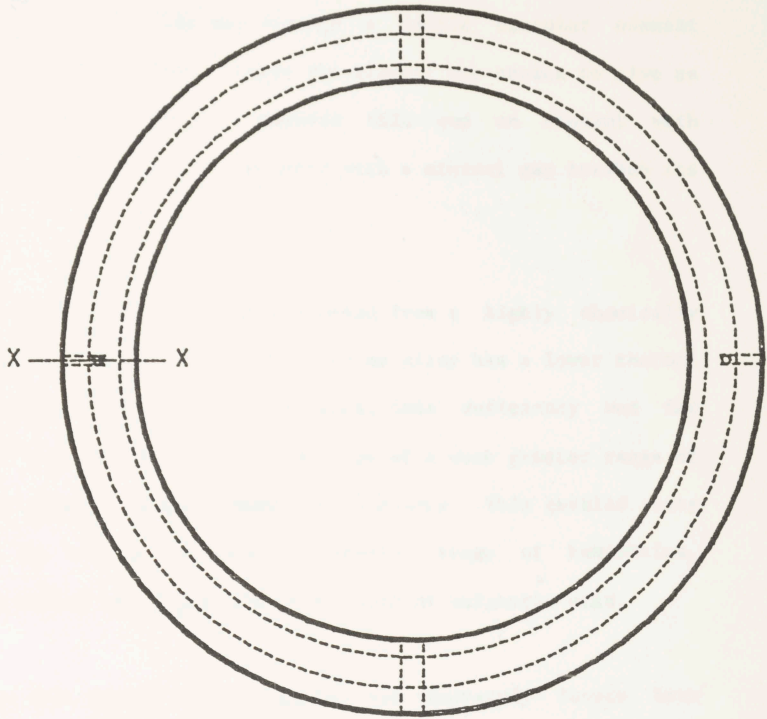
PLAN



SECTION X-X

HEATED PLATE

FIGURE 2.1



PLAN



SECTION X-X

Guard Ring

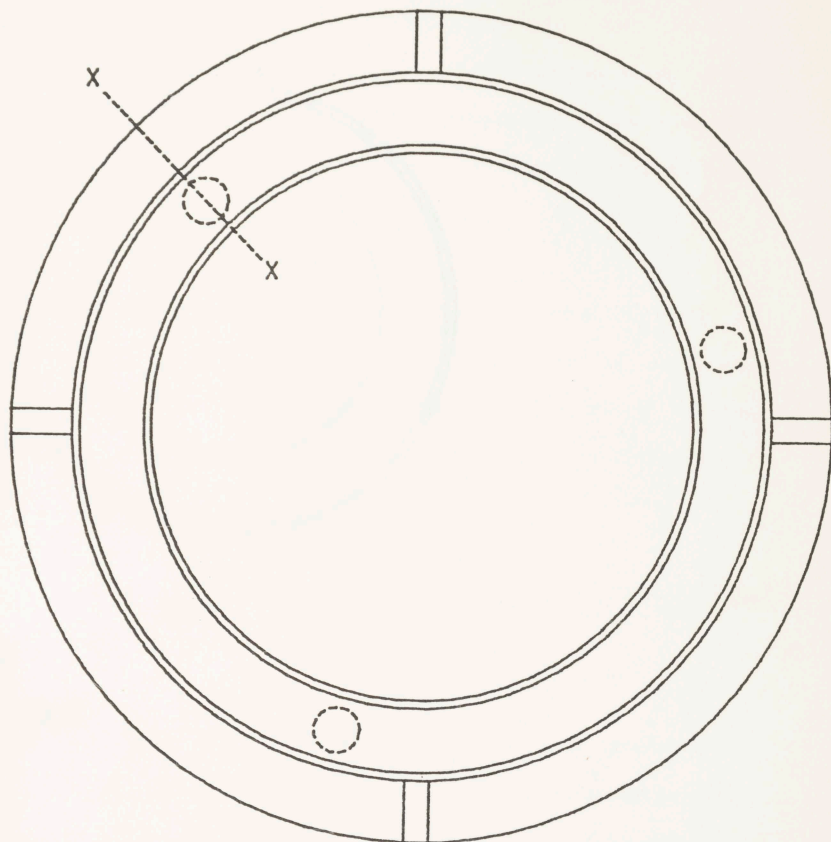
FIGURE 2.2

The energy supply to the ring was through a single circular element attached to its lower face. Again the element was chosen to give as uniform a heat flux as possible. Towards this end an element with virtually zero dead length was mounted with a minimal gap between its two ends.

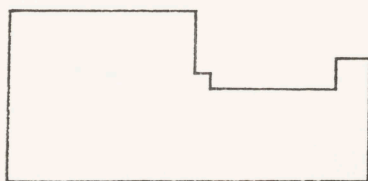
Both the ring and the plate were constructed from a highly chemically resistant stainless steel. Although such an alloy has a lower thermal conductivity than the more normal materials, this deficiency was far outweighed by the potential for the use of a much greater range of liquids, which might otherwise damage the surfaces. This enabled tests to be carried out over an equivalently greater range of humidities, such as are provided by varying concentrations of sulphuric acid.

The insulating base served to both support and accurately locate both the plate and guard ring, while minimising heat loss in all but the upward direction(Fig.2.3). It was fashioned from a very rigid and strong insulating material and provided with three adjustable feet to enable the instrument to be accurately levelled. Suitable slots were cut in its upper surface to admit the liquid supply tubes. Additional insulation was provided under the plate in the form of a layer of glass fibre and a sheet of expanded polystyrene foam.

The fabric support was an aluminium frame as shown in Fig 2.4. This frame had slots cut into its upper surface at 2cm intervals to facilitate the accurate location of the mesh of monofilaments or wire used to support the test specimens. This spacing was chosen because it was small enough to give minimal deviation from flatness for all fabric samples under consideration, while being large enough for the mesh itself to cover an insignificant fraction of the total surface area.



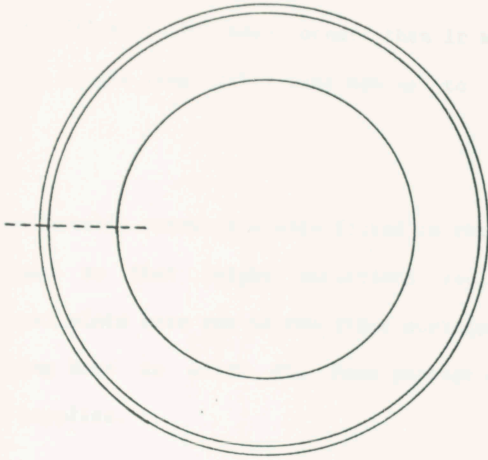
PLAN



SECTION X-X

Insulating Base

FIGURE 2.3



PLAN



ELEVATION

Fabric Support frame

FIGURE 2.4

Loops of nylon monofilament were individually held across the frame by small aluminium brackets. These brackets allowed for tension adjustments where necessary. The advantage of this system being that, should a filament breakage occur then it would only be necessary to replace a single loop rather than having to remount a complete new mesh.

Three adjustable screws are also fitted to the horizontal surface of the frame so that height variations could readily be achieved. Additional slots were cut in the frame corresponding to those in the insulating base to allow the free passage of the tubes carrying the liquid supplies.

2.3 HEATER CONTROL

The accuracy of guarded hot plate systems relies on the maintenance of very precise temperatures and on the measurement of the energy consumed by the test area or plate component of the instrument. Both the plate and the guard ring must therefore be controlled to the same temperature but by separate heater control circuitry.

2.3.1 MODES OF CONTROL

Heater control systems generally fall into two basic categories- on/off and proportional. Both systems have their relative merits and limitations. If the power response to temperature is considered, it will be of the form shown in Fig.2.5(a) and Fig.2.5(b) for on/off and proportional respectively.

Power Supplied as a Function of Temperature

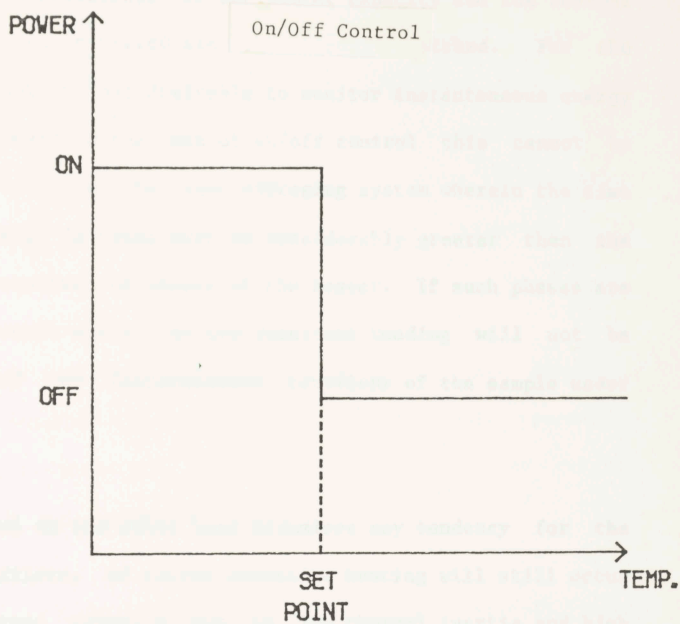


FIGURE 2.5 (a)

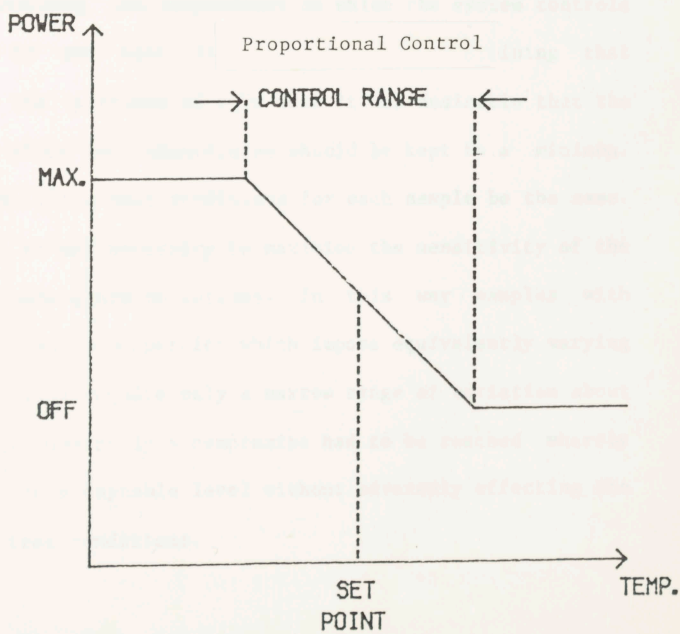


FIGURE 2.5 (b)

The main problem with the on/off system is that it is very prone to large temperature oscillations if the heater capacity and the thermal inertia of the mass to be heated are not suitably matched. For the purposes of this work it was desirable to monitor instantaneous energy consumption. Obviously in the case of on/off control this cannot be achieved without resorting to some averaging system wherein the time over which the average is taken must be considerably greater than the time between consecutive on phases of the heater. If such phases are more than a few seconds apart then the resultant reading will not be truly indicative of the instantaneous behaviour of the sample under test.

Proportional control on the other hand minimises any tendency for the temperature to oscillate. Of course excessive hunting will still occur if there is a gross mismatch due to low thermal inertia and high sensitivity of the control system. Clearly Fig.2.5 implies that, for a given temperature setting, the temperature to which the system controls will be determined by the heat flow demanded in maintaining that temperature. For the purposes of this work it was desirable that the difference between these two temperatures should be kept to a minimum. Only in this way will the test conditions for each sample be the same. To achieve this end it was necessary to maximise the sensitivity of the control system to temperature variations. In this way samples with very different insulation properties which impose equivalently varying loads on the system will require only a narrow range of variation about the set temperature. Obviously a compromise had to be reached whereby hunting was kept to an acceptable level without adversely effecting the reproducibility of test conditions.

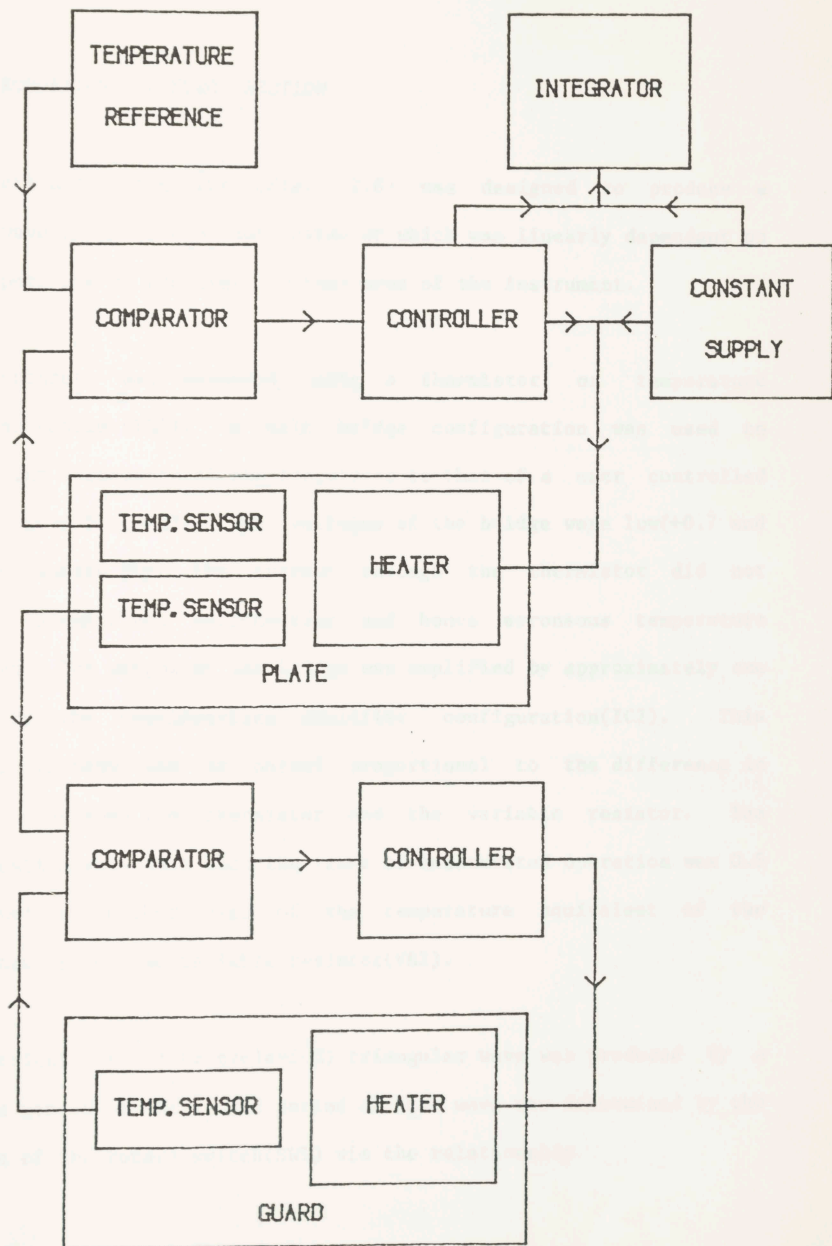
2.4 CIRCUIT DESIGN

Given the above considerations a proportional control system was constructed. The design allows for considerable flexibility in total heat capacity, control sensitivity and output facilities. A basic outline of the system is shown in Fig.2.6. There are three features which are of fundamental importance to the successful operation of this equipment.

1/ The control circuitry for the heater and guard were completely separate. This ensured the maintenance of a minimal temperature gradient between the plate and guard, irrespective of the relative magnitude of the energy demand imposed on them.

2/ The design was such that the guard temperature was compared directly to the plate temperature and the difference between these two quantities was minimised by the action of the guard controller. The plate temperature was controlled by comparison to a user operated temperature reference. This combination means that only a single adjustment was needed to change both the plate and the guard to a new temperature setting. Also it means that the two could not inadvertently be set to different values and thus give spurious results.

3/ The power supplied to the plate came from two sources, one controlled and the other fixed. This facility was intended as a way to maximise sensitivity while avoiding the problems of hunting, as described previously. Since the controller was only responsible for a fraction of the total power it was possible to keep the control range narrow without producing an excessively steep slope in the power versus



Temperature Control and Power Monitoring
Outline

FIGURE 2.6

temperature relationship(Fig.2.7).

2.4.1 PROPORTIONAL CONTROL SECTION

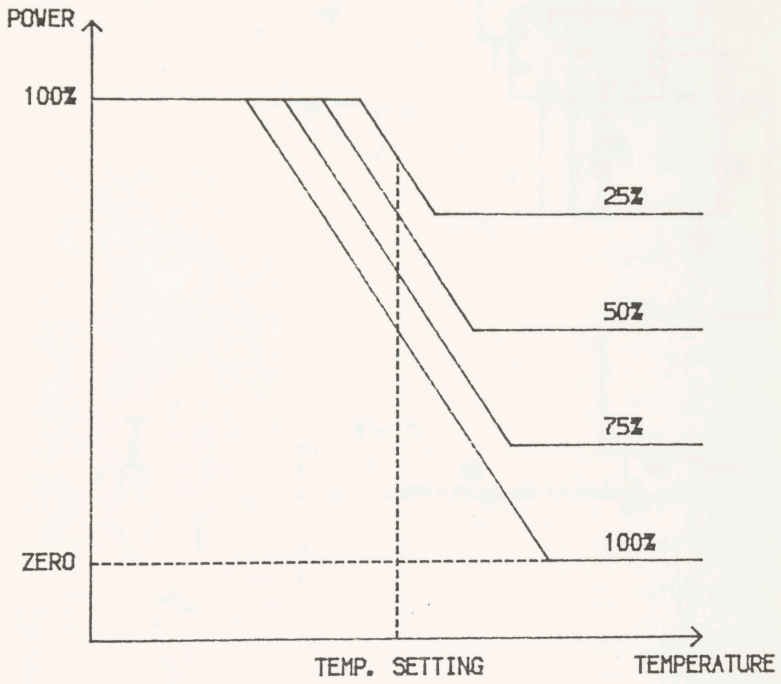
This section of circuitry (Fig. 2.8) was designed to produce a square-wave output, the duty-cycle of which was linearly dependent on the temperature of the plate or test area of the instrument.

The temperature was measured using a thermistor or temperature dependant resistor(TH1). A half bridge configuration was used to compare the resistance of the thermistor to that of a user controlled variable resistor(VR2). The voltages of the bridge were low(+0.7 and -0.7V) to ensure that the current through the thermistor did not produce significant self-heating and hence erroneous temperature detection. The output of the bridge was amplified by approximately one hundred by the non-inverting amplifier configuration(IC2). This amplifier thereby had an output proportional to the difference in resistance between the thermistor and the variable resistor. The amplification was such that the range of unsaturated operation was 0.5 degree Celsius either side of the temperature equivalent of the resistance set on the variable resistor(VR2).

A symmetrical(i.e. duty cycle=50%) triangular wave was produced by a waveform generator(IC1). The period of this wave was determined by the position of the rotary switch(SW1) via the relationship

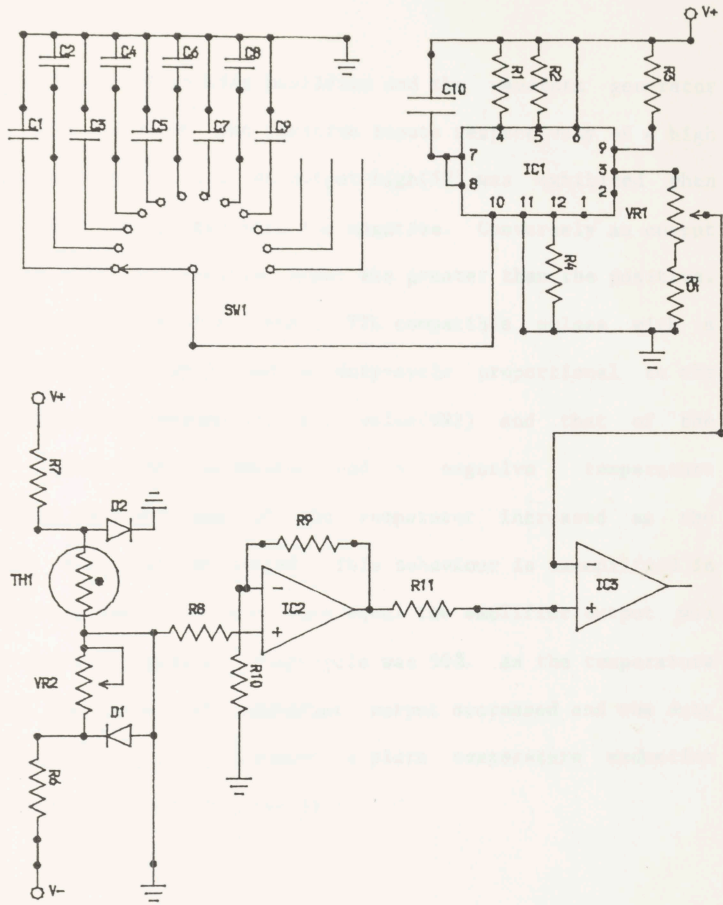
$$\text{Period} = 0.5 C \text{ (seconds)}$$

where C is the capacitance (in microfarads) connected through the



Heater Supply Response to Temperature

FIGURE 2.7



Component values given in Appendix 2

FIGURE 2.8
COMPARATOR SECTION

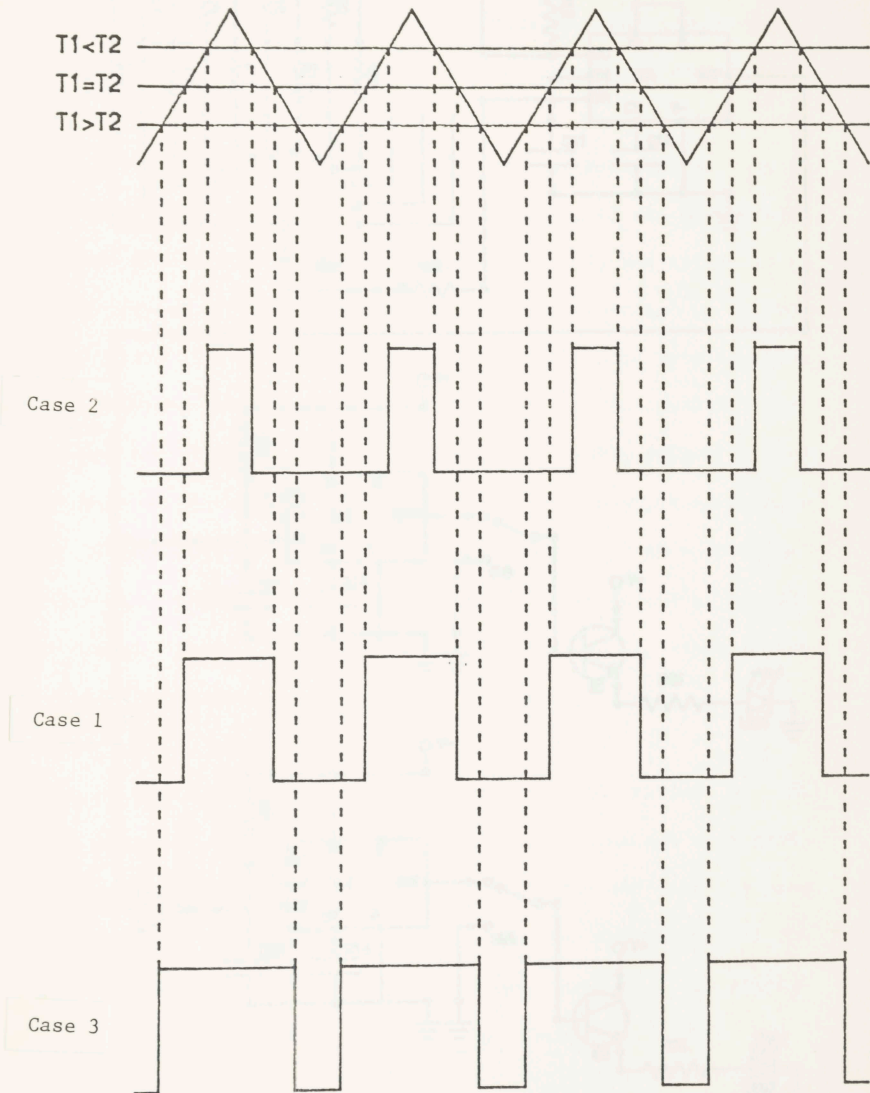
switch. The potentiometer(VR1) allowed the amplitude to be varied between 0.5 and 3.0 volts.

The outputs of the non-inverting amplifier and the waveform generator were fed to the positive and negative inputs respectively of a high speed voltage comparator(IC3). An output high(5V) was exhibited when the positive input was greater than the negative. Conversely an output low(0V) results when the negative input was greater than the positive. Thus the output consisted of a chain of TTL compatible pulses with a fixed frequency(set by SW1) and a duty-cycle proportional to the temperature difference between the set value(VR2) and that of the plate(TH1). Since the thermistor had a negative temperature coefficient then the 'on' time of the comparator increased as the temperature of the plate decreased. This behaviour is exemplified in Fig.2.9. When the two resistances were equal the amplifier output was zero(case 1) and the comparator duty-cycle was 50%. As the temperature of the plate increased the amplifier output decreased and the duty cycle was reduced(case 2). Conversely, a plate temperature reduction led to an increased duty-cycle(case 3).

2.4.2 PULSE GENERATION SECTION

In order to provide two out of phase pulse chains the circuitry shown in Fig.2.10 was constructed.

An astable multivibrator based on an integrated circuit timer(IC4) is used to produce a square wave with a duty cycle of approximately 50%. The frequency of its output is set by a rotary switch(SW2) and determined by the relationship:



Comparator Operation

FIGURE 2.9

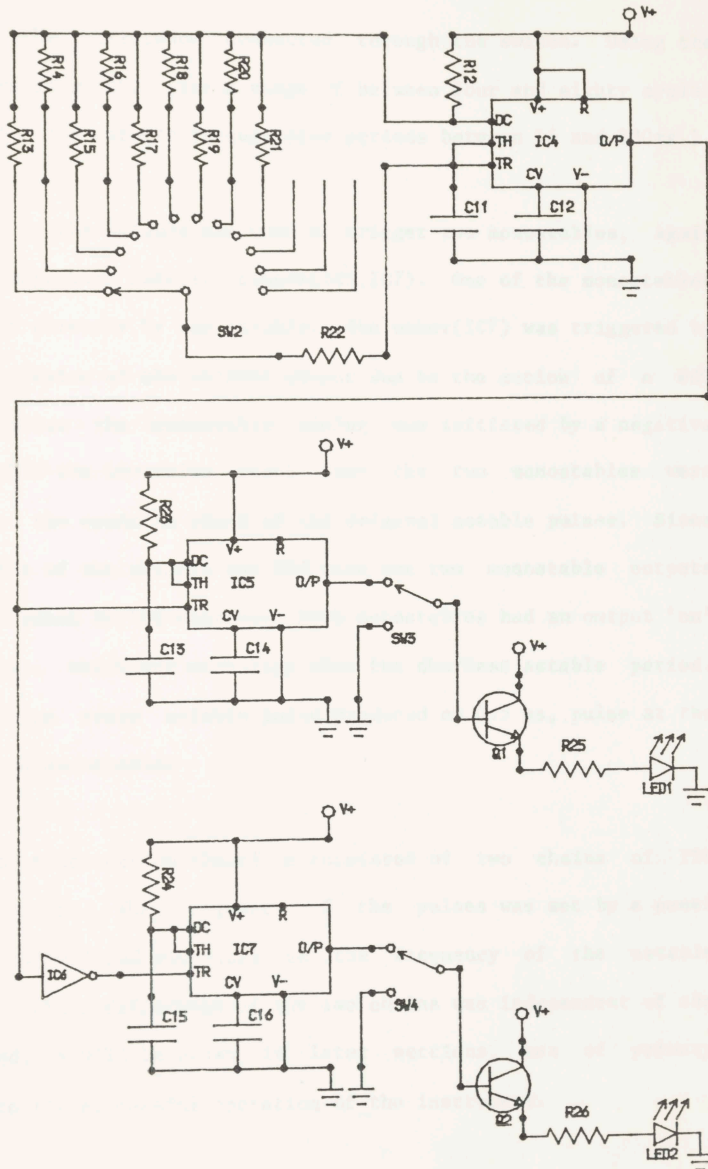


FIGURE 2.10
PULSE GENERATION

$$\text{frequency} = \frac{\text{constant}}{R} \quad (\text{Hz})$$

where R is the resistance connected through the switch. Using the components as shown this gave a range of between four and eighty cycles per second for the astable frequency (or periods between 16 and 330ms.).

The signal from the astable was used to trigger two monostables, again based on integrated circuit timers (IC5, IC7). One of the monostables was triggered directly by the astable. The other (IC7) was triggered by an inverted version of the astable output due to the action of a NOT gate (IC6). Since the monostable timing was initiated by a negative going edge then the inversion meant that the two monostables were triggered by the opposite edges of the original astable pulses. Since the duty cycle of the astable was 50% then the two monostable outputs were out of phase by 180 degrees. Both monostables had an output 'on' time of 0.5 ms. which was much less than the shortest astable period. For this reason every astable pulse produced an 0.5 ms, pulse at the output of each monostable.

The output of this section therefore consisted of two chains of TTL compatible pulses. The frequency of the pulses was set by a panel mounted switch (SW2) and was equal to the frequency of the astable output. The phase difference of the two chains was independent of the frequency and, as will be shown in later sections, was of primary importance to the successful operation of the instrument.

The panel mounted light emitting diode (LED1) was simply intended as a visible indicator of the correct operation of the section.

2.4.3 OUTPUT DRIVER SECTION

Information from the comparator section had to be combined with the chains of the previous section to provide an output to the plate heater. The circuitry involved in this procedure is shown in Fig.2.11. One of the pulse chains from the pulse generation section(IC5) was used without modification to trigger a further monostable with a fixed output 'on' time of 6.0 ms.

The second pulse chain(IC7) was fed, along with an inverted version(IC9) of the comparator section output, to a NAND gate(IC10). The output of the NAND gate was an interrupted chain of negative pulses. The gaps in the chain corresponded to times when the comparator section output was high(5V). This interrupted chain was in turn used to trigger another monostable(IC11) which had a variable timing period set by the rotary switch(SW4). The times ranged from 1.5 to 12.0m.s..

These two monostable outputs(IC8,IC11) were fed to the base of a high power Darlington transistor(Q3). This had the effect of switching the regulated supply to the heater whenever one of the monostables was giving an output high. Clearly one monostable was supplying an uninterrupted chain to the heater while the other chain was broken by the temperature feedback. This meant that the proportional control section was only responsible for a preset fraction of the total output potential of the heater. Such an arrangement ensured a smooth response over a wide range of experimental situations.

Another visual display(LED2) was provided to indicate the interrupted nature of the pulse chain and hence to show when the plate temperature

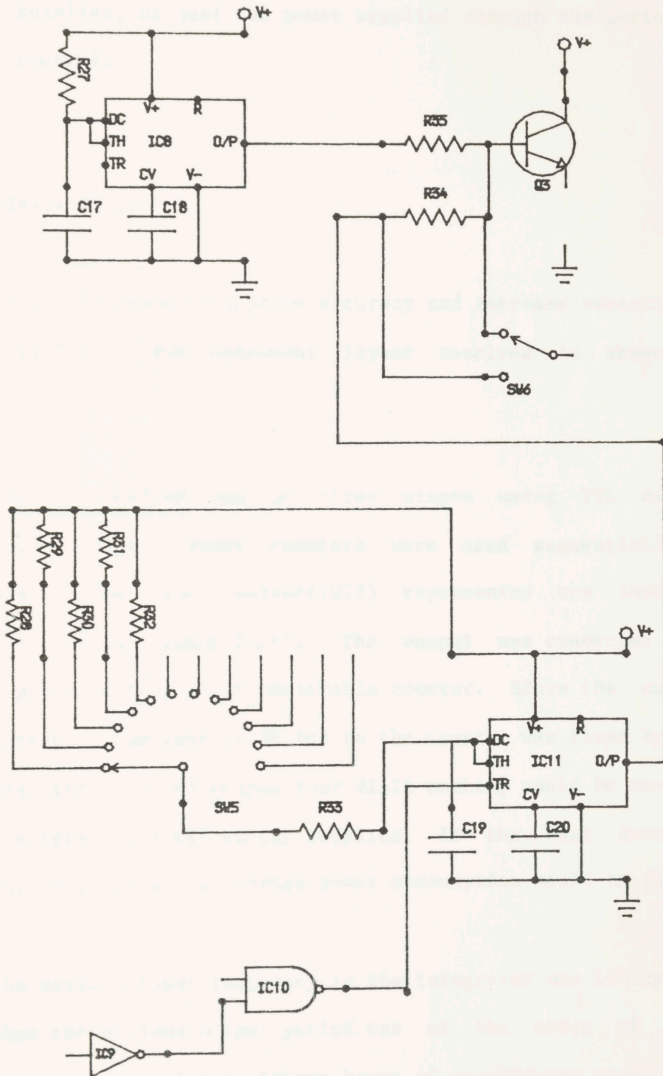


FIGURE 2.11
OUTPUT DRIVER

was near the set point. Output to the integrator section was through a toggle switch(SW6). This allowed the choice of integrating either the total power supplied, or just the power supplied through the action of proportional control.

2.4.4 INTEGRATOR SECTION

An integrator was included to improve accuracy and increase versatility as described earlier. The component layout involved is shown in Fig.2.12.

The integration was carried out in three stages using TTL decade counters(IC12,IC13,IC14). These counters were used sequentially so that each pulse at the final output(IC12) represented one thousand pulses at the initial input(IC14). The output was connected to a commercially produced four digit resettable counter. Since the amount of energy represented by each pulse fed to the counter was fixed by the panel settings then the displayed four digit number, could be readily interpreted in terms of total energy supplied. If the test duration was also recorded, then the average power consumption could be found.

Given that the maximum input frequency to the integrator was 160 cycles per second then the minimum output period was of the order of five seconds. This gave at least sixteen hours of unambiguous readout on the counter. For most applications the range was considerably greater than this figure. The resolution of the integrator was given by the period between output pulses, which for most purposes was of the order of ten seconds. Such a figure was more than adequate even for the most rapid transient experiments envisaged for the instrument. The

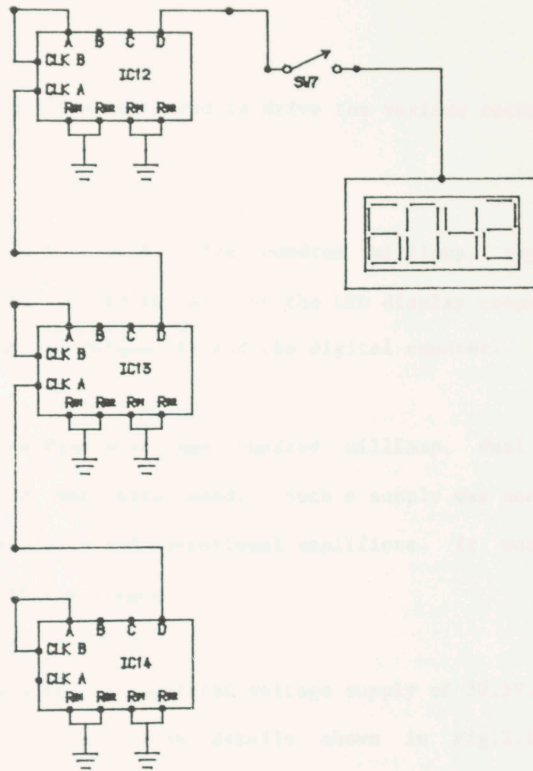


FIGURE 2.12

INTEGRATOR

combination of facilities for long term and high resolution testing was thus achieved.

2.4.5 POWER SUPPLIES

Four separate power supplies were used to drive the various sections of the instrument.

1/ Display driver.

A commercially produced five volt, five hundred milliamp, regulated power supply was used to drive all of the LED display components. These included the indicators(LED1-4) and the digital counter.

2/ Dual rail supply.

A commercially produced five volt, one hundred milliamp, dual rail, regulated power supply was also used. Such a supply was needed to power the waveform generator and operational amplifiers. It was also used to set up the bridge voltages.

3/ Plate heater supply

The plate heater required a regulated voltage supply of 30.5V. This was achieved using the construction details shown in Fig.2.13. A standard transformer(TR1), bridge rectifier(BR1) and smoothing capacitor(C26) arrangement was used to produce a D.C. voltage of about 38V. This voltage being suitable for regulation by a five ampere, variable voltage regulator(REG1). The output voltage being set by the variable resistor(VR6).

4/ Guard heater supply.

Since there is no need to monitor the power supplied to the guard it was not deemed necessary to use a regulated supply for this purpose. Hence a second smoothed D.C. supply was constructed according to the same design as the first part of the plate power supply. This

consisted of similar transformer(TR1), fuses(F1,F2), bridge rectifier(BR1) and output capacitors(C26,C27) to those shown in Fig.2.13.

2.4.6 COMBINED OPERATION OF PLATE CONTROL CIRCUITRY.

As has already been indicated the plate heater supply was made up from two components. Due to the action of the pulse generation section these two components determined the amount of energy supplied on alternate pulses. The pulse chain for the continuous supply was, of course, unbroken. The fraction of the maximum output capacity supplied by the action of this chain was given by the product of the astable frequency multiplied by the period of the relevant output monostable. Given that the period of this monostable was fixed(6.0m.s.), then the continuous power was set by the frequency of the astable as set by the switch(SW3). This range of frequencies was shown earlier to be between eighty and four cycles per second, giving a power fraction of between 0.5 and 0.02. Knowing that the total power capacity was set by the voltage regulator(30.5V) and the heater resistance(19.3 Ohm) to a value of 60.0 Watts then the power fractions translated into the power range selection (Table 2.1).

The second output pulse chain, which was broken by the action of the voltage comparator, NAND gate combination, was used as the proportional temperature controller. As in the case of the continuous supply, the power fraction was set by the astable frequency and the relevant output monostable period. Given that both pulse chains are derived from the same astable, then clearly the power switched by the controller was

ASTABLE FREQ.(Hz)	POWER FRACTION	CONTINUOUS POWER(W)
4.0	0.02	1.25
5.0	0.03	1.75
8.0	0.04	2.5
10.0	0.06	3.5
16.0	0.08	5.0
20.0	0.13	7.0
32.0	0.16	10.0
40.0	0.25	14.0
64.0	0.32	20.0
80.0	0.50	28.0

Table 2.1

Relationship Between Astable Frequency and Power Supplied
Through Controller

equal to the product of the continuous power and the ratio of the control monostable period to that of the continuous monostable. This ratio was set by the switch(SW4) and has the following values.

0.25 0.50 0.75 1.0 2.0

Obviously the ratio 2.0 could only be selected when the power was set to 14.0 Watts or less, or when the continuous output was switched off(SW4).

The overall operation can best be understood in terms of the waveforms which appeared at certain points in the circuitry(Fig.2.14).

The voltage comparator output(A) was determined by the effect the temperature of the plate has on the input crossover locations. Two out of phase pulse chains(C,D) were produced by triggering a pair of monostables by the opposite edges of a square-wave(B). One of these chains(D) was fed to a NAND gate along with the comparator output(A). This comparator produced an interrupted pulse chain(E).

Both the continuous(C) and the interrupted(E) chains were used to trigger monostables to produce output pulses with accurately set 'on' times(F and G respectively). These two chains were then fed simultaneously to the base of the output transistor(H) which supplied the heater.

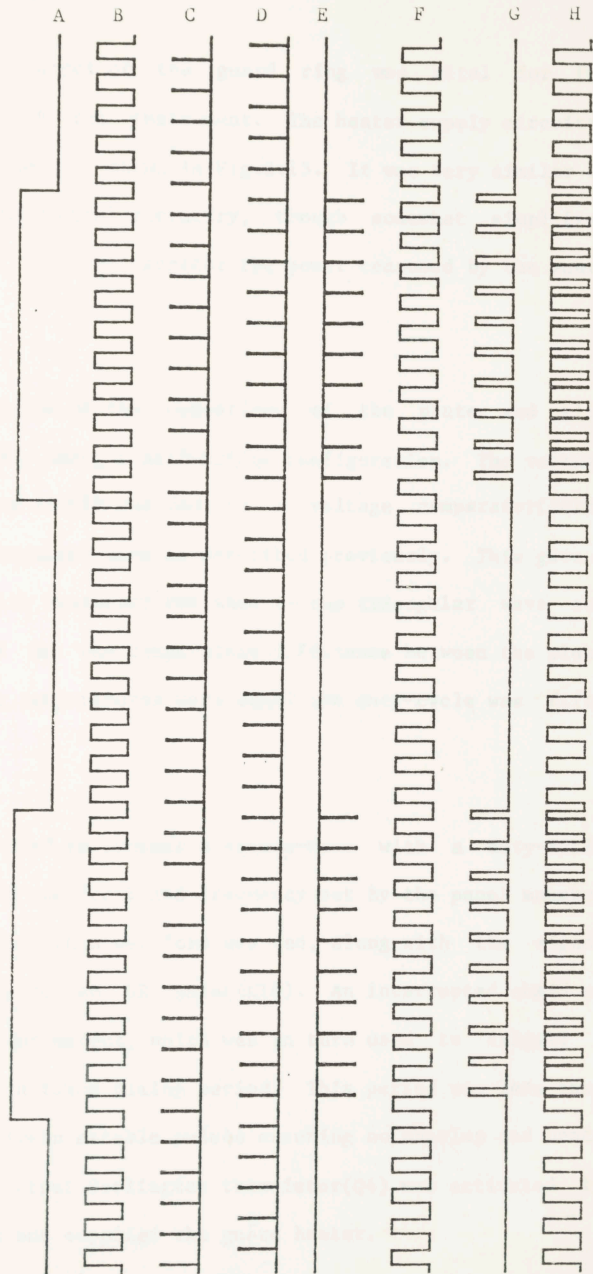
The waveforms shown in Fig.2.14 are consistent with settings of

10.0 W on the switch controlling the continuous power

50% on the switch setting the power fraction for the controller

0.5 sec on the triangular wave time switch

3.0 deg on the control range variable resistor



Waveforms as Seen at Certain Points in the Control Circuitry

FIGURE 2.14

2.4.7 GUARD RING HEATER CONTROL

Accurate temperature control of the guard ring was vital for the successful operation of the instrument. The heater supply circuitry employed for this purpose is shown in Fig.2.15. It was very similar in principle to the plate control circuitry, though somewhat simplified since there was no need to monitor the power consumed by the guard ring.

The first stage consisted of the comparison of the plate and ring temperatures (TH2, TH3) using a half-bridge configuration. The voltage produced was amplified (IC15) and fed to a voltage comparator (IC16) along with the triangular wave as described previously. This gave a square-wave output with frequency the same as the triangular wave and duty-cycle determined by the temperature difference between the plate and ring. When these temperatures were equal the duty-cycle was fifty per cent.

An astable (IC17) was used to produce a square-wave with a duty-cycle close to one hundred per cent and frequency set by the panel mounted variable resistor (VR5). This waveform was fed, along with the signal from the comparator, to an OR gate (IC18). An interrupted chain of pulses was the resultant output, which was in turn used to trigger a monostable (IC19) with a fixed timing period. This period was less than the minimum time between astable pulses ensuring no overlap and hence linear response. An output Darlington transistor (Q4) was activated by the monostable output and supplied the guard heater.

The circuitry was such that an increase in ring temperature led to a more positive amplifier output and hence a larger duty-cycle at the

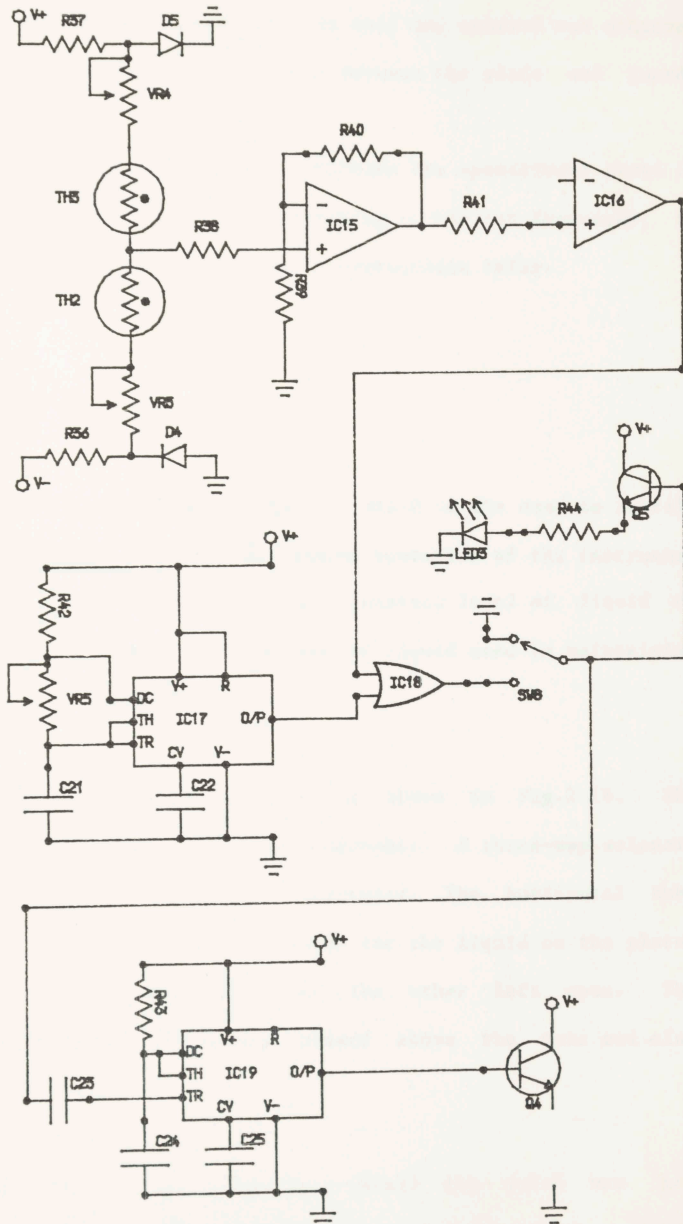


FIGURE 2.15
GUARD SUPPLY

comparator output. This gave fewer pulses per triangular wave at the output of the OR gate, which in turn meant fewer pulses from the monostable and Darlington transistor. In this way control was achieved by minimising the temperature difference between the plate and guard.

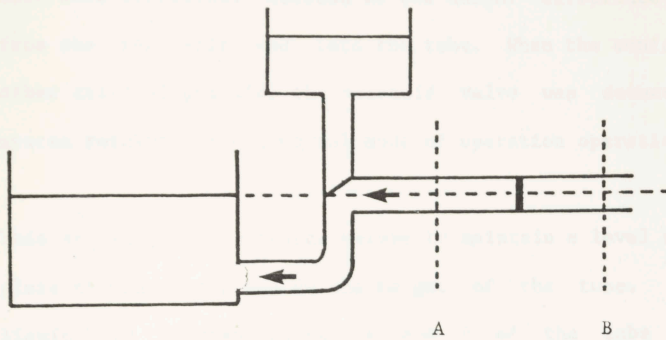
A visual display(LED3) is provided to indicate the operational state of the ring control circuitry and, when flashing at the set frequency, to show that the ring temperature was at an appropriate value.

2.5 LIQUID SUPPLY SYSTEM

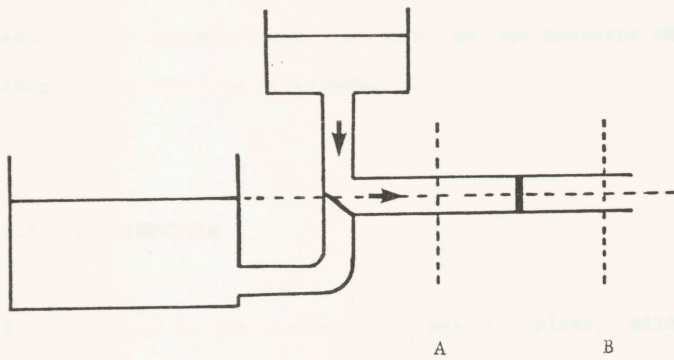
The design of the liquid supply system was based on the need to fulfill two principle requirements. For the proper operation of the instrument it was necessary to be able to maintain a constant level of liquid on the plate. At the same time, the mass of liquid used in maintaining that level had to be monitored.

A schematic diagram of the approach used is shown in Fig.2.16. The system supplying the plate had three components. A three-way solenoid valve, a horizontal tube and a liquid reservoir. The horizontal tube was located at the same height as desired for the liquid on the plate. One end was connected to the valve and the other left open. The reservoir was held at a constant height above the tube and also connected to the valve.

In the normal mode of operation(Fig.2.16(a)) the valve was not energised and the liquid supplying the plate was drawn along the tube. When the meniscus reached a certain point(A) the solenoid valve was energised. In this mode of operation (Fig.2.16(b)) the reservoir and



(a)



(b)

Operation of Liquid Supply System

FIGURE 2.16

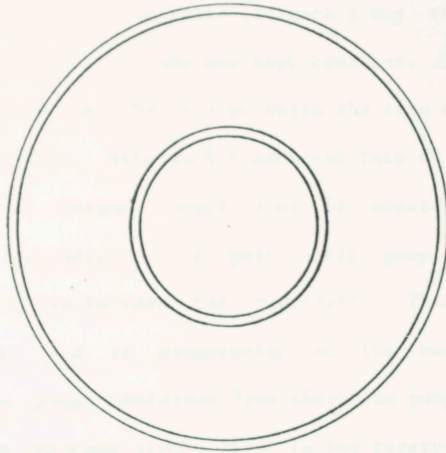
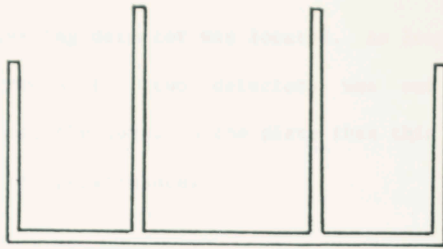
tube were connected. Because of the height difference liquid flowed from the reservoir and into the tube. When the meniscus reached the other critical point(B) the solenoid valve was deenergised and the system returned to the normal mode of operation operation(Fig.2.16(a)).

This sequence of operations served to maintain a level of liquid on the plate at the same place as the height of the tube. The volume of liquid held between points A and B of the tube could be set by adjusting the positions of the detectors. This represented the amount of liquid evaporated during the time interval between any two consecutive energisations. If this time was measured then the rate of evaporation could be calculated.

2.5.1 CONSTRUCTION

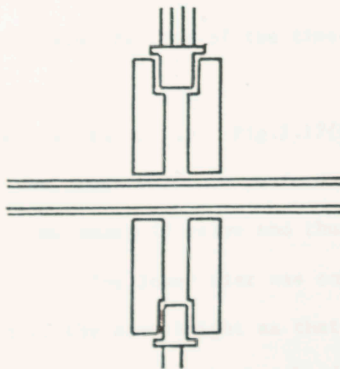
The tube used in the construction was of glass, with internal and external diameters of five and seven millimeters respectively. Near each end the tube was held in a nylon cylinder which had a suitable hole drilled along its axis to accept its seven millimeter diameter. These cylinders were rigidly clamped in a frame that allowed for individual height adjustments at each end of the tube. Similar drilled nylon cylinders were used to house emitter/detector pairs for the detection of the meniscus(Fig.2.17(a)).

There were certain difficulties in finding tube of near perfect straightness and of setting the two ends of the tube to exactly the same height. For this reason the open end of the tube was set slightly higher than the end connected to the valve. The level of liquid on the plate was therefore set by the height of the tube at the point where



Liquid Supply Reservoir

(b)



Infra-red Detector

(a)

FIGURE 2.17

the solenoid activating detector was located. As long as the volume of liquid held between the two detectors was not sufficient to significantly change the level on the plate then this arrangement would not detract from the performance.

The liquid reservoir was constructed in such a way that the head of water used to replenish the tube was kept constant. This was desirable as a way to ensure that the rate at which the tube refilled was fixed over very long periods. With such a constant rate of flow any tendency for the meniscus to overshoot would also be constant and could be allowed for in calibration. A peristaltic pump is used to give a continuous flow of liquid into the reservoir. This flow was much greater than the rate of evaporation so the reservoir constantly overflowed into a larger container from which the pump drew its water. The result was a constant liquid level in the reservoir. The position of the reservoir could be varied as the tube position was varied to give the constant head of liquid desired. For the rates of evaporation encountered in this work a head of one centimetre was used. This figure produced a refill rate that minimised overshoot but kept the refill time as a negligible fraction of the time between refills.

The liquid reservoir is shown in Fig.2.17(b). The two-tiered arrangement allowed the reservoir to perform two functions. The top tier was connected to the solenoid valve and thus used to supply the tube and hence the plate. The lower tier was connected directly to the guard ring and held at the same height as that desired for the liquid on the instrument. This meant that the height difference between the two tiers represents the head used in refilling the tube.

2.5.2 LIQUID SUPPLY CIRCUITRY

The liquid supply system relied on the detection of the meniscus inside the glass tube. Detectors are placed at two positions along the tube. When the lower one detected the meniscus a timing circuit was activated which, in turn energised the solenoid valve. Liquid then flowed into the tube until the second detector sensed the meniscus. The output change from this detector served to terminate the timing period and return the valve to its normal state.

The detection of the meniscus was achieved by the use of an infra-red light emitting diode with a suitably matched light activated switch. They were positioned(Fig.2.17(a)) on opposite sides of the tube so that the liquid flowed between them. When the meniscus moved between the source and detector the curvature of the liquid-air interface bent the light and greatly reduced the intensity as seen by the light activated switch. With a suitable adjustment of the sensitivity control the switch gave an output 'low' when the meniscus is present and an output 'high' otherwise.

The first light activated switch was connected to the trigger of a resettable monostable. The sensitivity of the switch was set by a variable resistor. When the meniscus broke the beam from the diode the resultant negative going edge initiated the monostable timing period. A relay was energised by the monostable through a transistor. This relay switched the more powerful supply and energised the solenoid valve.

When the tube had been filled the beam from the second light emitting diode to its associated light activated switch was interrupted by the

meniscus. The output low was used to reset the monostable i.e. terminate the timing period and rearm the monostable in preparation for the next trigger input. As the monostable output returned to zero the transistor, relay and solenoid valve resumed their original states.

In normal operation the tube refilled in approximately five seconds. The timing period used was about thirty seconds. If something should go amiss with the second detector and the monostable not be reset, then this limited timing period ensured that the solenoid valve was not kept in an energised condition indefinitely.

2.6 RECORDING FACILITIES

To maximise versatility three separate outputs were taken from the control circuitry. The quantities measured were the instantaneous power supplied to the plate, the integrated value of that power and the times at which the solenoid valve was energised to refill the tube.

The instantaneous power was measured by using the proportional control section operational amplifier output (IC2). It was this voltage that set the duty-cycle of the comparator and hence the power supplied by the controller. A low pass filter was used to eliminate any high frequency pick-up before feeding the signal to a three pen chart recorder. This active filter was based on a high impedance operational amplifier and had its time constant set to about ten seconds.

In order to record the integrated power an output was taken from the last stage of the integrator section, as described earlier. This signal was fed to a further decade counter and the subsequent output

used to control an integrated circuit analogue switch. The two output terminals of this switch were used to operate the chart recorder's event marker. This produced a spike on the paper for every ten pulses entering the counter. Or, in other words, an output spike for every ten thousand pulses fed to the plate heater.

Recording the volume of liquid supplied was also based on an integrated circuit analogue switch. This switch was fed with the output from the second light activated switch and used to operate the event marker on the third channel of the chart recorder. Every refill of the tube was indicated by a spike on the recording.

The accuracy of the readings taken from the recorder depend, to a large extent, on the precision of the paper drive. For the recorder used, the difference between the quoted and measured values of the paper drive settings was better than one half of one per cent.

These three outputs combined with the readout on the digital counter provided all the information needed to assess the performance of the samples under test.

CHAPTER 3

THE MEASUREMENT OF FABRIC THICKNESS

3.1 INTRODUCTION

The measurement of fabric thickness presents considerable difficulties, both in terms of the instrumentation required and the interpretation and application of the results.

Any definition of fabric thickness is dependent on the envisaged use of the fabric. The problems are due to the surface properties of the fabrics produced from staple fibres in particular. Under smaller loads the fabric effectively forms three layers. The top and bottom layers were due to the load supporting capacity of the surface hairs and the centre layer represents the bulk of the fibre content of the fabric. When the pressure is increased the two outer layers were greatly compressed while the central layer undergoes only a comparatively small change. For some applications the surface fibres will contribute to the performance of the fabric giving an effective thickness which includes the uncompressed outer layers. In other applications the surface fibres will play no part in determining the performance of the fabric giving a greatly reduced effective fabric thickness.

A further major difficulty concerns the choice of test duration for fabric thickness measurements. As will be shown by the results that follow, there can be significant differences between test results achieved using different test times. This is a consequence of the

rearrangement of surface fibres in low pressure tests and stress relaxation within the fabric at higher pressures. In addition, the amount by which the thickness changes (or the amount by which the pressure falls for a constant thickness test) during a test is dependent on the applied load. In other words, a plot of thickness against pressure for a rapid test may have a different shape to the same plot based on results for a long term or equilibrium test.

3.2 TEST METHODS AND RESULTS

Most instruments used in the assessment of fabric thickness are based on the measurement of the separation of two parallel flat surfaces which are used to apply a known pressure to the fabric. By varying the applied pressure, the thickness response of the fabric can be assessed. Clearly the measured thickness values only have meaning in relation to the applied pressure for this, very specific, 'sandwich' situation. As has already been indicated, the effective thickness of the fabric could well depend on the particular end-use proposed for the fabric. The situation could arise whereby two fabrics with the same measured thickness could perform quite differently in a situation supposedly governed by thickness.

3.2.1 THE RELATIONSHIP BETWEEN THICKNESS AND PRESSURE.

A large number of primarily empirical equations have been suggested for the relationship between measured fabric thickness and the applied pressure.

Peirce(28) proposed that, at a pressure P , the fabric thickness, $d(P)$ will be given by:

$$d = d_0 e^{-cP} \quad 3.1$$

where d_0 is the thickness at zero pressure and c is a constant.

Hoffman and Beste(29) used a compressometer to assess the performance of fabrics and found that Peirce's equation(EQ. 3.1) could not be applied with sufficient accuracy. An alternative formulation was suggested:

$$P = c (d_0 - d)^a \quad 3.2$$

where c is a constant. The exponent, a , was found, for all samples tested, to be equal to 1.25 at low pressure and then to change suddenly to a value of 3 at medium to high pressures.

By considering only the bending forces, Van Wyk(30) developed a theoretical model to predict the pressure versus thickness relationship for samples of bulk wool fibre. The resultant expression was given as:

$$P = \frac{c Y^3}{\rho} \left(\frac{1}{v_p} - \frac{1}{v_0} \right) \quad 3.3$$

where v_p and v_0 are the volume of the sample at pressure P and zero respectively, ρ is the fibre density, Y is Young's modulus, m is the total mass of fibre and c is a constant. From van Wyk's experiments it appeared that, at the commencement of compression, a wool sample obeys Hooke's Law which implied the equation:

$$P = \frac{c' Y^3}{\rho} \left(\frac{1}{v_p} - \frac{1}{v_0} \right) \quad 3.4$$

where c' is a constant.

Bogarty et al(31) carried out a series of experiments on a range of blended serges using a Scheifer compressometer. Over the range of pressures from 0.002 to 2.0 lb/sq.in.(14 to 14000 Pa) the results were found to conform to the relationship:

$$d = a + \frac{b}{P + 0.05} \quad 3.5$$

where a and b are constants. The relationship is analogous to van der Waal's equation, where a represents the volume occupied by the gas molecules and the value 0.05lb/sq.in. allows for the internal pressure.

A Schiefer compressometer was also used by Larose(32) for an investigation of the compression properties of fabrics. Over the pressure range considered (0.1 to 1.0 lb./sq.in. or 700 to 7000 Pa) Larose found that the following formulation gave the best fit for the fabrics tested:

$$d_0 - d = c \ln(P) \quad 3.6$$

where c is a constant. This equation was found to be inadequate for the wool and cotton battings also tested.

Larose also compared his experimental results with the different

expressions available at the time. Peirce's formula was found to be inadequate and the other equations (Eq. 3.2, Eq. 3.3) suffered either from the limited range of pressures over which they were applicable or because the various coefficients could only be found experimentally for each fabric considered.

3.3 TEST INSTRUMENT

The instrument constructed for the measurement of fabric thickness employed the same general principles as those previously described. The main difference between the instrument employed here and those of previous workers was that the thickness was set by the operator and the load measured by the device rather than the converse which was more commonly the case.

A vertical section of optical bench was used to support a horizontal arm. The height of the arm could be adjusted to an accuracy of 0.02 mm using the vernier scale on the vertical support. An aluminium plate was suspended from the arm through a flexible coupling. This plate was centred above an electronic balance which had been fitted with a flat measuring table. The fabric sample to be tested was placed on the measuring table and the plate lowered to the desired height. The applied load was registered by the balance. After suitable calibration of the vernier scale it was possible to achieve rapid readings of fabric thickness over a wide range of loads. The test area used was 100sq.cm. which minimised edge effects and allowed for simple conversion of the balance reading to pressure units.

Before any measurements could be made on fabrics it was necessary to

calibrate the instrument to allow for any travel in the electronic balance mechanism or in the plate support elements. The relationship between the applied load and the zero thickness reading on the vernier was found. All results quoted have been based on this calibration curve.

3.4 EXPERIMENTAL

Of primary concern to the assessment of fabrics as thermal insulators is the low pressure region of the thickness versus pressure relationship. The British standard test (BS4745) for fabric thermal resistance specifies that a pressure of 7 Pa. should be applied to the fabric during the test and should also be used in the measurement of the fabric thickness. This allows the results to be expressed in units of resistivity as well as resistance. This particular pressure has been suggested as the value at which the knitted staple fibre fabric has been compressed to its geometric thickness(33). The relevance of the geometric thickness and hence the recommended pressure to the performance of a fabric as an insulator will be discussed in the chapter relating to dry heat transfer.

Several different formulations have been used to represent the relationship between the thickness of a fabric and the pressure exerted perpendicularly to its surface. For fabrics produced from staple fibres in particular, the compression can be divided into several stages which are likely to display considerable overlap. These stages have long been recognised and can be seen as originating from at least four sources. The first stage invariably involves the compression of the layer of fibres protruding from the bulk of the fabric. The second

stage can be associated with the removal of any creases or buckling of the fabric. In the third stage the actual bulk of the fabric is compressed, bringing the fibres closer together. The final stage corresponds to the compression of the fibres, which requires substantially higher pressure than encountered by a fabric in normal use.

The experimental work undertaken for this chapter was divided into two sections. In the first section the low pressure region was investigated using both rapid and steady-state methods. In the second section a wider range of pressures was employed using only the rapid technique.

3.4.1 LOW PRESSURE

For the purposes of this section the pressure range 0.25 to 250 Pa was used. This range had a geometric mean at about the pressure associated with the geometric thickness of the fabric as discussed earlier. This range of pressure could therefore be expected to encompass the compression of the protruding fibre layer and the transition to the stiffer bulk compression region (assuming the samples are not buckled).

The low pressure measurements were divided into two sets. The first set consisted of a rapid sequence of increasing loads. Eleven readings of thickness were taken at loads from 0.25 to 256 Pa. The experiment was carried out with minimal delay between readings.

The second set was carried out to find the steady-state thickness values for the same eleven pressure settings. Readings were only taken

when the electronic balance output had not changed significantly over a period of not less than twenty minutes. A typical result is shown in Figure 3.1.

It is immediately apparent from these results that there is no indication of a transition between two different compression mechanisms over the range of pressures used. As anticipated the plot of pressure against thickness displays an increasingly negative slope as the thickness is reduced. The plot of the logarithm of pressure against thickness is also shown. This second plot was, for all fabrics, well represented by a straight line.

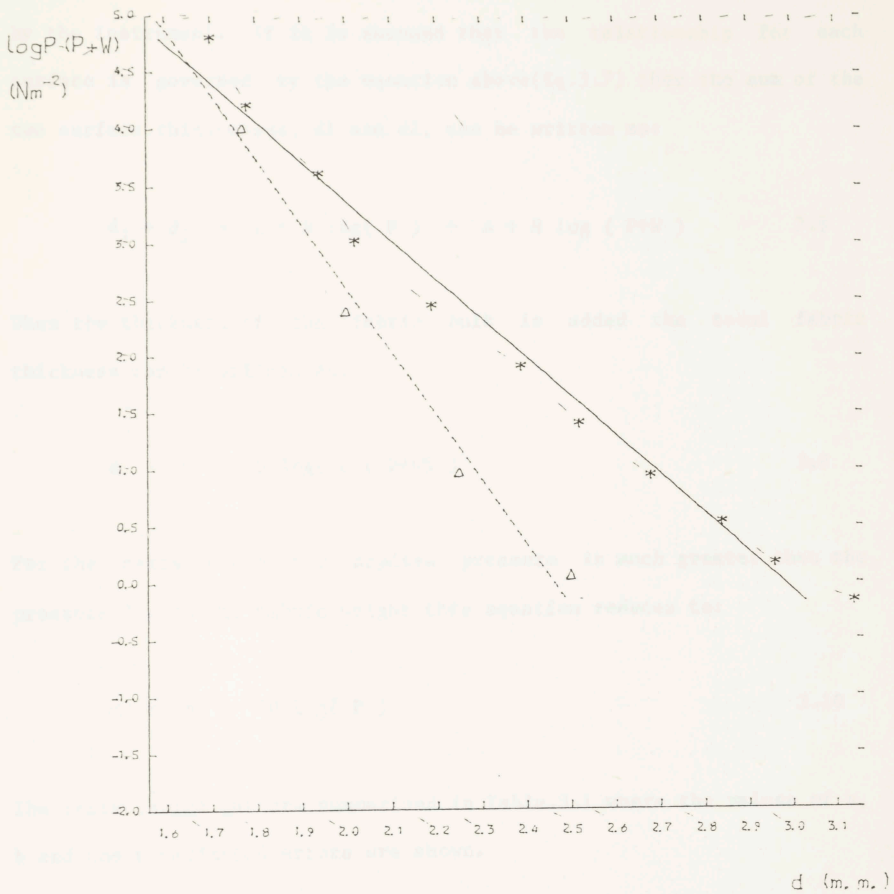
In general the rapid and steady-state measurements followed a similarly shaped curve with the steady-state results offset toward the low pressure and lower thickness directions. This was also demonstrated in the logarithmic plots where, for most fabrics, the two sets of results produced approximately straight lines though of different slope. The equation for the line of best fit relating the thickness, d , to the pressure, P , is given by:

$$d = A + B \log (P) \quad 3.7$$

where the coefficients, A and B the intercept and slope respectively, were calculated for each fabric sample and for each of the two sets of test conditions.

If the relationship between thickness and pressure in the low pressure region is considered then it is clear that the surface fibres at the two faces of the fabric are subjected to different pressures. At the lower surface the pressure includes the contribution of the sample mass

SAMPLE: 2



LINEAR REGRESSION: $d = a + b \log P (P+W)$

—*— $a = 2.98 (0.03)$ $b = -0.29 (0.004)$

- - - Δ - - - $a = 2.46 (0.03)$ $b = -0.18 (0.005)$

FIGURE 3.1

per unit area, W , as well as the pressure applied to the upper surface by the instrument. If it is assumed that the relationship for each surface is governed by the equation above (Eq.3.7) then the sum of the two surface thicknesses, d_1 and d_2 , can be written as:

$$d_1 + d_2 = A + B \log(P) + A + B \log(P+W) \quad 3.8$$

When the thickness of the fabric bulk is added the total fabric thickness can be written as:

$$d = a + b \log(P(P+W)) \quad 3.9$$

For the cases where the applied pressure is much greater than the pressure due to the fabric weight this equation reduces to:

$$d = a + 2B \log(P) \quad 3.10$$

The tests carried out are summarised in Table.3.1 where the values of a , b and their estimated errors are shown.

The relationship between thickness and pressure (Eq.3.9) was derived empirically and without any reference to the physical mechanisms which could be involved. For the purposes of interpreting heat transfer results at low pressures it served as a description rather than as an explanation.

I.D.	W	STEADY-STATE				RAPID			
		a	s(a)	b	s(b)	a	s(a)	b	s(b)
2	2.55	2.46	0.03	-0.177	0.005	3.65	0.05	-0.461	0.008
26	2.56	3.07	0.08	-0.294	0.012	3.73	0.03	-0.442	0.005
28	2.32	3.27	0.09	-0.389	0.012	4.25	0.03	-0.569	0.004
30	2.92	3.25	0.06	-0.295	0.008	3.94	0.03	-0.443	0.006
31	3.04	2.98	0.05	-0.258	0.007	3.77	0.02	-0.410	0.003
33	2.95	3.03	0.06	-0.271	0.009	3.65	0.02	-0.388	0.003
35	3.22	3.29	0.05	-0.298	0.009	3.91	0.01	-0.390	0.002
36	2.89	2.82	0.03	-0.256	0.004	3.39	0.02	-0.362	0.003
37	3.36	3.28	0.05	-0.287	0.008	3.93	0.02	-0.405	0.003
39	2.67	2.89	0.07	-0.250	0.012	3.50	0.02	-0.376	0.003
40	1.82	2.56	0.09	-0.234	0.015	3.12	0.03	-0.355	0.004
41	1.81	2.41	0.06	-0.248	0.009	2.99	0.02	-0.364	0.003
45	1.46	3.39	0.05	-0.339	0.008	4.17	0.05	-0.525	0.009
46	3.37	2.72	0.02	-0.204	0.003	3.33	0.03	-0.357	0.004
47	3.84	4.62	0.09	-0.503	0.014	5.14	0.01	-0.549	0.002
48	2.65	2.88	0.05	-0.276	0.006	3.24	0.02	-0.332	0.003
50	2.73	4.05	0.08	-0.277	0.009	4.48	0.02	-0.357	0.003
51	1.80	3.15	0.09	-0.419	0.012	3.42	0.03	-0.494	0.005
52	3.08	2.43	0.18	-0.232	0.026	3.54	0.04	-0.509	0.007
53	2.93	3.14	0.09	-0.345	0.012	3.25	0.01	-0.336	0.002
55	3.73	3.38	0.06	-0.297	0.009	4.17	0.09	-0.516	0.015
56	2.73	2.92	0.04	-0.265	0.007	3.37	0.02	-0.368	0.003
57	2.38	3.88	0.02	-0.327	0.003	4.38	0.02	-0.384	0.003
58	4.80	5.05	0.21	-0.479	0.031	5.50	0.02	-0.544	0.003

Table 3.1

Coefficients of Linear Relationship Between Thickness and Pressure Under Steady-State and Rapid Testing

3.4.2 EXTENDED PRESSURE RANGE

The second series of thickness measurements was made over a much wider range of pressures, 0.5 to 3000 Pa. Nineteen readings were taken for each sample. The technique was again based on increasing the load with minimal delay between readings.

The results of these tests are summarised in Table 3.2 and a typical example is shown in Figure 3.2. The plot of $\log P(P+W)$ against d generally displays two linear regions. The magnitude of the slope was generally greater on the high pressure line indicating that the modulus of the fabrics were changing more rapidly in that region. There were only two exceptions to this general description of the relationship between thickness and pressure. The samples 50 and 57 displayed a reduced slope in the high pressure region as compared to the low pressure region. Both of these samples however had somewhat atypical structures. The sample 50 was a 'thermal knit' with a very uneven mass distribution. The sample 57 had a brushed surface and hence a comparatively dense mass of protruding surface fibres. The unbrushed version of the same fabric(48) conformed to the more normal type of $\log P(P+W)$ versus thickness plot which implied that the unusual nature of the 57 plot was due to its surface structure.

The value of the intersection between the high and low pressure regions of the relationship between thickness and pressure are given in Table 3.3. The values of P associated with the transition between the two regions is considerably higher than the value of 7 Pa used for the measurement of thermal insulation (BS4745). From the steady-state thickness measurements (Table 3.1) it is evident that stress relaxation does not occur to a large enough extent for a pressure of 7 Pa

I.D.	Low Pressure		High Pressure	
	a	b	a	b
2	3.646	-0.461	2.805	-0.204
3	3.537	-0.396	2.930	-0.224
4	3.639	-0.357	2.826	-0.167
5	3.798	-0.388	3.133	-0.210
6	3.797	-0.410	3.304	-0.249
7	3.743	-0.380	3.099	-0.183
8	3.767	-0.389	3.204	-0.219
9	3.595	-0.635	2.934	-0.177
10	4.130	-0.415	3.447	-0.202
11	4.368	-0.437	3.520	-0.196
12	4.325	-0.431	3.449	-0.180
13	2.758	-0.304	2.200	-0.170
14	2.961	-0.376	2.100	-0.155
17	3.503	-0.400	2.643	-0.187
19	4.683	-0.411	4.057	-0.225
20	4.037	-0.400	3.219	-0.187
21	3.866	-0.368	3.346	-0.228
22	3.337	-0.340	2.864	-0.220
23	3.685	-0.418	3.156	-0.249
25	4.101	-0.434	3.375	-0.224
26	3.733	-0.442	3.120	-0.246
27	4.269	-0.528	3.072	-0.246
28	4.247	-0.569	2.651	-0.202
30	3.941	-0.443	3.168	-0.222
31	3.766	-0.410	2.904	-0.187
33	3.646	-0.388	2.762	-0.161
35	3.905	-0.390	3.115	-0.193
36	3.386	-0.362	3.607	-0.168
37	3.931	-0.405	3.241	-0.227
39	3.496	-0.376	2.925	-0.217
40	3.120	-0.355	2.611	-0.216
45	4.167	-0.525	2.759	-0.252
46	3.328	-0.357	3.348	-0.191
47	5.135	-0.549	4.044	-0.292
48	3.238	-0.332	2.654	-0.203
49	5.063	-0.563	3.861	-0.240
52	3.541	-0.509	2.231	-0.155
51	3.422	-0.494	2.168	-0.166
53	3.250	-0.336	2.532	-0.159
54	3.305	-0.386	2.670	-0.213
60	4.684	-0.498	3.678	-0.188
55	4.165	-0.516	3.004	-0.181
56	3.971	-0.368	2.528	-0.158
57	4.380	-0.384	4.580	-0.433
58	5.504	-0.544	4.113	-0.222

Coefficients of the linear relationship between thickness and the logarithm of pressure - rapid test

Table 3.2

SAMPLE 27

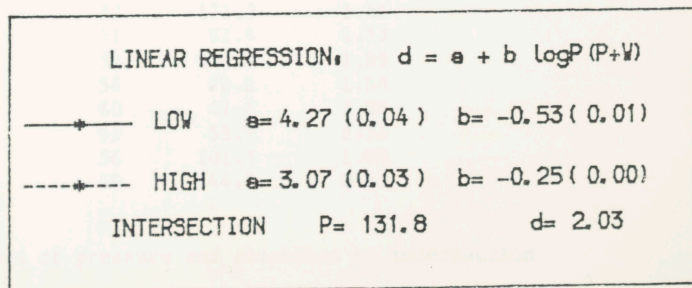
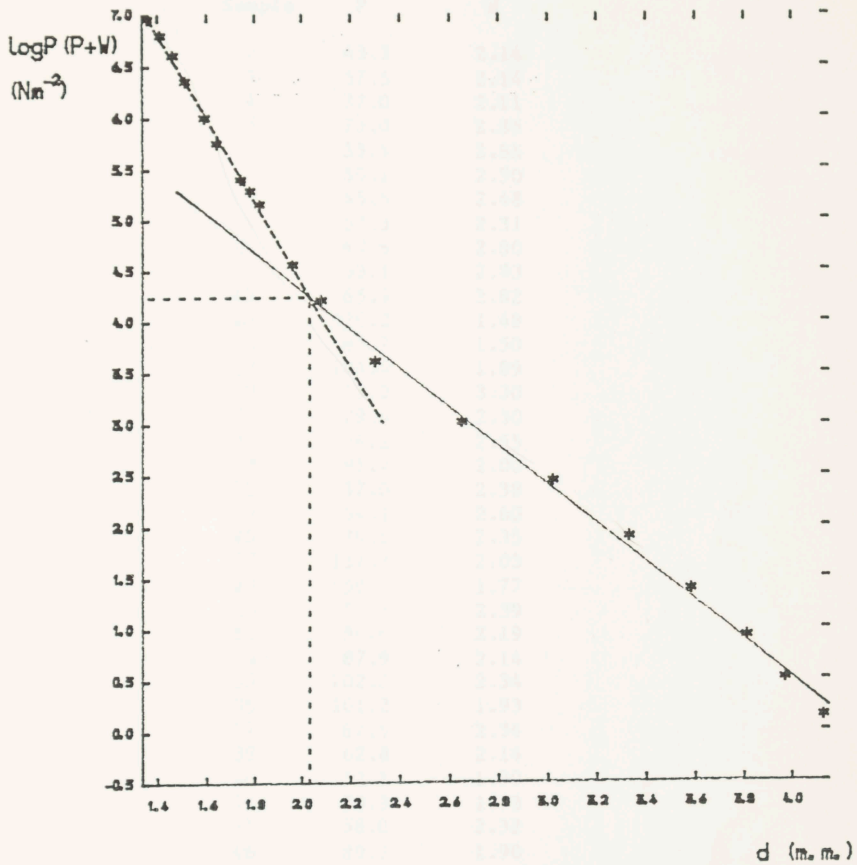


FIGURE 3.2

Sample	P	d
2	43.3	2.14
3	57.5	2.14
4	37.0	2.11
5	73.0	2.35
6	33.4	2.55
7	50.1	2.50
8	45.5	2.48
9	57.3	2.31
10	49.6	2.80
11	63.1	2.83
12	65.3	2.82
13	120.2	1.49
14	87.7	1.50
17	104.4	1.89
19	43.0	3.30
20	79.4	2.50
21	56.2	2.55
22	91.7	2.00
23	37.0	2.38
25	54.1	2.60
26	36.5	2.35
27	131.8	2.03
28	150.1	1.77
30	55.8	2.39
31	84.6	2.19
33	87.9	2.14
35	102.2	2.34
36	101.2	1.93
37	87.5	2.36
39	62.8	2.14
40	52.1	1.90
41	50.3	1.73
45	58.0	2.32
46	89.2	1.90
47	131.6	2.81
48	183.2	1.74
49	72.8	2.97
52	171.3	1.66
51	82.4	1.53
53	106.7	1.89
54	70.2	1.88
60	41.8	3.02
55	53.7	2.38
56	101.5	1.90
58	144.7	3.15

Values of pressure and thickness at intersection

Table 3.3

($\log P(P+W) = 1.82$ for $W = 2.5$ Pa) to be associated with the transition thickness. If the transition noted here can be associated with the onset of the compression of the bulk of the fabric then thermal insulation measurements made at a pressure of 7 Pa will include contributions from the air layers maintained by fibres protruding from the fabric surfaces. The thickness of such air layers according to the results here will vary between samples making the comparison of thermal resistance values unreliable.

CHAPTER 4

DRY HEAT TRANSFER THROUGH FIBROUS ASSEMBLIES.

Many different experimental and theoretical approaches have been applied to the problems of measuring and predicting the insulation properties of fibrous structures. Because of the complexity of real systems a variety of idealised fibre arrangements have been considered. The complexity is increased by the presence of the three mechanisms of heat transfer, conduction, radiation and convection. These three mechanisms will be discussed separately in the sections that follow. The formulations will then be combined and compared to a range of experimental results.

4.1 HEAT CONDUCTION

The basis of heat conduction can be expressed through Fourier's Law shown here in scalar form:

$$dE = -k \frac{\partial T}{\partial n} dA dt \quad 4.1$$

where dE represents the incremental heat flow(J), k is known as the thermal conductivity($W/m \text{ degK}$), $\frac{\partial T}{\partial n}$ is the temperature gradient(degK/m), dA is the elemental area through which the heat flows(m^2) and dt is the time interval. Expressed in terms of the heat flux $q(W/m^2)$ Fourier's Law can be rewritten as:

$$q = -k \frac{\partial T}{\partial n} \quad \text{scalar} \quad 4.2$$

$$q = -k \nabla T \quad \text{vector} \quad 4.3$$

By using the divergence theorem the net flow of heat into an elemental volume due to conduction can be shown to be:

$$Q_1 = -k \nabla^2 T \quad 4.4$$

Energy may also enter the elemental volume due to the presence of inner heat sources (e.g. electrical heater element). Let the energy released by such sources be given by $Q_2 = q_v (\text{W/m}^3)$. Since energy must be conserved these two sources of heat must lead to a storage of energy within the volume under consideration. This stored energy can be expressed in terms of the temperature, specific heat, C , and density, ρ , using the relationship:

$$Q_3 = C \rho \frac{\partial T}{\partial t} = Q_1 + Q_2 \quad 4.5$$

$$\text{or} \quad C \rho \frac{\partial T}{\partial t} = k \nabla^2 T + q_v \quad 4.6$$

The most commonly used form of the differential equation of heat conduction is given by:

$$\frac{\partial T}{\partial t} = a \nabla^2 T + \frac{q_v}{C\rho} \quad 4.7$$

$$\text{where } a = k/C\rho \quad 4.8$$

The quantity $a (\text{m}^2/\text{s})$ introduced in EQ.4.7 is known as the thermal diffusivity.

In the absence of inner heat sources or sinks ($q_v=0$) and under steady-state conditions ($\partial T/\partial t=0$) the heat equation reduces to:

$$\nabla^2 T = 0 \quad 4.9$$

which is known as Laplace's equation. It is this equation, or some version of it, that forms the mathematical basis of any discussion of heat transfer by conduction. The operator ∇^2 is commonly referred to as the Laplacian and can be written in a variety of forms dependent on the co-ordinate system in use:

$$\nabla^2 = \frac{\partial^2}{\partial x^2} + \frac{\partial^2}{\partial y^2} + \frac{\partial^2}{\partial z^2} \quad (\text{Cartesian}) \quad 4.10$$

The simplest case encountered in the study of heat transfer by conduction is that of steady-state, one dimensional heat flow in a uniform medium. Consider an isotropic, homogeneous and infinite sheet of material the two surfaces of which are maintained at temperatures T_1 and T_2 . If the x direction is taken as being parallel to the temperature gradient (i.e. perpendicular to the sheet surface) then Laplace's equation in Cartesian co-ordinates becomes:

$$\frac{d^2 T}{dx^2} = 0 \quad 4.11$$

By integrating this formula and applying the boundary conditions the temperature distribution and heat flux can readily be found.

$$\begin{aligned} \text{Boundary conditions at } x = 0 & \quad T = T_1 \\ & \quad x = d \quad T = T_2 \end{aligned}$$

$$T(x) = T_1 - \frac{(T_1 - T_2)x}{d} \quad 4.12$$

Estimation of heat transfer by conduction is dependent on an estimation of the effective value of the thermal conductivity. This value can be found experimentally or by calculation from the known conductivities and spatial distribution of the components of the system under consideration.

4.1.1 CONDUCTION OF HEAT IN FIBROUS MATERIALS.

The conduction of heat in a fibrous material presents a much more complex problem than the simple example already considered. A great variety of approaches have been employed in the development of theoretical models to explain or predict the diversity of experimental results. Several of these models are based on considerations of thermal conduction as the sole mode of energy exchange, and therefore form a useful starting point for a physical description of the heat transfer process.

The study of conductivity in fabrics effectively commenced with the work of Schumeister in 1877(34). He proposed that the conductivity of a mixture of fibres can be estimated by the relationship:

$$k = \frac{1}{3} (k_a v_a + k_f v_f) + \frac{2}{3} \left(\frac{k_a k_f}{k_a v_f + k_f v_a} \right) \quad 4.13$$

where k_a, v_a and k_f, v_f are the conductivity and volume fraction of the air and the fibre respectively. The choice

of the coefficients is based on an assumed random distribution of fibres whereby 1/3 of the fibres and air are parallel to the flow of heat and 2/3 are perpendicular to that flow.

An alternative solution was proposed by Lees in 1900(35). This model insulator is formed from infinitely long prisms of square cross-section. If the conductivities of the two components are again denoted by k_a and k_f then the resultant system conductivity is given by:

$$k = (k_a k_f)^{0.5} \quad 4.14$$

Lees extended this model to allow for different volume ratios of the two components to give:

$$k = k_a^v k_f^{(1-v)} \quad 4.15$$

The formulations of both Lees and Schumeister were used by Baxter(36) in analysing the results of his experimental work. Both relationships were found to compare reasonably well to the data. Baxter suggested that, from the known conductivity of horn keratin and the measured conductivities of his wool fabrics, the best fit could be achieved by changing the coefficients of Schumeister's formula to 0.29 and 0.71.

This equation was then used to calculate the values of fibre conductivity for other fibre types from the measured fabric conductivities and packing densities. The apparently high thermal conductivities measured for fabrics of low density were attributed by Baxter to convection.

A more rigorous three-dimensional approach to the conduction of heat through a fabric-air mixture has been carried out by Drummond(37). Using a fabric model where the fibres are regarded as three sets of parallel cylinders, the heat equation can be solved. The resultant equation for the conductivity of this model system was very complex, involving Bessle functions in a series solution. This model can be extended to include the case where the fibre distribution is not isotropic.

The formulations which have been described so far discuss the overall conduction through fibrous assemblies. Other workers have preferred to consider the conduction along the solid paths and through the surrounding air separately.

Many difficulties are encountered in attempting to derive an exact analytical solution to the problem of conduction in a random fibre arrangement. For this reason most derivations rely on the assumption of an orderly arrangement of fibres. One such model was used by Strong(38) to estimate the contribution of conduction through the fibres. The fibres are regarded as all having the same diameter and forming a symmetrical lattice. The intersection points are regarded as forming circular contact areas. Using this model it can be shown that the total rate of heat flow, Q , per square centimeter area of the fibre lattice for a temperature difference of T across each contact unit is given by:

$$Q = \frac{4 \pi r^2 k n \Delta T}{r \ln(4 r / \Delta r) + 2 l} \quad 4.16$$

where n is the number of fibre intersections per square centimeter.

The quantity Δr represents the compression of the radius corresponding to the pressure flattening at the area of contact and is equal to the area of contact divided by πr . Calculated values of the fibre contribution were compared to experimental results. It was found that as the fibre diameter increased, the difference between the measured and calculated values diverged. This was assumed to indicate that the model used gave too many fibre contacts compared to the real situation.

Heat conduction through the gaseous component of a fibrous insulation can be approached using the kinetic theory of gases. According to the kinetic theory the probability that a molecule, after one collision, will collide with another molecule of gas before moving a distance x is given by:

$$P_g = 1 - \exp(-x/l_g) \quad 4.17$$

where l_g is known as the mean free path of the gas. Similarly the probability that a molecule after one collision will collide with a fibre before moving a distance x is given by:

$$P_f = 1 - \exp(-x/l_f) \quad 4.18$$

In this case l_f is the mean free path for a molecule-fibre collision.

Verschoor and Greebler(39) suggested that, for the purposes of this type of calculation, the fibres in an insulator can be regarded as forming into planes. These planes are parallel to one another and perpendicular to the temperature gradient. The fibres are all

of the same diameter, d , and occupy a volume fraction denoted by v_f . If an incremental thickness Δx of such an insulator is considered then the volume of fibre per unit area it contains will be given by $v_f \Delta x$. Dividing this total fibre volume by the cross-sectional area of a fibre yields the length of fibre within the volume element. The total projected fibre area is given by the product of the total fibre length and the fibre diameter:

$$A = \frac{4 v_f \Delta x}{\pi d} \quad 4.19$$

This represents the fibre collision cross-section per unit area of the insulator as seen by the gas molecules. As such it can be equated to the probability of a gas molecule having a collision with a fibre before moving a distance x . The two probability formulations may be equated to give:

$$\frac{4 v_f \Delta x}{\pi d} = 1 - \exp(-x/l_f) \quad 4.20$$

By changing x to Δx and using only the first order terms of a power series expansion of the exponential the following, more useful equation results:

$$l_f = \frac{\pi d}{4 v_f} \quad 4.21$$

The effective mean free path in a fibrous insulator allows for both types of collision and can be shown to be closely approximated by:

$$l = \frac{l_g l_f}{l_g + l_f} \quad 4.22$$

Through the kinetic theory of gases it is known that the conductivity of a gas is proportional to the mean free path of its molecules. Assuming that this relationship holds for the model system the conductivity of the gaseous component of the gas-fibre mixture can be expressed as:

$$k_{g,m} = k_g \left(\frac{l_f}{l_g + l_f} \right) \quad 4.23$$

The value for l_f has already been calculated and the value for k_g is effectively dependent only on the molecular species present and the temperature (that is, independent of pressure). Values for l_g are found to be proportional to temperature and inversely proportional to the pressure of the gas. For the purpose of this work l_g can be taken as dependent on pressure only since temperature variations are only small and their effect negligible. Similarly, the temperature dependence of l_g (l_g proportional to $T^{0.7}$) can be ignored at present. These relationships are shown in the following properties of air at standard atmospheric conditions.

$$l_g = \frac{6.72 \times 10^{-3}}{p} \quad 4.24$$

$$k_g = 2.53 \times 10^{-2} \quad 4.25$$

These values when substituted into Eq.4.23 give:

$$k_{g,m} = \frac{0.020 P d/v_f}{6.72 \times 10^{-3} + 0.79 P d/v_f} \quad 4.26$$

With a gas pressure near atmospheric and fibres of about 10micron diameter, the value of Pd is far greater than 6.72×10^{-3} and $k_{g,m}$ is therefore approximately equal to 0.025 W/m degK . It requires very large changes in fibre diameter or pressure to cause any appreciable change in the conductivity of the gas within the insulator.

4.2 RADIATION

The normal starting point for any discussion of radiant energy exchange is Planck's Law for spectral emissive power:

$$E_\lambda = \frac{2 \pi^5 c_1}{15 \lambda^5} \left(\exp \left(c_2 / \lambda T \right) - 1 \right)^{-1} \quad 4.27$$

where λ = wavelength (m)

c_1 = Planck's first constant ($5.944 \times 10^{-17} \text{ Wm}^2$)

c_2 = Planck's second constant ($1.4388 \times 10^{-2} \text{ m degK}$)

T = temperature (degK)

Planck's Law was formulated theoretically for a black body emitter, that is, a non-selective emitter. For non-black bodies it is necessary to obtain the wavelength dependence experimentally. The overall emissive power E_0 can be found by integrating Planck's equation E_λ over λ and is known as the Stefan Boltzmann Law:

$$E = \sigma T^4 \quad (\text{W/m}^2) \quad 4.28$$

where σ is the Boltzmann constant ($5.6687 \times 10^{-8} \text{ W/m}^2 \text{ degK}^4$). This Law can also be extended to the case of grey body radiation to give:

$$E = \epsilon \sigma T^4 \quad (\text{W/m}^2) \quad 4.29$$

where ϵ is the emissivity of the body ($=E/E_0$). A further feature of black or grey bodies is that the absorptivity and the emissivity must be equal.

The simplest case of radiative transfer is that between two infinite parallel surfaces separated by a non-participating medium. The energy leaving either surface $E_{L,1}$ is given by the sum of its own energy emission and the amount of power coming from the other surface which it reflects (that is, does not absorb) as follows:

$$E_{L,1} = E_1 + (1 - \epsilon_1) E_{L,2} \quad 4.30$$

$$E_{L,2} = E_2 + (1 - \epsilon_2) E_{L,1} \quad 4.31$$

These equations can be solved readily for $E_{L,1}$ and $E_{L,2}$ and the difference between these two quantities is a measure of the radiant exchange:

$$q = \epsilon_2 \frac{E_1 - \epsilon_1 E_2}{\epsilon_1 + \epsilon_2 - \epsilon_1 \epsilon_2} \quad (\text{W/m}^2) \quad 4.32$$

In the case where $\epsilon_1 = \epsilon_2 = \epsilon$ and using Eq.4.29 for the emissive power, the result is:

$$q = \frac{\sigma}{2/\epsilon - 1} (T_1^4 - T_2^4) \quad (\text{W/m}^2) \quad 4.33$$

The temperature difference term can be expanded as follows:

$$T_1^4 - T_2^4 = (T_1^2 + T_2^2)(T_1 + T_2)(T_1 - T_2) \quad 4.34$$

If the difference between the two temperatures is small compared to their average value then the approximation shown below can be applied:

$$T_1^4 - T_2^4 = (T_1 - T_2) 4T_m^3 \quad 4.35$$

where:

$$T_m = (T_1 + T_2)/2 \quad 4.36$$

Substitution into Equation 4.33 gives a simplified version of the equation for heat flux due to radiation exchange:

$$q = \frac{4\sigma}{(2/\epsilon - 1)} T_m^3 (T_1 - T_2) \quad 4.37$$

4.2.1 RADIANT EXCHANGE WITHIN FIBROUS MATERIALS.

It is now useful to consider the radiation exchange between the two surfaces when a fibrous assembly is placed between them. To analyse the contributions of individual fibres would require an exact knowledge of their distribution throughout the system. Since this information is not normally available, it is necessary to produce a model of the insulator.

One such model was proposed by Verschoor and Grebler(39). They proposed that the fibres within the insulator be considered as a series of parallel plates, arranged perpendicularly to the flow of heat. Each plane absorbs a fraction of the incident radiant energy, denoted by a . If the middle plate is considered then the radiant energy arriving from all plates nearer to the heated surface will be given by:

$$q = \frac{4 \sigma T_m^3 L_f \Delta T}{d a^2} \quad 4.38$$

where total thickness is, d , the fibre plate separation, L_f and the total temperature drop, ΔT .

An alternative approach to the problems of estimating the radiative transfer through fibrous assemblies has been employed by Strong(38). This approach is analogous to the kinetic theory based examination previously described for gaseous conduction.

The resultant formulation is given by Eq.4.39, for the effective conductivity due to radiation:

$$k_r = H \pi R \sigma T_m^3 / v_f A \quad 4.39$$

where H is a factor determined by the fibre orientations, such that $H=2.67$ for a random three dimensional distribution and $H=3.24$ for fibres randomly oriented within planes lying perpendicular to the temperature gradient. Strong and his colleagues compared this formulation with that obtained by regarding the radiation transfer as the diffusion of photons to give the result:

$$k_r = \frac{16}{3} \pi \sigma T_m^3 \quad 4.40$$

If these two equations are compared for the three dimensional random arrangement, the resultant expression for the mean free path, l , is given by:

$$l = \pi R / 2 \epsilon v_f \quad 4.41$$

which is the same as Equation 4.21, with the addition of the emissivity term.

4.3 CONVECTION

4.3.1 PROPERTIES OF FLUIDS.

An understanding of the transfer of heat by convection requires that the physical significance of various fluid properties be understood. The conductivity, k , and the specific heat, C , have already been described. Of particular importance to convection are the properties relating to changes in density and the influence of forces.

For the purposes of this work it is best to concentrate on convection within gases. In order to simplify any analysis, it is generally assumed that the physical properties of the gas involved are constant within the investigated temperature range (except for density).

The viscosity of a gas relates the tangential force to the velocity gradient as follows:

$$s = \mu \frac{dw}{dn} \quad 4.42$$

where s is the tangential force, dw/dn is the velocity gradient and μ is the viscosity. For present applications μ for a given gas can be expressed as a function of temperature alone. Frequently, the term μ/ρ appears in calculations and this ratio is known as the kinematic viscosity and is denoted here by ν .

Of obvious importance is the coefficient of thermal expansion of a gas. This can be expressed as:

$$\beta = -\frac{1}{\rho} \left(\frac{\partial \rho}{\partial T} \right) \quad 4.43$$

From the relationships for the ideal gas it can be shown to be equal to the reciprocal of the absolute temperature.

$$\beta = 1/T \quad 4.44$$

It is this temperature dependence of density that produces the necessary force distribution to give free convection.

Frequently, the large number of variables involved in calculations of heat transfer by convection can be grouped together into relatively few dimensionless numbers. Provided these dimensionless numbers are used only over appropriate ranges of conditions, they provide a simple approach to the solution of some complex systems.

Four dimensionless numbers are of particular relevance to convection. They are the Nusselt number Nu , the Reynolds number Re , the Grashof number Gr , and the Prandtl number Pr . Expressed in terms of the physical properties of the gas and the system dimensions, they are:

$$Nu \equiv H l / k \theta \quad 4.45$$

$$Re \equiv w l / \nu \quad 4.46$$

$$Gr \equiv g \beta l^3 \theta / \nu^2 \quad 4.47$$

$$Pr \equiv \nu/a$$

4.48

where H = heat transfer coefficient

l = characteristic dimension

θ = temperature drop

a = thermal diffusivity

In order to use these quantities appropriately it is useful to understand their physical significance. The Nusselt number represents the ratio of the heat flow by convection to the heat flow by conduction in the gas at rest. The Reynolds number characterises the ratio of the inertial and the viscous forces. As such the Reynolds number determines the pattern of fluid flow around or over the solid body placed in the path of the stream of fluid. The Grashof number characterises the buoyancy force appearing in the fluid due to density differences. It is the ratio of the buoyancy force $\beta g \theta l$ to the viscous drag force $\mu v/l$, where v is taken as being proportional to μ/l .

These products of dimensional analyses have been extensively used for a variety of heat exchange situations. The relationships that exist between the different groups have been experimentally determined and must be applied within the limitations of the available experimental information.

4.3.2 CONVECTION FROM FABRIC SURFACES.

Convective heat transfer is due to the bulk motion of fluid. It is the energy content of the moving fluid which constitutes the heat transfer. This process is invariably complex with many properties of both the solid interfaces and the fluid being involved. Convective transfer falls into two categories - free convection and forced convection.

Free convection is the result of density variations and hence buoyancy effects within the fluid. Such variations in density can be caused by temperature differences between regions of the fluid or by differing concentrations of molecular species. Forced convection as the name implies, is due to externally induced fluid flow. This can be in the form of a fan pushing air past a surface or a pump circulating coolant. Clearly, while both of these forms of heat transfer depend on the rate of movement of the fluid, they are governed by a different set of relationships. For this reason they will be discussed separately.

Free convection originates due to the non-uniform distribution of mass forces within a fluid. Throughout the range of insulation systems and environments considered here, these mass forces are due to the effect of gravity on the density distribution within the gas.

Both theory and experiment show that, unless Pr is very small, only the product $GrPr$ is needed to predict free convective transfer for situations where the fluid currents are slow enough that inertial stresses are small compared with the viscous forces. In other words, provided that conditions of laminar flow are maintained, the

relationship between the Nusselt, Grashof and Prandtl numbers can be expressed as(40):

$$\text{Nu} = c (\text{Gr Pr})^{0.25} \quad 4.49$$

The values of the coefficient c will be determined by certain system parameters. When the value of GrPr becomes large the inertial forces become significant and turbulent flow results. In such systems the group relationship becomes:

$$\text{Nu} = c (\text{Gr Pr})^{0.33} \quad 4.50$$

The transfer of heat by convection within a fibre assembly can be described in terms of an effective layer separation. If the formulation for a horizontal layer of thickness d is considered then:

$$k/k_a = 1 \quad \text{Gr Pr} < 10^3 \quad 4.51$$

$$= 0.105 (\text{Gr Pr})^{0.3} \quad \text{for } 10^3 < \text{Gr Pr} < 10^6 \quad 4.52$$

$$= 0.40 (\text{Gr Pr})^{0.2} \quad \text{for } \text{Gr Pr} > 10^6 \quad 4.53$$

The value of GrPr for air at 30 deg C is given by $\theta d^3 10^9$. If, for example, θ is of the order of 10 degC then d must be greater than 5mm before convective transfer will begin. A plot of the product GrPr is shown in Figure.4.1. The line $\text{GrPr}=10^3$ indicates the onset of convection. For all combinations of θ and d below this line convection will be insignificant.

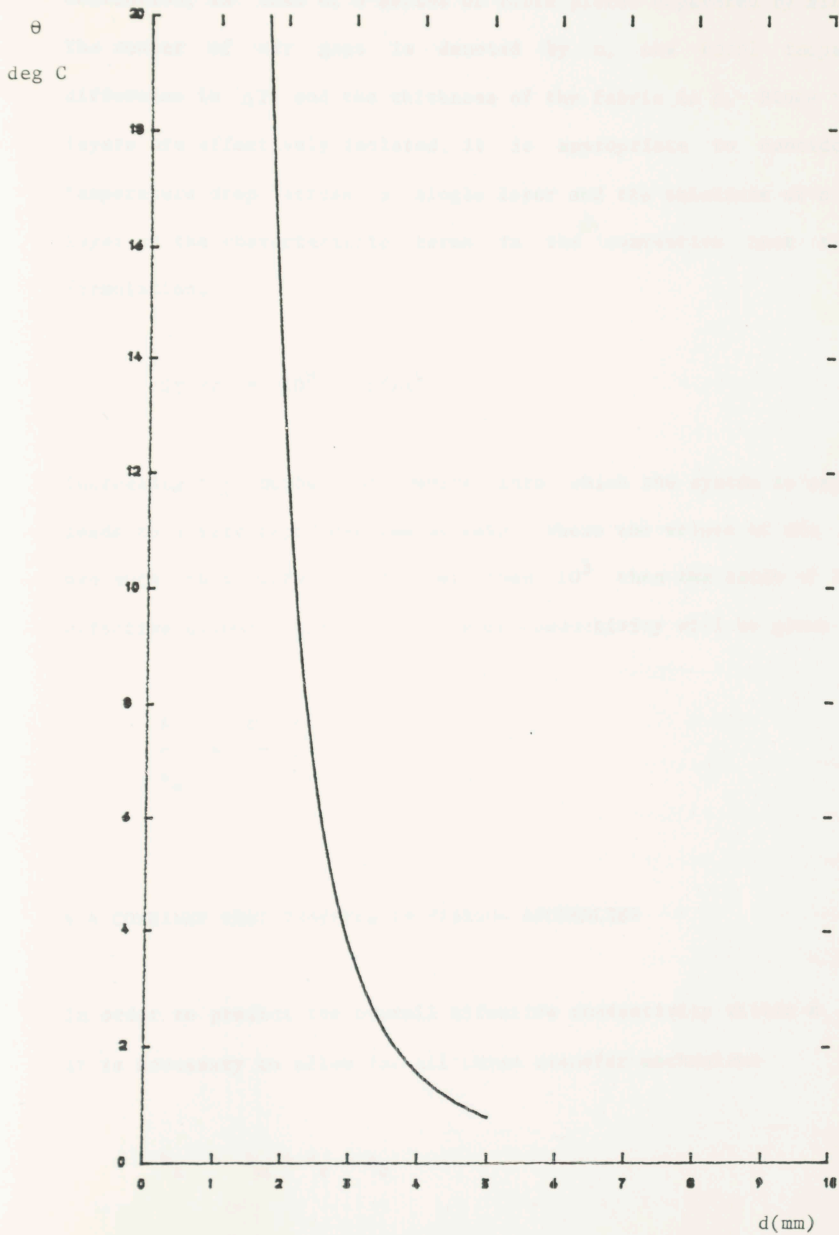


FIGURE 4.1

Values of Temperature Difference and Thickness at the onset of Convection

The simplest model that can be used for a fabric in the context of convention, is that of a series of fibre plates separated by air gaps. The number of air gaps is denoted by n , the total temperature difference is ΔT , and the thickness of the fabric is d . Since the air layers are effectively isolated, it is appropriate to consider the temperature drop across a single layer and the thickness of a single layer as the characteristic terms in the convective heat transfer formulations.

$$\text{Gr Pr} = 10^9 T d^3/n^4 \quad 4.54$$

Increasing the number of layers into which the system is separated leads to a very rapid decline in GrPr . Where the values of d/n and θ are such that GrPr is greater than 10^3 then the ratio of the effective conductivity to the gaseous conductivity will be given by:

$$\frac{k}{k_a} = \frac{c (\text{Gr Pr})^{0.25}}{n} \quad 4.55$$

4.4 COMBINED HEAT TRANSFER IN FIBROUS ASSEMBLIES

In order to predict the overall effective conductivity within a fabric it is necessary to allow for all three transfer mechanisms

$$k_t = k_m + k_r + k_c \quad 4.56$$

The contribution made by the conduction, k_m , can best be estimated from the formulae of Schumeister/Baxter or Drummond. If k_m is plotted against v_f for a range of fibre conductivities, the result is

as shown in Figure.4.2. From these graphs it is possible to evaluate the conduction of heat from the known fibre volume fraction and fibre conductivity. Knowledge of the fabric thickness allows the the thermal resistance to be calculated.

A comparison between the two formulations for thermal conductivity is shown in Figure.4.3. The difference between them is insignificant compared to the errors in most experiments.

The effective conductivity due to radiation can be approached from the equation of Strong(38). This formulation requires knowledge of the fibre diameter and emissivity as well as the fractional volume occupied by the fibres. The radiation loss is proportional to the fibre diameter and inversely proportional to the volume fraction

By way of confirmation of this result experimentally obtained values for effective conductivity were plotted against air pressure(38). When the pressure was extremely low the gaseous conduction and convection could be ignored. Similarly, because the structures concerned were very open the fibre conduction was low. This implied that at very low pressure, most of the effective conductivity was due to radiation. The predicted radiation values were compared to the overall effective conductivity values and were shown to agree well at the lowest pressures.

The final contribution to the total heat flow comes in the form of convection. As has already been indicated the onset of convection occurs when $GrPr$ becomes greater than 10^3 . Beyond this value the convective loss is determined from Eq.4.52. Where the system can be visualised as a number of layers this becomes:

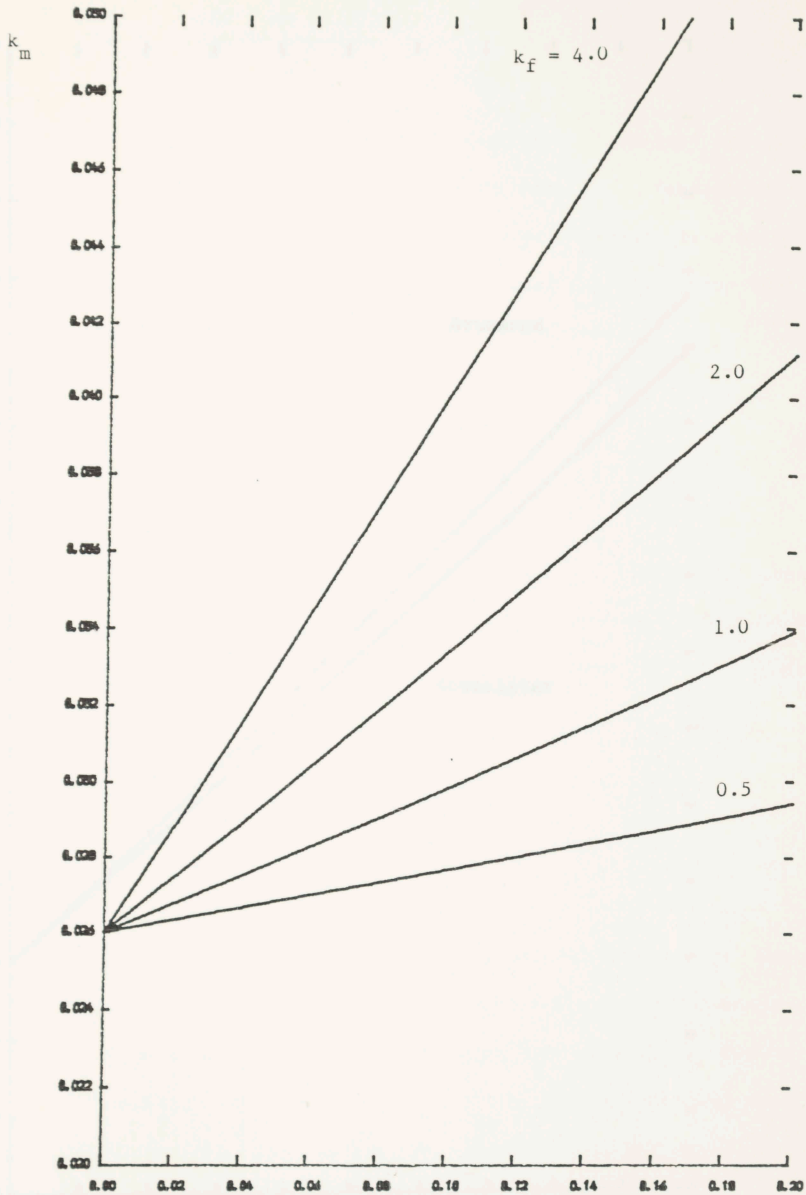


FIGURE 4.2

Fabric Conductivity as a Function of Fibre Volume Fraction
for Different Values of Fibre Conductivity

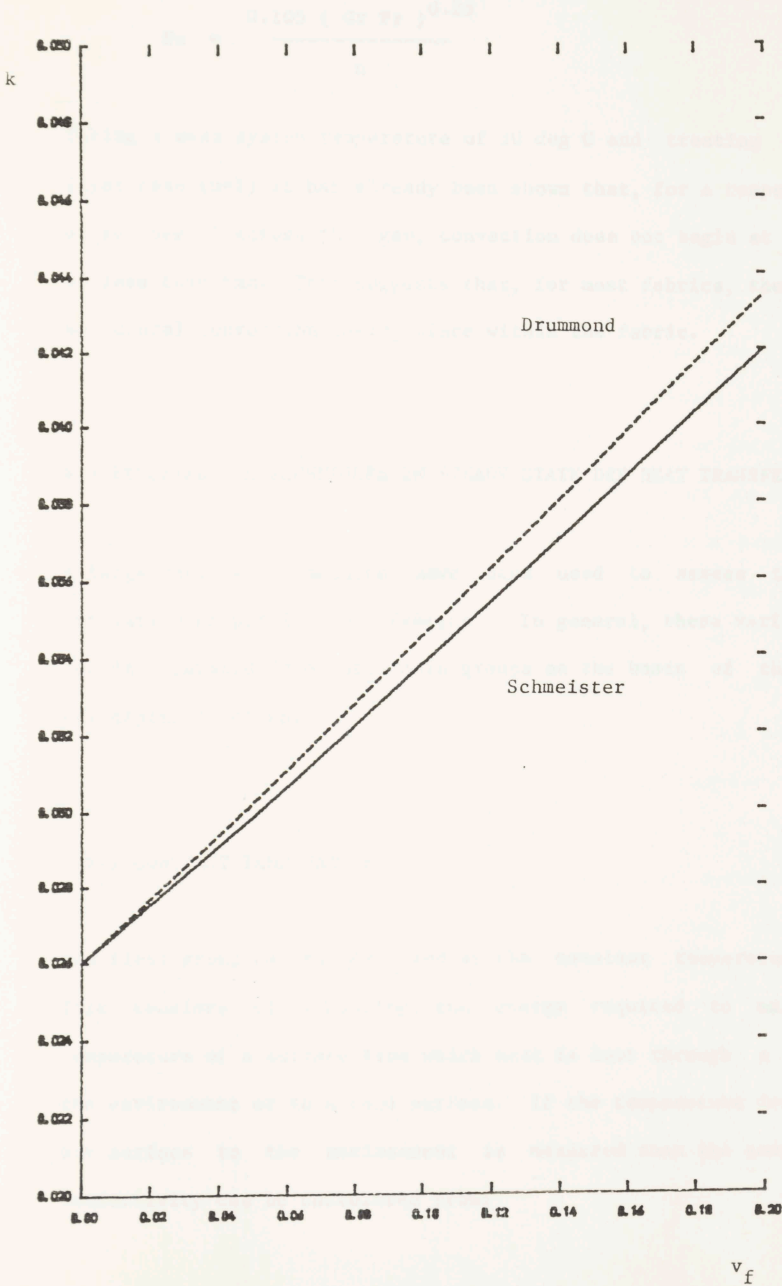


FIGURE 4.3

Fabric Conductivity as a Function of Fibre Volume Fraction
Derived Theoretically

$$\text{Nu} = \frac{0.105 (\text{Gr Pr})^{0.25}}{n} \quad 4.57$$

Taking a mean system temperature of 30 deg C and treating the single layer case ($n=1$) it has already been shown that, for a temperature drop of 10 deg C across that gap, convection does not begin at a thickness of less than 5mm. This suggests that, for most fabrics, there will be no natural convection taking place within the fabric.

4.5 EXPERIMENTAL TECHNIQUES IN STEADY STATE DRY HEAT TRANSFER

A large variety of methods have been used to assess the thermal insulation properties of fabrics. In general, these various methods can be separated into three main groups on the basis of the physical principles involved.

4.5.1 CONSTANT TEMPERATURE

The first group can be described as the constant temperature method. This consists of measuring the energy required to maintain the temperature of a surface from which heat is lost through a fabric to the environment or to a cold surface. If the temperature drop from the hot surface to the environment is measured then the sample thermal conductivity can be calculated from:

$$k = \frac{q d}{\Delta T} \quad 4.58$$

If the thickness is not known then the thermal resistance is usually quoted:

$$R = \frac{\Delta T}{q} \quad 4.59$$

Guarded hot-plate systems are a good example of this type of measurement system. The device, already described in this work, for the simultaneous measurement of heat and vapour flow, falls into this category. For absolute measurements the most important feature is that all of the heat lost by the measuring area must pass through the sample. Also it is desirable that edge effects should not encroach on the part of the sample in contact with the measurement section. These requirements are necessary to ensure that the whole of the measurement area is supplying the same heat flux. If they are fulfilled then calculations can be carried out according to Eqs.4.58 and 4.59 depending on whether or not a cold plate is used. Such simplicity of interpretation of data is a valuable asset of this approach.

Guarded hot-plates have been used with considerable success both for conventional textile products and in a wide variety of engineering applications. Though the physical appearance of the various systems differs greatly, the underlying principles are always the same.

4.5.2 RATE OF COOLING AND RATE OF HEATING

As the name suggests this method is based on the measurement of the rate of change of temperature of a calibrated mass surrounded by the insulator being tested. Although it is not a true steady state test, the rate of change of temperature is usually so slow that any deviation from a steady state result can be ignored.

Knowing the specific heat, temperature, area and mass of the cooling object, the following approximate relationship for its stored energy is used:

$$q = \frac{dE}{A dt} = \frac{M C}{A} \left(\frac{dT}{dt} \right) \quad 4.60$$

This can be equated to the Equation 4.58, to give:

$$k = - \frac{M C d}{A (T - T_a)} \left(\frac{dT}{dt} \right) \quad 4.61$$

If both the temperature and the rate of change of temperature are measured at some time, and the ambient temperature T_a and properties of the heated block are known, then an estimate of k can be made.

The equation Eq.4.61 can now be integrated to give:

$$\Delta T = \Delta T_0 \exp (- t k A / M C d) \quad 4.62$$

This formula can be applied by measuring the time taken for the temperature difference to drop to $1/e$ of a starting value (T_0).

This time will then equal the relaxation time of the system or:

$$t = M C d/A k \quad 4.63$$

and hence k is given by:

$$k = M C d/A t \quad 4.64$$

This particular fraction is merely the most convenient in terms of the time dependence of the temperature: any value could be used.

4.5.3 THERMAL RESISTANCE REFERENCES

A heat flow transducer functions as a thermal resistance reference. If such a transducer is placed in a heat flux then a temperature difference proportional to the heat flux will be produced between its faces. This temperature difference or some electrical equivalent of it will appear as the output. In terms of the heat flow equation:

$$\Delta T = q/k_{\text{ref}} \quad 4.65$$

These transducers can be very small and are hence very useful in measuring the heat flow within clothing in use. Of course, by the nature of the transducer it will, used in this manner, interfere with heat flow pattern and cause an error in the reading. This problem can be minimised by careful choice of transducer and is often outweighed by the advantages stemming from its convenience.

The so called Tog-meter is similarly based on the use of a sheet reference material of known thermal resistance. In this case, however,

the reference is used in series with a sample. Assuming that the heat flowing through both the reference and the sample is the same, then the ratio of their thermal resistances will equal the ratio of their temperature drops:

$$\frac{R}{R_{\text{ref}}} = \frac{\Delta T}{\Delta T_{\text{ref}}} \quad 4.66$$

This technique will be described more fully later, where the apparatus used for some of the dry heat transfer testing will be described.

4.6 EXPERIMENTAL

Several different approaches have been used in the investigation of the flow of heat through fabrics under the influence of a temperature gradient. These various experimental techniques have already been discussed. For the purposes of this work two methods were considered most applicable. The first is based on the guarded-hot plate instrument, the construction of which was described in Chapter 2. The second makes use of the thermal resistance comparison approach of the so called Tog-meter.

The Tog-meter has been used in a variety of forms and one of these forms is regarded as the standard (BS4745) method for assessing the thermal insulation of fabrics.

This type of instrument has three basic requirements for successful operation:

1. The availability of a reference material with precisely known thermal resistance;
2. The establishment of the same steady heat flux through both the reference and test sample;
3. A provision for the measurement of the temperature drop across the reference and across the sample.

In general for a one dimensional heat flow situation the heat flux q is given the relationship:

$$q = - \Delta T / R \quad 4.67$$

where q is the heat flux, R is the thermal resistance and T is the temperature drop. The minus sign indicates that the heat flow is in the opposite direction to the temperature gradient for a positive value of thermal resistance. Given that, in the Togmeter, the quantity q is the same for both the reference material and the sample then:

$$R_s \Delta T_{ref} = R_{ref} \Delta T_s \quad 4.68$$

where the subscript, s , refers to the sample and the subscript, ref , refers to the material. The temperature drops are measured by the reference instrument and assuming the thermal resistance of the reference material is known, then the sample thermal resistance can be found using:

$$R_s = R_{ref} \Delta T_s / \Delta T_{ref} \quad 4.69$$

4.6.1 DESCRIPTION OF THE APPARATUS

A complete description of the instrument can be found in other sources(41). Only a brief indication of its features will be given here.

The temperature gradient is established through the action of a heated plate. Its supply of heat comes from two circular elements which are mounted in an aluminium frame and clamped to the base of the plate. Insulation is provided to give a more uniform temperature distribution over the layer of reference material. In this equipment a 1.3cm thick sheet of marianite was used as the reference. The cold plate consists of a layer of Tufnol which is fixed to a Dural disc of the same size. When the sample is placed between the Tufnol and the marianite its thickness can be set using three micrometers and if desired a pressure applied using three knurled nuts. Temperature measurements are made using thermocouples embedded in both faces of the marianite and in the Tufnol. These thermocouples are all near the centre of the apparatus where the heat flux will be uniform. Only three thermocouples are required because the sample and reference are in contact which means that the thermocouple in the top face for the marianite is also monitoring the temperature of the lower surface of the fabric, that is:

$$R_s = R_{ref} \left(\frac{T_3 - T_2}{T_2 - T_1} \right) \quad 4.70$$

where T_3 is the temperature of the lower face of the marianite, T_2 is the temperature of the marianite-sample interface and T_1 is the temperature of the upper fabric surface. This whole system is supported by a frame and can be pivoted and locked at any angle.

4.6.2 TEMPERATURE CONTROL

As originally built the temperature of the hot-plate was controlled through a thermocouple mounted on its base. This thermocouple was used as the sensor for an on/off controller with mains voltage being fed to the heater. This arrangement led to temperature oscillations which in turn produced variations in the heat flow through the system. Such variations of course invalidate Eq.4.66 and caused difficulties in interpretation of the results. This system also had the disadvantage that the effective "skin" temperature (that is, the temperature of the interface between the reference and the sample) was not the same for all samples. For a given hot-plate temperature setting the temperature at this point is dependent on the fabric thermal resistance. Therefore, samples with different properties were being exposed to different test conditions. Any attempt to control this "skin" temperature with the original circuitry would have resulted in even more severe temperature oscillations and the system would have become quite unworkable.

In order to remedy this situation a completely new control system was constructed for the testing reported here. This controller operated at a considerably lower heater supply voltage and exhibited a proportional temperature response. It was used in such a way that the middle thermocouple was maintained at the same temperature thus giving the constant "skin" temperature desired.

The design was based on a commonly used proportional control configuration but, with greatly improved sensitivity due to the temperature feedback arrangement. This high sensitivity was accompanied by the use of a reduced heater supply voltage and gave

the desired temperature stability.

A commutating auto-zero operating amplifier was used to amplify the signal from the appropriate thermocouple. This type of amplifier was chosen because of its extremely low drift and offset which are so important in any small signal amplification. The output was fed to a differential amplifier along with the voltage equivalent of the desired temperature setting. This setting was derived from a panel mounted multiturn potentiometer. The differential amplifier output was thus proportional to the difference between the temperature measured by the thermocouple and that set by the operator. The gain of the differential amplifier was set by a variable resistor and served as a sensitivity control. An integrated circuit zero voltage switch was used to compare the temperature difference signal to an internally generated sawtooth waveform. When the edge of the sawtooth crossed the temperature difference signal, the triac was turned off. The triac properties and timing are such that the switching always occurred at the zero voltage point of the sinusoidal voltage controlled by the triac and thence fed to the heater. This had the effect of minimising electrical noise which could interfere with other circuitry. The period of the sawtooth in turn set the period of the energy supplied. With the values chosen the period was three seconds. The time constant of the Tog-meter was much larger than this value; a necessary prerequisite for temperature stability. The transformer used to drive the heaters was chosen so that the output duty-cycle would be around fifty percent for most of the testing envisaged. This feature optimised the stability and allowed high levels of temperature sensitivity to be used.

4.7 THERMAL INSULATION RESULTS

4.7.1 TOG-METER

Thermal insulation measurements were carried out on a range of knitted fabrics. Both the tog-meter and the guarded plate were used. For each sample the tog-meter was set to a series of different plate separations. The largest plate separation being considerably greater than the thickness of the fabric as measured at the lowest pressures in the previous chapter. The smallest plate separations led to considerable compression of the sample fabrics taking the fabric thickness well below the value associated with the onset of compression of the bulk of the fabric. The guarded hot-plate measurements were carried out with the fabric samples open to the atmosphere.

The Tog-meter tests were divided into two groups. For the first group readings were taken using 0.2mm steps in the plate separation while for the other group 0.5mm steps were used.

Clearly the first group of tests generated far more information about the thermal resistance properties of the fabrics. However, the time involved in achieving this detail was prohibitive and would have limited the range of samples to be tested. From this group the form of the thermal resistance versus plate separation relationship could be seen and a model proposed. This model could in turn be applied to the results of the second group of tests and its applicability for a wide range of fabrics was assessed.

A typical plot of thermal insulation(degCm^2/W) versus thickness is shown in Fig.4.4. The line of best fit is based on a least mean squares regression assuming that the line should pass through the origin. From this plot it is clear that the results do not conform to a linear relationship. The measured values appear to form two regions, both of which show marked curvature.

The presence of the two regions and the sharpness of the intersection suggest an abrupt change in the influence of the changing thickness. Given the two layer nature of the insulators under test it would seem reasonable to suggest that the two regions represent first the compression of the layer of air and protruding fibres and then the compression of the bulk of the fabric as the thickness is further reduced.

This interpretation of the results is very similar to that made in relation to the thickness v pressure results of the previous chapter. The shape of the two regions of the thermal insulation versus thickness plot can be interpreted in terms of the changing thickness of the air layer for the upper region and changing thickness and hence density of the bulk of the fabric in the lower region.

As was discussed earlier in this chapter the conductivity of a fibrous assembly can be estimated by several different theoretical derivations. If the model developed by Schumeister(34) is considered then the fabric conductivity is given as a function of the volume fraction of fibre in the sample. Ignoring convection but including the heat transfer by radiation as derived by Strong(38) gives:

$$k = a(k_a(1-v_f)+k_f v_f) + (1-a) \left(\frac{k_a k_f}{k_a v_f + k_f(1-v_f)} \right) + \frac{F}{v_f} \quad 4.71$$

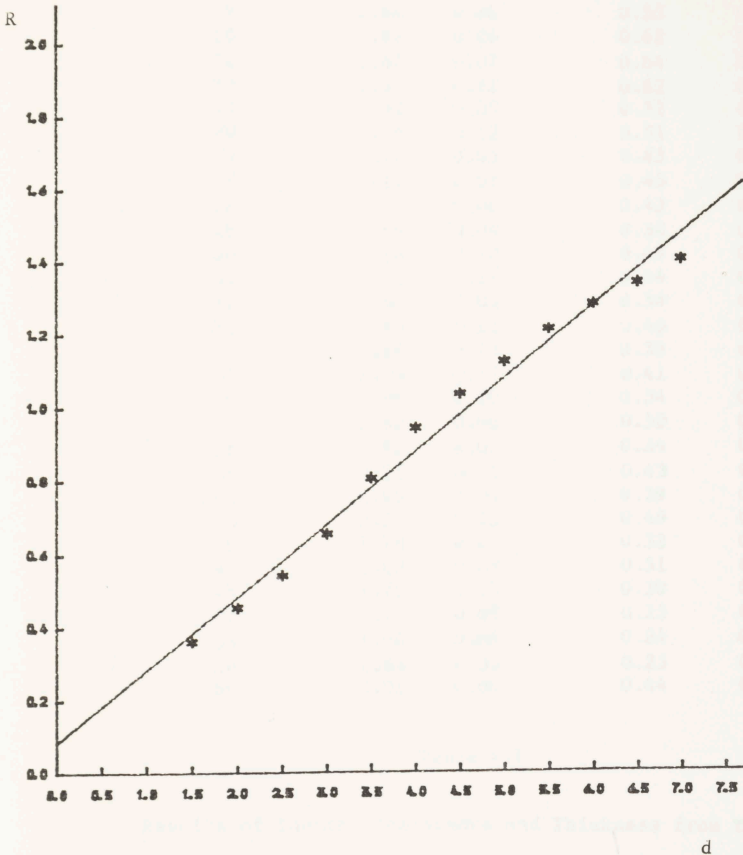
The two coefficients in this equation, a and F , are determined by the size and distribution of the fibres within the fabric.

Where the Tog-meter plate separation is greater than the uncompressed thickness of the fabric bulk the changing thermal resistance will be associated with the changing thickness of the layer of protruding fibres and air. If the thickness of this layer remains less than five mm then once again convection need not be considered. The overall resistance of this air layer can therefore be estimated as the combined radiation and conduction and written as:

$$R_s = \frac{1}{k_a/d_a + 6.3} \quad 4.72$$

Assuming that the fibre conductivity and fabric weight are known and using the formula of Schumeister/Baxter to find k_f then the above relationships contain only two unknowns, the thickness of the bulk of the fabric d and the factor F governing the heat transfer by radiation within the fabric.

Using a least mean squares regression procedure the data from the Tog-meter was analysed and the values of d giving the best fit were found. These values along with their standard deviations are shown in Table.4.1 and examples of the lines of best fit along with the experimental data are shown in Figs.4.5 and 4.6.



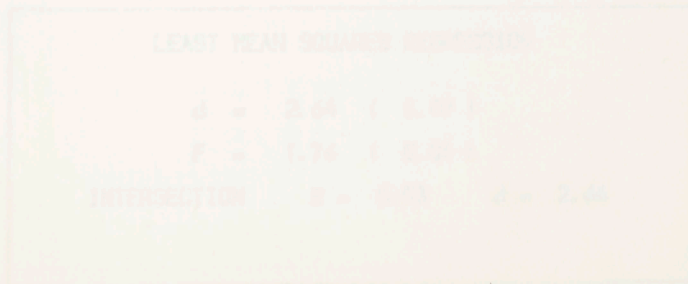
Thermal Resistance(Togs) as a Function of Thickness(mm)

FIGURE 4.4

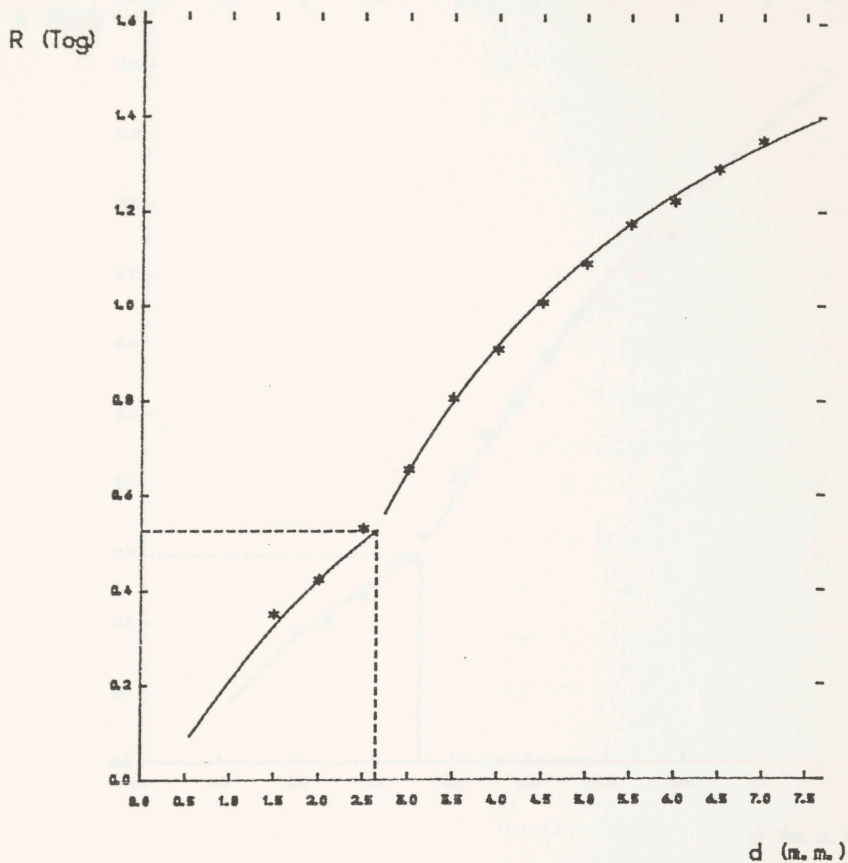
Sample	d (mm)	error	R (Tog)	error
6	2.61	0.07	0.50	0.01
9	2.64	0.06	0.53	0.02
10	2.87	0.06	0.62	0.03
11	2.87	0.07	0.64	0.02
12	2.93	0.12	0.62	0.04
13	2.52	0.05	0.32	0.03
20	2.24	0.12	0.51	0.03
24	2.11	0.05	0.43	0.02
27	2.17	0.05	0.43	0.03
28	2.21	0.06	0.43	0.04
29	1.89	0.04	0.34	0.02
30	2.38	0.12	0.45	0.03
31	2.38	0.11	0.44	0.04
32	1.90	0.03	0.34	0.02
33	2.44	0.11	0.46	0.03
34	1.87	0.13	0.33	0.03
35	2.35	0.17	0.41	0.04
36	1.91	0.10	0.34	0.03
37	2.62	0.06	0.50	0.02
38	1.92	0.07	0.34	0.03
39	2.25	0.18	0.43	0.03
41	1.65	0.05	0.29	0.03
45	2.26	0.13	0.49	0.05
46	1.78	0.05	0.32	0.03
47	2.63	0.09	0.51	0.02
48	1.75	0.05	0.30	0.03
52	1.73	0.05	0.25	0.04
53	1.94	0.04	0.24	0.05
56	1.98	0.03	0.23	0.03
60	3.01	0.04	0.44	0.03

Table 4.1

Results of Thermal Resistance and Thickness from Togmeter



SAMPLE 9



LEAST MEAN SQUARES REGRESSION

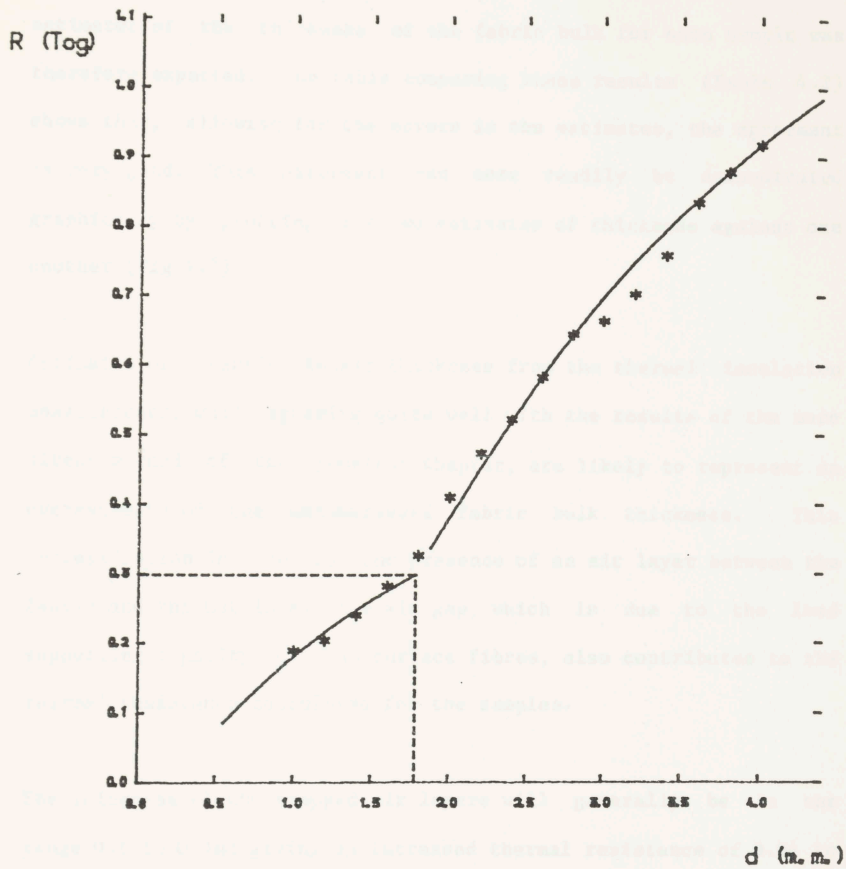
$$d = 2.64 \quad (0.07)$$

$$F = 1.76 \quad (0.04)$$

$$\text{INTERSECTION} \quad R = 0.53 \quad d = 2.64$$

FIGURE 4.5

SAMPLE W (1.25)



LEAST MEAN SQUARES REGRESSION

$$d = 1.78 \quad (0.07)$$

$$F = 3.66 \quad (0.46)$$

$$\text{INTERSECTION} \quad R = 0.30 \quad d = 1.78$$

FIGURE 4.6

The model of the fabric used to calculate the thickness was, as has already been indicated, the same as that used to interpret the thickness versus pressure results. A close correlation between the estimates of the thickness of the fabric bulk for each sample was therefore expected. The table comparing these results (Table 4.2) shows that, allowing for the errors in the estimates, the agreement is very good. This agreement can more readily be demonstrated graphically by plotting the two estimates of thickness against one another (Fig.4.7).

Estimates of effective fabric thickness from the thermal insulation measurements, while agreeing quite well with the results of the more direct method of the previous chapter, are likely to represent an overestimate of the uncompressed fabric bulk thickness. This overestimation is due to the presence of an air layer between the fabric and the hotplate. The air gap, which is due to the load supporting capacity of the surface fibres, also contributes to the thermal resistance calculated for the samples.

The thickness of the trapped air layers will generally be in the range 0.1 to 0.3mm giving an increased thermal resistance of 0.04 to 0.10 Togs. (1 Tog = $0.1 \text{ degC m}^2/\text{W}$).

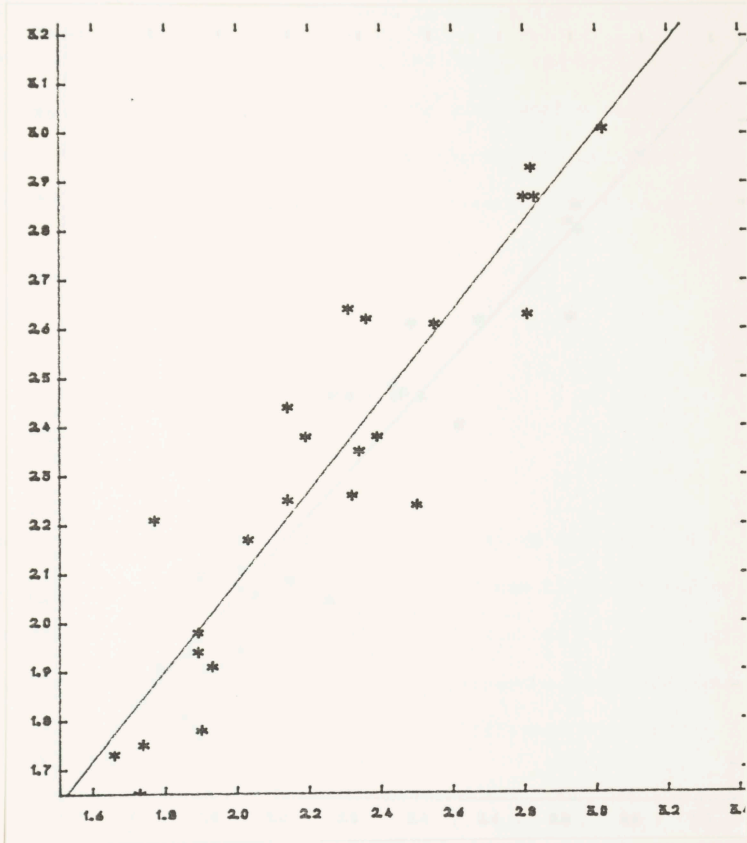
From a comparison of the thickness estimates from the two different measurement procedures shown in Figure 4.7 a linear relationship was found with a slope of nearly unity and an intercept of 0.1mm. On average the difference between the thickness estimates for a given sample was 0.1mm which agrees with the indication from the steady-state measurements of the previous chapter.

Sample	d (mm) Tog-meter	d (mm) direct
6	2.61	2.55
9	2.64	2.31
10	2.87	2.80
11	2.87	2.83
12	2.93	2.82
13	2.52	1.49
20	2.24	2.50
27	2.17	2.03
28	2.21	1.77
30	2.38	2.39
31	2.38	2.19
33	2.44	2.14
35	2.35	2.34
36	1.91	1.93
37	2.62	2.36
39	2.25	2.14
41	1.65	1.73
45	2.26	2.32
46	1.78	1.90
47	2.63	2.81
48	1.75	1.74
52	1.73	1.66
53	1.94	1.89
56	1.98	1.89
60	3.01	3.07

Table 4.2

Thickness Values Estimated from Thermal Resistance Testing
and from Direct Measurements

d
direct



d
Tog-meter

FIGURE 4.7

Comparison of Thickness Estimates

The results also give information about the fabric performance when under compression. The thermal resistance results for thicknesses below the transition thickness are shown in Figure 4.8. The thermal resistance is plotted against thickness for each result with the line of best fit being calculated for the wool samples only. From these results the relationship between thermal resistance and thickness can be represented by a linear equation passing through the origin:

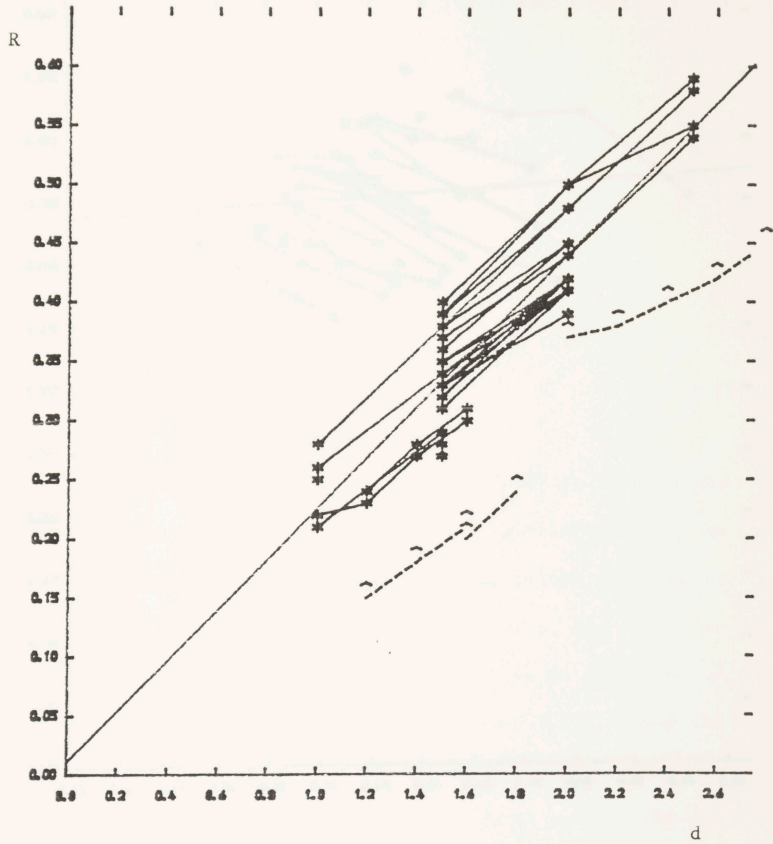
$$R = 0.022 d \text{ (degC m}^2\text{/W)} \quad 4.73$$

or $r = 2.15 (\pm 0.2) \text{ Togs/cm} \quad 4.74$

A further plot using the data and variables is shown in Figure 4.9. In this case the results for each individual sample are joined by straight lines. This data suggests that the scatter is not due solely to random errors in the measurement procedure but represents actual differences between the properties of different samples.

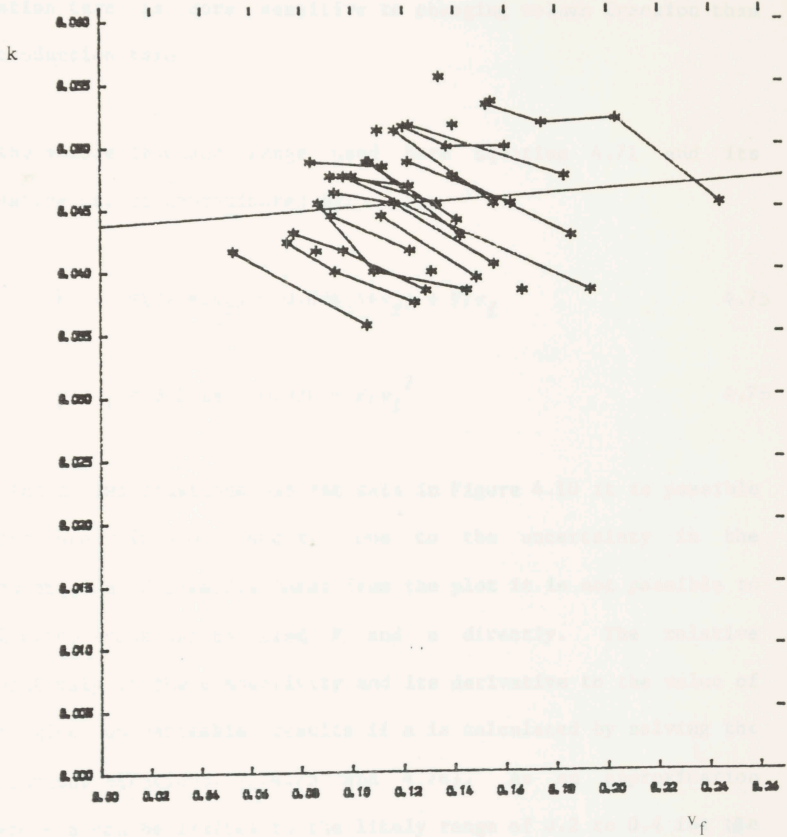
The relationship between thermal resistance and thickness as suggested by Equation 4.71 implies that the volume fraction along with the choice of coefficients, a , and, F , determine the conductivity for a given fibre type. A plot of thermal conductivity as a function of volume fraction is shown in Figure 4.10. The plot shows only wool samples and the points for each individual sample are joined by straight lines.

Within this narrow range of volume fraction the relationship between the conductivity and the volume fraction can be taken as approximately linear. The different samples give a series of



Fabric Thermal Resistance as a function of Thickness

FIGURE 4.9



Fabric Conductivity as a Function of Fibre Volume Fraction

FIGURE 4.10

roughly parallel lines with a negative gradient. This implies that, for a given sample, as the volume fraction decreased the thermal conductivity increased. From Equation 4.71 this means that the radiation term is more sensitive to changing volume fraction than the conduction term.

For the volume fraction range used here Equation 4.71 and its derivative can be approximated by:

$$k = a(0.141v_f) + 0.026(1+v_f) + F/v_f \quad 4.75$$

$$dk/dv_f = 0.141a + 0.026 - F/v_f^2 \quad 4.76$$

From these two equations and the data in Figure 4.10 it is possible to calculate values of F and a. Due to the uncertainty in the values of the derivative taken from the plot it is not possible to solve these equations to find F and a directly. The relative insensitivity of the conductivity and its derivative to the value of a can give unreasonable results if a is calculated by solving the simultaneous equations. (Eq. 4.75 and 4.76). As an approximation therefore a can be limited to the likely range of 0.2 to 0.4 for the calculation of F. The results of the calculations for two of the cases from Figure 4.10 are shown in Table 4.3 where the value for F is found to be in the range 0.001 to 0.003.

At very low volume fractions it is apparent that the radiation term accounts for a large fraction of the conductivity and is the most important term in the derivative of conductivity with respect to volume fraction.

The values of γ and δ are likely to be functions of the dimensions and distribution of the fibres within the fabric and are therefore not likely to be calculated theoretically. The calculations carried out here, while giving a qualitative idea of the order of magnitude of γ are subject to the same limitations as those mentioned above.

	Case 1	Case 2
$k =$	0.039	0.05
$v =$	0.078	0.15
$\frac{dk}{dv} =$	-0.10	-0.06

4.7.2 Sample Calculations

$a = 0.2$	$F =$	0.0008	0.0025
$a = 0.4$	$F =$	0.0005 to 0.0009	0.0017 to 0.0032

Table 4.3
Results of Sample Calculations of the Radiation factor, F, from the Measured Relationship Between Conductivity and Volume Fraction

Results of Sample Calculations of the Radiation factor, F, from the Measured Relationship Between Conductivity and Volume Fraction

where k is the conductivity of the fibres, γ is the volume fraction of the fibres and δ is the radiation factor respectively and v is the power conducted by the heating wire to maintain the plate temperature. Below the plate the area of 0.12^2 m² the power is conducted by an electrically insulated heat sink.

Each fibre sample was tested at least four times with individual tests being further subdivided into a number of readings. The conductivity measured in each case was the average of the readings over all the tests carried out on each sample.

In the case of the present test plate the area of heat sink was

The values of F and a are likely to be functions of the dimensions and distribution of fibres within the fabric and are therefore very difficult to calculate theoretically. The calculations carried out here, while giving some indication of the magnitude of F are subject to large errors due to the uncertainties in the measured values and the small differences between readings used to find the derivative in particular.

4.7.2 GUARDED HOT-PLATE

The plate temperature was set to 33 degC and the heat loss through the fabric and the ambient temperature were recorded. From these values the total thermal resistance of the fabric air system could be found from the following equation:

$$R = (T_p - T_a) / 10 P \quad 4.77$$

where $R(\text{degC m}^2/\text{W})$ is the total thermal resistance, T_p and T_a are the temperatures of the plate and the ambient respectively and P is the power consumed by the heating elements to maintain the plate temperature. Because the plate has an area of 0.1m^2 the power is multiplied by ten in Eq.4.77 to convert it to a heat flux.

Each fabric sample was tested at least four times with each individual test being further subdivided into 3 or 4 hourly readings. The results are summarised in table.4.4 where the values represent the averages over all the tests carried out on each sample.

In the case of the guarded hot plate the loss of heat from the

Sample	R (Togs)	Sample	R (Togs)
1	1.19	33	1.19
2	1.23	34	1.19
3	1.14	35	1.22
4	1.23	36	1.19
5	1.21	37	1.24
6	1.22	38	1.16
7	1.17	39	1.17
8	1.22	40	1.14
9	1.23	41	1.14
10	1.27	47	1.27
11	1.28	48	1.21
12	1.22	50	1.26
13	1.13	51	1.19
14	1.13	53	1.22
15	1.14	54	1.18
16	1.16	55	1.14
17	1.18	56	1.17
18	1.07	57	1.37
19	1.27	61	1.18
20	1.19	62	1.25
21	1.21	63	1.19
22	1.15	64	1.15
23	1.20	65	1.12
24	1.17	66	1.42
25	1.20	67	1.39
26	1.15	68	1.39
27	1.19	69	1.43
28	1.20	70	1.36
29	1.17	71	1.39
30	1.18	72	1.37
31	1.19	73	1.38
32	1.16	74	1.31

Table 4.4

Comparison of Thermal Resistance Values from the Togmeter
and the Guarded Hotplate

surface of the fabric is by both radiative and convective processes. The contribution of radiation can be estimated with a reasonable degree of certainty. Convective losses however are considerably more difficult to calculate from first principles. Empirical relationships for convective loss from a flat horizontal surface vary greatly depending on the exact dimensions of the surface and the temperatures involved.

For this reason it was not possible to compare the results from the guarded hot plate and the Tog-meter directly. As a first approximation however the difference between the thermal resistance as measured on the guarded hot plate and the thermal resistance of the uncompressed fabric bulk as measured on the Tog-meter should be roughly constant for all samples and should represent the surface resistance of the fabric. These difference values, along with the two sets of thermal resistance results are shown in Table.4.5.

A graphical representation of the relationship between the thermal resistance measured on the guarded hotplate and as estimated from the Tog-meter is shown in Figure 4.11. Despite the large amount of scatter the relationship can be approximated to a straight line. The intercept of 1.1 gives an estimate of the fabric surface resistance while the slope of 0.3 implies that the thermal resistance of the fabric on the guarded hotplate is considerably less than between the plates of the Tog-meter.

The scatter of the results and the fact that the fabric contribution to the total thermal insulation is small for the hotplate leads to considerable uncertainty as to the accuracy of the relationship derived from the data. The relationship suggests that the fabric

Sample	R (Togs) Tog-meter	R (Togs) Hotplate	Difference
6	0.50	1.22	0.72
9	0.53	1.22	0.69
10	0.62	1.27	0.65
11	0.64	1.28	0.64
12	0.62	1.22	0.60
13	0.32	1.13	0.81
20	0.51	1.19	0.68
24	0.43	1.17	0.74
27	0.43	1.19	0.76
28	0.43	1.19	0.76
29	0.34	1.17	0.83
30	0.45	1.18	0.73
31	0.44	1.19	0.75
32	0.34	1.15	0.81
33	0.46	1.19	0.73
34	0.33	1.19	0.86
35	0.41	1.22	0.81
37	0.50	1.24	0.74
38	0.34	1.16	0.82
39	0.43	1.17	0.74
41	0.29	1.14	0.85
47	0.51	1.27	0.76
48	0.30	1.21	0.91
56	0.23	1.17	0.94
Mean	0.43	1.20	0.76

TABLE 4.5

The Relationship Between Thermal Resistance Values as Measured on the
the Togmeter and the Guarded Hotplate

thermal resistance is reduced when the upper surface is open to the atmosphere. The most likely cause of this change is the establishment of convection of air movement associated with convective heat transfer. The flow of air within the sample, without more details, is not possible to analyze. This apparent reduction in thermal resistance is probably due to the fact that the air within the sample, without more details, is not possible to analyze. This apparent reduction in thermal resistance is probably due to the fact that the air within the sample, without more details, is not possible to analyze.

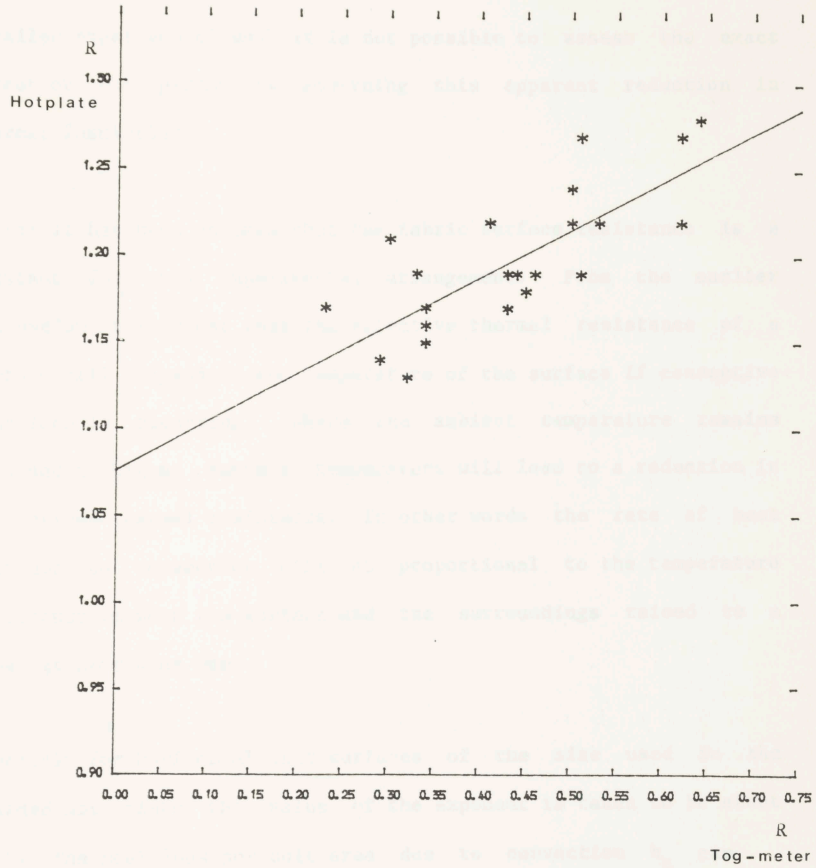


FIGURE 4.11

where T_s = fabric surface temperature
 T_a = ambient temperature
 A = constant

thermal resistance is reduced when its upper surface is open to the environment. The most likely cause of the change is the establishment of patterns of air movement associated with convective heat exchange disturbing the air within the fabric. Without more detailed experimental work it is not possible to assess the exact extent or the parameters governing this apparent reduction in thermal insulation.

So far it has been assumed that the fabric surface resistance is a constant for this experimental arrangement. From the earlier discussion it is clear that the effective thermal resistance of a surface will depend on the temperature of the surface if convective heat loss is occurring. Where the ambient temperature remains constant a higher surface temperature will lead to a reduction in the surface thermal resistance. In other words the rate of heat loss due to convection will be proportional to the temperature difference between the surface and the surroundings raised to a power greater than one.

Generally for horizontal flat surfaces of the size used in the guarded hot plate the value of the exponent is taken to be about 1.33. The heat loss per unit area due to convection h_c can therefore be written as:

$$h_c = A (T_s - T_a)^{1.33} \quad 4.78$$

where T_s = fabric surface temperature
 T_a = ambient temperature
 A = constant

The total heat loss from the surface must also include the radiation term and can be equated to the heat flux, q , as supplied electrically to the hot-plate.

$$q = A (T_s - T_a)^{1.33} + 6.3 (T_s - T_a) \quad 4.79$$

which can be rearranged to give:

$$q/(T_s - T_a) = A (T_s - T_a)^{0.33} + 6.3 \quad 4.80$$

The term on the left represents the heat transfer coefficient of the fabric surface which is equal to the inverse of its thermal resistance. Using the value of the surface film resistance of 1.08(Tog) and from the known temperatures the value for, A , was found to be about 1.2.

CHAPTER 5

STEADY-STATE HEAT AND VAPOUR FLOW

5.1 EXPERIMENTAL PROCEDURE.

The guarded hotplate described in Chapter 2 was employed for the simultaneous measurement of heat and vapour flow through the samples selected. The output from the instrument consisted of:

- 1/ A recording of instantaneous heat supplied to the plate.
- 2/ Integrated power reading to give total energy consumed.
- 3/ Short term energy printout indicating every 10,000 heater supply pulses.
- 4/ Markers indicating the refilling of the liquid supply tube which corresponds to 2cm^3 of liquid evaporation.

The test duration was in all cases at least eight hours. Such a length of time was deemed necessary to allow for steady-state conditions to be reached followed by sufficient recording time to minimise errors.

Heat was supplied to the base of the hot-plate on which there was a layer of liquid. Above the liquid was an air gap and above that is the fabric supported by an open mesh. The total separation between the fabric and the plate was one centimetre. The level of the liquid could be set via the positioning of the liquid supply system which also

caused equal but opposite changes in the air gap thickness. In addition the instrument could be operated with a stream of air flowing over and parallel to the fabric surface.

5.2 RESULTS

5.2.1 AIR GAPS, NATURAL CONVECTION

Measurements total energy flow and rate of water vapour transfer were made for three different levels of water on the hot plate and guard ring. The levels chosen were 3, 5 and 7mm giving air gaps of 7, 5 and 3mm respectively, between the liquid surface and the lower fabric surface.

The results of this series of test are shown in Table 5.1. It is immediately apparent from this data that the transfer of heat and vapour is not particularly sensitive to the choice of fabric for the range of fabrics and experimental conditions used. This apparent insensitivity can be understood if the relative contributions to the heat and vapour resistance are considered. In the previous chapter it was found that the thermal resistance of the interface between the top surface of the fabric and the environment was generally of the order of twice the thermal resistance of the bulk of the fabric. The additional air layer between the liquid and the lower surface of the fabric is likely to add a resistance of one to two times that of the fabric for thicknesses of 3 and 7mm respectively. Thus even a doubling of the fabric thermal resistance will lead only to 20 to 25% change in the measured thermal resistance. Similarly a large proportion of the

Sample	Energy Loss-Heat			Energy loss-Vapour		
	7 mm	5 mm	3 mm	7 mm	5 mm	3 mm
79	74	78	80	90	92	94
59	76	79	80	93	96	102
80	75	78	80	94	97	99
81	80	81	85	95	99	102
61	80	85	86	102	103	104
82	82	84	90	108	111	115
64	81	84	85	84	90	93
8	74	75	78	81	86	88
9	70	75	79	85	87	90
10	73	74	80	86	86	91
11	70	72	79	83	87	88
12	70	75	79	87	88	90
13	75	76	80	84	90	93
14	73	75	78	82	84	85
15	72	74	79	84	86	86
16	70	73	79	83	85	89
17	80	81	85	95	99	101
18	74	76	79	97	100	103
19	75	78	81	92	93	95
20	75	76	79	90	92	93
21	84	85	87	95	98	101
22	72	74	79	91	94	96
23	80	81	84	92	99	105
24	82	82	86	90	95	99
25	86	91	92	98	104	114
26	78	79	80	86	93	95

Table 5.1

Energy Loss Due to Heat and Vapour Flow for Different Air Gaps

vapour resistance of the samples under test is due to the layers of air on either side of the fabric.

A summary of this data is given in table 5.2 where the values of heat and vapour resistance alone with their ratio are shown for the 26 samples tested.

Due to the time involved in testing and the relative insensitivity the remaining 28 samples were tested at only the two larger liquid fabric separations to give the data in table 5.3 and the summary of that data in table 5.4

Several points of interest emerged from this data. The contributions of heat and evaporative energy transfer are within about twenty per cent of one another for all fabrics and air gaps tested. This emphasises the importance of water vapour transfer in maintaining the overall energy balance. In addition the relative values of heat and vapour resistance remained roughly the same as the air gap was reduced. However, because of the errors in measuring such small changes it is difficult to draw any definite conclusions from this data.

5.2.2 MINIMAL AIR GAP, FORCED CONVECTION.

In order to emphasise the influence of the fabric on the heat and vapour transport properties a further set of measurements was made.

For this set, the fabric support system was removed and replaced by a sheet of cellophane stretched tightly across the plate and guard ring. The cellophane was held in place by a rubber ring on the outer wall of

Sample	1/R			1/W			W/R		
	7 mm	5 mm	3 mm	7 mm	5 mm	3 mm	7 mm	5 mm	3 mm
79	6.2	6.5	6.7	22.6	23.0	23.6	0.27	0.28	0.28
59	6.4	6.6	6.7	23.4	24.2	25.7	0.27	0.27	0.26
80	6.3	6.5	6.7	23.6	24.4	25.0	0.27	0.27	0.27
81	6.7	6.8	7.1	23.9	24.9	25.6	0.28	0.27	0.28
61	6.7	7.1	7.2	25.7	25.9	26.2	0.26	0.27	0.28
82	6.9	7.0	7.5	27.0	27.9	29.0	0.26	0.25	0.26
64	6.8	7.0	7.1	21.0	22.5	23.5	0.32	0.31	0.30
8	6.2	6.3	6.5	20.3	21.7	22.2	0.31	0.29	0.29
9	5.9	6.3	6.6	21.5	22.0	22.7	0.28	0.29	0.29
10	6.1	6.2	6.7	21.5	21.8	22.8	0.28	0.29	0.29
11	5.9	6.0	6.6	20.9	21.8	22.1	0.28	0.27	0.30
12	5.9	6.3	6.6	21.8	22.1	22.7	0.27	0.29	0.29
13	6.3	6.4	6.7	21.0	22.5	23.5	0.30	0.28	0.29
14	6.1	6.3	6.5	20.6	21.0	21.5	0.30	0.30	0.30
15	6.0	6.2	6.6	21.0	21.5	21.7	0.29	0.29	0.30
16	5.9	6.1	6.6	20.9	21.5	22.4	0.28	0.28	0.30
17	6.7	6.8	7.1	24.0	25.0	25.3	0.28	0.27	0.28
18	6.2	6.4	6.6	24.5	25.2	26.0	0.25	0.25	0.25
19	6.3	6.5	6.8	23.2	23.3	23.8	0.27	0.28	0.29
20	6.3	6.4	6.6	22.5	23.0	23.3	0.28	0.28	0.28
21	7.0	7.1	7.3	24.0	24.6	25.4	0.29	0.29	0.29
22	6.0	6.2	6.6	23.0	23.7	24.2	0.26	0.26	0.27
23	6.7	6.8	7.0	23.0	25.0	26.3	0.29	0.27	0.27
24	6.9	6.9	7.2	22.7	23.8	24.8	0.30	0.29	0.29
25	7.2	7.6	7.7	24.6	26.2	28.5	0.29	0.29	0.27
26	6.5	6.6	6.7	21.5	23.3	23.9	0.30	0.28	0.28
Mean	6.4	6.6	6.8	22.7	23.5	24.3	0.28	0.28	0.28

Table 5.2

Values of Conductance (1/R) and Vapour Transfer Coefficient (1/W) and their Ratio for Different Air Gaps

Sample	Energy flow-Heat		Energy flow-Vapour	
	7 mm	5 mm	7 mm	5 mm
2	74	81	93	99
4	75	80	95	99
6	69	78	96	105
7	64	70	97	110
8	72	82	95	99
9	70	79	95	102
10	70	79	97	101
11	70	81	95	99
12	72	78	92	101
13	75	79	100	103
14	78	82	100	106
15	75	80	99	110
16	75	80	93	101
17	75	81	95	101
18	76	84	99	105
20	70	73	95	105
21	73	79	97	99
22	81	85	90	101
23	81	86	90	95
24	84	88	92	94
25	79	82	93	96
26	79	84	96	101
28	75	81	89	100
29	75	81	97	106
30	70	81	99	101
31	78	86	95	101
33	69	72	98	115
34	80	82	98	98
35	76	80	95	99
36	74	81	101	101
37	73	76	95	99
38	79	86	97	100
40	80	82	95	101
43	78	81	101	101
44	76	82	99	103
45	82	84	94	98

Table 5.3

Sample	1/R		1/W		W/R	
	7 mm	5 mm	7 mm	5 mm	7 mm	5 mm
2	6.2	6.8	23.3	24.8	0.27	0.27
4	6.3	6.7	24.0	24.8	0.26	0.27
6	5.8	6.5	24.2	26.3	0.24	0.25
7	5.4	5.9	24.3	27.8	0.22	0.21
8	6.0	6.9	24.0	24.8	0.25	0.28
9	5.9	6.6	24.0	25.6	0.25	0.26
10	5.9	6.6	24.3	25.3	0.24	0.26
11	5.9	6.8	24.0	24.8	0.25	0.27
12	6.0	6.5	23.0	25.4	0.26	0.26
13	6.3	6.6	25.1	25.8	0.25	0.26
14	6.5	6.9	25.1	26.6	0.26	0.26
15	6.3	6.7	24.8	27.8	0.25	0.24
16	6.3	6.7	23.3	25.5	0.27	0.26
17	6.3	6.8	24.0	25.5	0.26	0.27
18	6.4	7.0	24.8	26.3	0.26	0.27
20	5.9	6.1	24.0	26.3	0.25	0.23
21	6.1	6.6	24.3	24.8	0.25	0.27
22	6.8	7.1	22.5	25.5	0.30	0.28
23	6.8	7.2	22.5	24.0	0.30	0.30
24	7.0	7.4	23.0	23.6	0.30	0.31
25	6.6	6.9	23.3	24.1	0.28	0.29
26	6.6	7.0	24.1	25.4	0.27	0.28
28	6.3	6.8	22.3	25.1	0.28	0.27
29	6.3	6.8	24.4	26.6	0.26	0.26
30	5.9	6.8	24.8	25.5	0.24	0.27
31	6.5	7.2	24.0	25.5	0.27	0.28
33	5.8	6.0	24.5	28.8	0.24	0.21
34	6.7	6.9	24.5	24.6	0.27	0.28
35	6.4	6.7	24.0	24.8	0.27	0.27
36	6.2	6.8	25.3	25.4	0.25	0.27
37	6.1	6.4	24.0	24.8	0.25	0.26
38	6.6	7.2	24.3	25.1	0.27	0.29
40	6.7	6.9	24.0	25.5	0.28	0.27
43	6.5	6.8	25.3	25.5	0.26	0.27
44	6.4	6.9	24.8	25.9	0.26	0.27
45	6.9	7.0	23.7	24.5	0.29	0.29
Mean	6.3	6.8	24.0	25.5	0.26	0.27

Table 5.4

the guard ring. The recesses on the plate and guard ring were filled with water so that the liquid was in contact with the cellophane.

A thin film of grease was used on the horizontal metal surfaces at the tops of the liquid retaining walls of the plate and guard ring to ensure that there could be no transfer of liquid between the two containers. The test samples were then placed directly on the cellophane thus eliminating the air gap which had been used for the previous measurements.

With this arrangement it was found that rapid condensation of water occurred within the fabric making it difficult to take steady-state readings before the fabric became saturated with water.

In order to eliminate or at least greatly reduce the rate of condensation within the fabric a chamber was constructed into which the apparatus could be placed. This chamber was fitted with three fans to draw air from the room over the fabric parallel to its surface. The air speed used was approximately 1.5 m/s. This forced convection also reduced the total heat and vapour resistances of the system and increased further the role of the fabric itself in determining the transfer properties. The results are shown in Table 5.5.

Sample	Heat	Vapour	l/R	l/W	w/R
1	218	392	18.2	98.0	0.19
2	190	330	15.9	82.5	0.19
3	171	345	14.3	86.5	0.17
6	123	335	10.3	84.0	0.12
7	125	341	10.4	85.3	0.12
8	125	338	10.4	84.7	0.12
10	116	328	9.7	82.1	0.12
11	137	357	11.5	89.5	0.13
12	157	372	13.2	93.2	0.14
13	164	397	13.7	99.4	0.14
14	173	381	14.5	95.3	0.15
15	181	368	15.2	92.1	0.16
16	179	378	14.9	94.7	0.16
17	171	362	14.3	90.6	0.16
19	139	336	11.6	84.2	0.14
20	160	353	13.3	88.4	0.15
21	139	374	11.6	93.6	0.12
23	160	351	13.3	88.0	0.15
24	130	378	10.9	94.7	0.11
25	120	404	10.0	101.1	0.10
27	134	389	11.2	97.4	0.12
28	160	353	13.3	88.4	0.15
29	169	356	14.1	89.0	0.16
30	160	349	13.3	87.5	0.15
31	160	347	13.3	86.8	0.15
32	149	368	12.5	92.0	0.14
33	179	320	14.9	80.1	0.19
35	130	380	10.9	95.0	0.11
36	120	371	10.0	92.8	0.11
37	130	341	10.9	85.5	0.13
38	160	344	13.3	86.1	0.15
43	179	338	14.9	84.6	0.18
44	160	349	13.3	87.3	0.15
45	139	326	11.6	81.6	0.14
47	130	314	10.9	78.5	0.14
48	193	333	16.1	83.3	0.19
50	129	304	10.8	76.2	0.14
53	190	320	15.9	80.3	0.20
56	134	378	11.2	94.7	0.12
57	149	255	12.5	63.9	0.20
58	149	308	12.5	77.0	0.16
60	144	328	12.0	82.1	0.15
75	206	435	17.2	109.0	0.16
76	399	500	33.3	125.1	0.27
77	181	427	15.2	106.9	0.14
78	279	449	23.3	112.4	0.21

Table 5.5

Heat and Vapour Transfer With Minimal Air Gap and Forced Convection

5.3 DISCUSSION OF RESULTS.

5.3.1 THERMAL RESISTANCE RESULTS.

The minimisation of the air layers on both sides of the fabric greatly increased the total energy flow through the fabric from less than 200 to over 500 W/m^2 . While the contribution from the flow of heat doubled the increase in the flow of water vapour was between three and fourfold. This caused a much lower ratio of the vapour to thermal resistance.

The main reason for the changing importance of the two sources of energy exchange is that there is no equivalent to radiation in vapour transfer. The radiant transfer across the air gap and between the fabric surface and the environment meant that the convection and conduction accounted for only a part of the heat flow. For the flow of water vapour the diffusion and convection accounted for the entire flow. Therefore, when the air gap was removed and forced convection introduced to minimise the surface resistances it had a greater impact on the vapour transfer.

The heat transfer component of the total energy flow can be compared to the results from the guarded hotplate quoted in Chapter 4 where there was no water vapour flow. the relationship between the sets of results can be seen in Figure 5.1 where the thermal resistance under the conditions used in this chapter are compared to those for the same fabrics under dry heat transfer conditions.

The lines of best fit shown in Figure 5.1 are based on a least mean squares regression procedure and the coefficients describing the linear

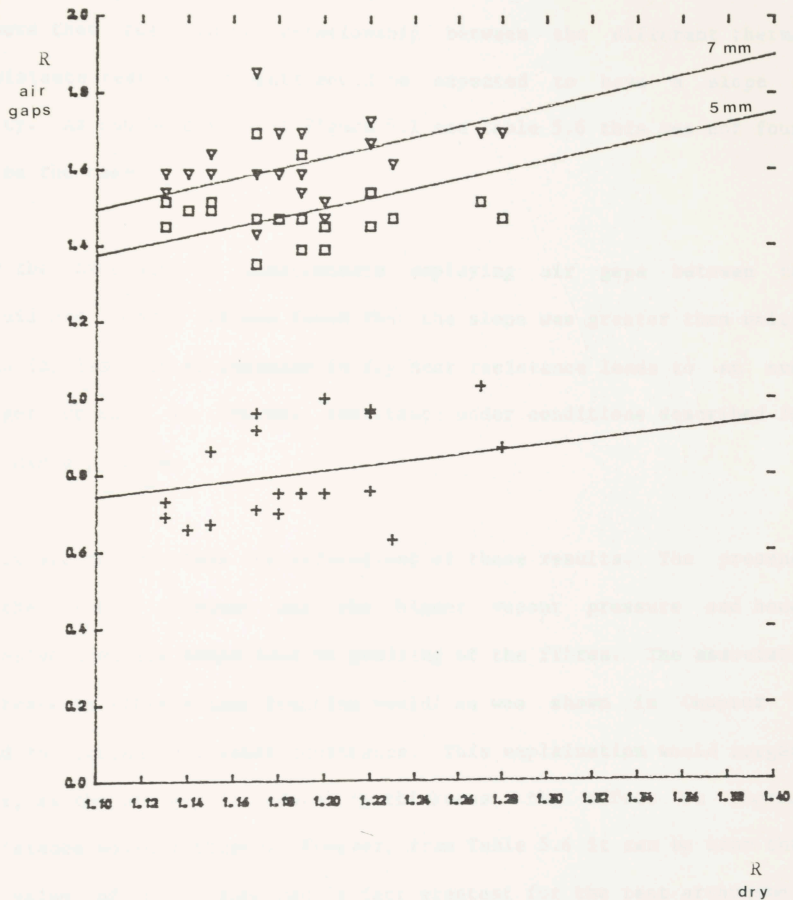


FIGURE 5.1

relationship are summarised in Table 5.6.

If the test conditions only effected the thermal resistance of the air layers then the linear relationship between the different thermal resistance test arrangements would be expected to have a slope of unity. As can be seen from Figure 5.1 and Table 5.6 this was not found to be the case.

For the three sets of measurements employing air gaps between the liquid and fabric it was found that the slope was greater than unity. This implies that an increase in dry heat resistance leads to an even larger increase in thermal resistance under conditions described for the air gap tests.

There are two possible interpretations of these results. The presence of the vapour gradient and the higher vapour pressure and hence relative humidity would lead to swelling of the fibres. The associated increase in fibre volume fraction would (as was shown in Chapter 4) lead to increased thermal resistance. This explanation would suggest that, as the air gap is reduced in thickness, the affect on thermal resistance would increase. However, from Table 5.6 it can be seen that the value of the slope was in fact greatest for the test arrangement using the largest air gap.

The alternative explanation is that the increasing air gap leads to an increase in the total thermal and vapour resistances and hence reduces the temperature and vapour pressure at the fabric surface. This would lead to a reduction in the convective losses from the surface to the environment. As was suggested in Chapter 4 the air movement produced by the density gradient could penetrate into the fabric. Thus a

Air gap (mm)	Intercept	Slope
7	0.0035	1.36
5	0.0071	1.24
0	-0.0040	0.68

Table 5.6

Coefficients of Linear Relationship Between Thermal Resistance Values for Different Air Gaps

reduction in the convective transfer would give rise to an increase in the thermal resistance of the fabric, as was observed.

The results of the tests carried out with a minimal air gap and forced convection are also shown in Figure 5.1 and Table 5.6. For these results the slope of the graph was substantially less than unity implying far greater penetration of the moving air into the fabric than occurred in the dry heat tests.

5.3.2 VAPOUR RESISTANCE RESULTS.

For the samples tested with the air gaps and natural convection at the top surface the average values of the energy equivalents of the vapour permeance were converted to vapour resistance values (sKPam^2/g) as shown in Table 5.7. From the work of Spencer-Smith(42) the vapour resistance of the air gap would be 5.16/mm. For the conditions used in the experimental work reported here the resistance at the top surface could be expected to be $90(\text{sKPam}^2/\text{g})(42)$. The measured values were compared to these estimates and the difference equated to the vapour resistance of the fabric itself.

These results suggest an increase in fabric vapour resistance as the air gap is reduced. This implies that the increased regain and fibre swelling has a greater influence on the vapour resistance than on the thermal resistance.

The relationship between the vapour resistance with a 7mm air gap and natural convection as compared to the case of zero air gap and forced

Sample	Total Vapour resistance			Fabric vapour resistance		
	7 mm	5 mm	3 mm	7 mm	5 mm	3 mm
79	185.5	181.8	177.2	59.3	66.0	71.7
59	178.9	172.8	163.2	52.8	57.0	57.8
80	177.2	171.8	167.6	51.1	56.0	62.2
81	175.0	168.2	163.7	48.9	52.4	58.2
61	162.8	161.8	160.0	36.6	46.0	54.5
82	155.1	150.1	144.6	29.0	34.3	39.1
64	199.4	186.1	178.4	73.3	70.3	72.9
8	206.0	193.2	188.6	79.9	77.4	83.1
9	195.2	190.5	184.9	69.1	74.7	79.4
10	194.5	192.5	183.6	68.4	76.7	78.2
11	200.1	191.8	189.9	74.0	76.0	84.4
12	191.8	189.9	184.2	65.7	74.1	78.8
13	199.4	186.1	178.4	73.3	70.3	72.9
14	203.0	199.4	195.2	76.9	83.6	89.7
15	199.4	194.5	193.2	73.3	78.7	87.7
16	200.1	195.2	187.3	74.0	79.4	81.9
17	174.5	167.6	165.7	48.3	51.8	60.2
18	171.2	166.1	161.3	45.1	50.3	55.9
19	180.7	180.1	176.1	54.5	64.3	70.6
20	186.1	181.8	180.1	60.0	66.0	74.6
21	174.5	170.2	164.7	48.3	54.4	59.2
22	182.4	176.7	172.8	56.3	60.9	67.4
23	181.8	167.6	159.5	55.7	51.8	54.0
24	184.9	176.1	169.2	58.7	60.3	63.7
25	170.2	160.0	146.9	44.1	44.2	41.4
26	194.5	180.1	175.0	68.4	64.3	69.5
Mean	185.5	178.9	173.5	59.4	63.1	68.0

Table 5.7

mates of Total and Fabric Vapour Resistances for Different Air Gaps

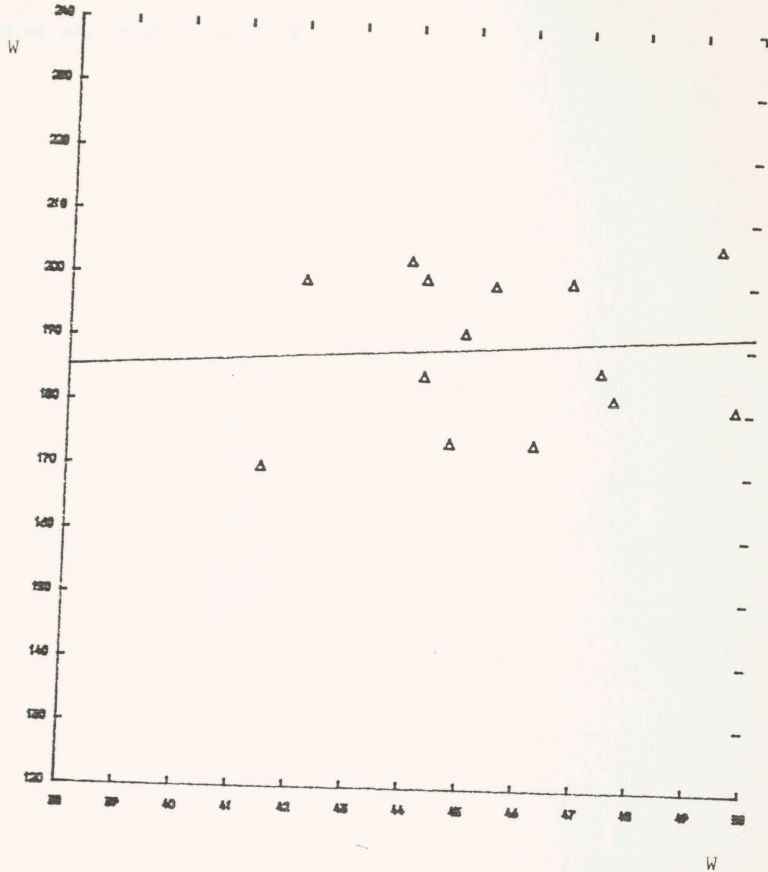


FIGURE 5.2

Relationship Between Vapour Resistance with 7mm Air Gap
and Minimal Air Gap

convection is shown in Figure 5.2. The apparent contribution of the fabric as reflected in the slope of the graph suggests that the vapour resistance of the fabric is reduced very substantially by the forced flow of air over its surface.

CHAPTER 6

TRANSIENT CONDUCTION

6.1 INTRODUCTION

The time dependence of heat transfer by conduction can be expressed through the differential equation of conduction:

$$\frac{\partial T}{\partial t} = a \nabla^2 T + \frac{q_v}{C} \quad 6.1$$

If the system contains no inner heat sources (i.e. $q_v=0$) then this expression reduces to Fourier's equation:

$$\frac{\partial T}{\partial t} = a \nabla^2 T \quad 6.2$$

Where a is known as the thermal diffusivity.

$$a = k/C\rho$$

In the case of the textile assemblies studied here the system can most easily be regarded as an infinite plate. Since the length and width are far greater than the thickness this approximation will lead to negligible errors while greatly simplifying the calculations by reducing the problem to a single dimension. The temperature gradient is generally perpendicular to the the surface of the fabric. Therefore it is most convenient to choose the orientation of the coordinate system such that the x axis is normal to the surface and hence parallel

to the flow of heat. Fourier's law can thus be written in a simplified form:

$$\frac{\partial T}{\partial t} = a \frac{\partial^2 T}{\partial x^2} \quad 6.3$$

The solution can be envisaged as the product of two functions, one of which is a function of time only and the other a function of position only.

$$T(x, t) = F(x) H(t) \quad 6.4$$

Substitution of this separable solution into Fourier's equation gives:

$$F \frac{dH}{dt} = a H \frac{d^2 F}{dx^2} \quad 6.5$$

which can be rearranged to give:

$$\frac{H'}{H} = a \frac{F''}{F} \quad 6.6$$

Since x and t are independent variables this equation can only be satisfied if both sides are equal to the same constant. Non-trivial solutions of F will only be obtained if the constant is negative. For convenience the constant will be denoted by minus S^2 . The resultant formulae are two readily soluble differential equations.

$$H' + S^2 H = 0 \quad 6.7$$

$$F'' + \frac{S^2}{a} F = 0 \quad 6.8$$

The general solutions of the two equations can be found by integration to be given by:

$$H(t) = \exp(-S^2 t) \quad 6.9$$

$$F(x) = A \sin\left(\frac{S}{\sqrt{a}} x\right) + B \cos\left(\frac{S}{\sqrt{a}} x\right) \quad 6.10$$

where A and B are the constants of integration. The full solution is given the steady-state solution along with the product of F and H summed over all possible values of S. Values of S for which the equations are soluble can be determined from the boundary conditions of the system under consideration. Similarly the steady-state solution can be found by applying EQ.4.12.

$$T(x,t) = T(x,\infty) + \sum [A_n \sin(Vx) + B_n \cos(Vx)] \exp(-S_n^2 t) \quad 6.11$$

$$\text{where } V = \frac{S}{\sqrt{a}} x$$

$$T(x, \infty) = C + D x$$

where A_n and B_n are constants for the nth eigenvalue.

This equation can be applied to many different single-layer systems provided that the boundary conditions are known. The more common examples of its use can be found in many sources. For the purposes of this work somewhat more complex situations must be considered if a deeper understanding of transient heat flow is to be acquired.

6.2 BOUNDARY CONDITIONS

For most applications relevant to work undertaken here only two types of boundary conditions need to be considered. The simplest of these arises from intimate contact between two surfaces. This condition gives the following pair of equations:

$$T_1 = T_2 \quad 6.12$$

$$k_1 \left(\frac{\partial T_1}{\partial x} \right) = k_2 \left(\frac{\partial T_2}{\partial x} \right) \quad 6.13$$

Where the subscripts 1 and 2 refer to the surfaces in contact.

The first of these equations (Eq. 6.12) implies that, because of the perfect contact between the two surfaces, their temperatures are equal. The second equation (Eq. 6.13) comes from the requirement of energy conservation and hence equates the heat flux through the two surfaces.

Of greater importance for most practical situations are the equations describing convective boundary conditions:

$$h (T_1 - T_2) = - k_1 \left(\frac{\partial T_1}{\partial x} \right) \quad 6.14$$

$$k_1 \left(\frac{\partial T_1}{\partial x} \right) = k_2 \left(\frac{\partial T_2}{\partial x} \right) \quad 6.15$$

Where h is the heat transfer coefficient of the convective boundary layer. The formulae for convective interfaces (Eqs. 6.12 and 6.13) equate the heat fluxes through the convective layer, the first surface

and the second surface, again on the basis of energy conservation.

For many problems involving one-dimensional heat flow these boundary conditions along with the general solution can be used to calculate the transient response of a system with known physical properties. Alternatively, from the measured response of the system, these equations can be used to find the relevant physical properties of the components which are involved. It is the latter of these two which is most useful in interpreting and utilising experimental data.

6.3 SOLUTION PROCEDURE

A complete solution for any problem must involve the evaluation of the coefficients $A_{i,n}$ and $B_{i,n}$ along with the steady-state temperature profile, as expressed by C_i and D_i .

For a system with i layers there will be $2i$ differential equations describing the boundary conditions. One equation will describe each of the innermost and outermost surface energy balance and two equations will arise for each interface between layers. This set of $2i$ differential equations can be treated as a system of simultaneous equations involving $2i$ unknowns ($A_{i,n}$ and $B_{i,n}$ for each layer).

It is important to note that the differential equation of heat conduction (Eq. 6.3) is an eigenvalue equation which can be rewritten as:

$$a \frac{\partial^2 T}{\partial x^2} + S^2 T = 0 \quad 6.16$$

where the eigenvalue is S^2 and the eigenfunction is the general solution as given in Eq. 6.9. This means that the solution F_n are orthogonal. The condition of orthogonality requires that the integral of the product of any two eigenfunctions will only be non-zero if the two function are identical. Thus if F_m and F_n are eigenfunctions of the same equation then:

$$\int_0^d F_m \cdot F_n \, dx = \begin{cases} 0 & \text{for } m \neq n \\ \neq 0 & \text{for } m = n \end{cases} \quad 6.17$$

This relationship is very useful in the evaluation of the various coefficients.

The details of the solution procedure are best described by using a specific set of boundary conditions and deriving the complete solution.

6.4 SINGLE LAYER, CONVECTIVE SURFACES.

In terms of the experimental work which is to follow this particular example is important, in that it can be used to calculate the properties of the hot-plate material used in the apparatus.

As the problem involves a single layer only, the subscripts i can be removed and the solution to Fourier's equation along with its derivative can be written as:

$$T(x,t) = C + D_x + \Sigma [A_n \sin(Vx) + B_n \cos(Vx)] \exp(-S_n^2 t) \quad 6.18$$

$$\frac{\partial T}{\partial x} = D + \Sigma V [A_n \cos(Vx) - B_n \sin(Vx)] \exp(-S_n^2 t) \quad 6.19$$

Subject to the following boundary conditions:

$$h_1 (T_1 - T(0,t)) = -k \frac{\partial T(0,t)}{\partial x} \quad 6.20$$

$$h_2 (T(d,t) - T_2) = -k \frac{\partial T(d,t)}{\partial x} \quad 6.21$$

Where $x=0$ is located at the inner surface and d is the thickness of the layer. When equations 6.18 and 6.19 are substituted into the equations for the boundary conditions and the terms involving the exponential are equated, the resultant expressions are:

$$\begin{aligned} h_1 \quad , \quad -k \quad C &= h_1 T_1 \\ h_2 \quad , \quad h_2 + k \quad D &= h_2 T_2 \end{aligned} \quad 6.22$$

$$\begin{aligned} kV \quad , \quad -h_1 \quad A_n &= 0 \\ h_2 \sin(Vd) + k \cos(Vd) \quad , \quad h_2 \cos(Vd) - kV \sin(Vd) \quad B_n &= 0 \end{aligned} \quad 6.23$$

The first of these equations (Eq. 6.22) can readily be solved for C and D to give:

$$C = T_1 - (T_1 - T_2) \frac{1/h_1}{R} \quad 6.24$$

$$D = - \frac{1}{d} [(T_1 - T_2)] \frac{d/k}{R} \quad 6.25$$

$$\text{where } R = \frac{d}{k} + \frac{1}{h_1} + \frac{1}{h_2} \quad 6.26$$

These results can readily be seen as conforming to the steady-state heat transfer equations developed in the previous chapter. The equation for C(Eq.6.24) states that the temperature at the inner surface of the conducting medium is less than the temperature T_1 by an amount proportional to the total temperature drop across the system multiplied by the ratio of thermal resistance of the inner convective layer to the total thermal resistance. The equation for D(Eq. 6.25) relates the temperature gradient within the conducting layer to the the temperature drop across the layer divided by its thickness.

For equation 6.23 to produce non-zero values of A and B it is essential that the matrix cannot be inverted. If this is to be the case then the determinant of the matrix must equal zero. The implication being that only those values of S_n which give rise to a determinant of zero can be used in the solution of Fourier's equation for this particular set of boundary conditions.

The determinant of the matrix can be written as:

$$\tan(Vd) - \frac{1 + h_1/h_2}{\frac{kV}{h_1} - \frac{h_2}{kV}} = 0 \quad 6.27$$

This equation can be solved to give a unique set of eigenvalues (S_n^2) which can be used in the solution of Fourier's equation. A graphical approach best illustrates the set of eigenvalues which will arise for a particular choice of system parameters. The eigenvalues can be found from the x coordinates of the intersection points of the two curves.

Defining the eigenvalues such that the determinant of the matrix is zero means that the two rows of the matrix are no longer independent and hence that a complete solution cannot be found. However, from Eq.6.21, the ratio of the coefficients can be shown, for any n, to be given by:

$$\frac{B_n}{A_n} = \frac{kV}{h_1} \quad 6.28$$

If this relationship is substituted into the equation for the position dependent general solution (Eq.6.10) the result can be written as:

$$F_n(x) = \sin(Vx) + \frac{kV}{h_1} \cos(Vx) \quad 6.29$$

Where A_n is now used as a factor external to the nth eigenfunction.

With the ratio of B_n to A_n established the final task is to calculate exact values of A_n . As was discussed earlier eigenvalue

equations give rise to an orthogonal relation which, for this specific case can be shown to be given by:

$$\int_0^d F_n(x) \cdot F_m(x) dx = \begin{cases} 0 & \text{for } n \neq m \\ N_n & \text{for } n = m \end{cases} \quad 6.30$$

$$\text{or } N_n = \int_0^d F_n^2(x) dx \quad 6.31$$

Where N_n is referred to as the norm. If the equation for F (Eq. 6.29) is substituted into the expression for the norm then:

$$N_n = \int_0^d \left[\sin(Vx) + \frac{kV}{h_1} \cos(Vx) \right]^2 dx \quad 6.32$$

The integration can be carried out to give:

$$N_n = \frac{k}{2a} \left[\left(\frac{B_n^2}{A_n^2} - 1 \right) \frac{1}{2V} \sin(2Vd) + \frac{B_n}{A_n} \frac{1}{2V} (1 - \cos(2Vd)) + \left(1 + \frac{A_n^2}{B_n^2} \right) d \right] \quad 6.33$$

If the situation at zero time is considered then the temperature profile can be written as:

$$T(x, 0) = C + Dx + \sum A_n F_n(x) \quad 6.34$$

If both sides of equation 6.34 are multiplied by a particular eigenfunction corresponding to the m .th eigenvalue and integration carried out over the region 0 to d then:

$$-\int_a^d T(x,0) F_m(x) dx = -\int_a^d \Sigma [T(x,\infty) + A_n F_n(x)] F_m(x) dx \quad 6.35$$

The terms on the right hand side of this equation can be separated to give:

$$-\int_a^d T(x,0) F_m(x) dx = -\int_a^d T(x,\infty) F_m(x) dx + A_m \int_a^d F_m^2(x) dx \quad 6.36$$

The last term in this expression is very similar to the definition of the norm (Eq.6.31) and after the appropriate substitution can be rewritten as:

$$-\int_a^d T(x,0) F_m(x) dx = -\int_a^d T(x,\infty) F_m(x) dx + A_m N_m \quad 6.37$$

After a simple re-arrangement an expression for A_m results:

$$A_m = \frac{1}{N_m} \int_a^d [T(x,0) - T(x,\infty)] F_m(x) dx \quad 6.38$$

In most cases the initial temperature distribution will be linearly dependent on x which means that the difference between the initial and the steady-state temperature distributions will also be linear. The integration in Eq.6.38 can therefore be carried out to give:

$$\begin{aligned}
 A_m = & \frac{1}{N_m} \frac{k}{a} \left[C_d \left(\frac{B_m}{A_m} \frac{1}{V} \sin(V d) - \frac{1}{V} (\cos(V d) - 1) \right) \right. \\
 & + D_d \left(\frac{1}{V^2} \sin(V d) + \frac{B_m}{A_m} \frac{1}{V^2} (\cos(V d) - 1) \right) \\
 & \left. - d \frac{1}{V} \cos(V d) + d \frac{B_n}{A_n} \frac{1}{V} \sin(V d) \right] \quad 6.39
 \end{aligned}$$

This now completes the solution for a single-layer convective boundary system. The application of the formulae will be demonstrated in the following chapter.

6.5 TWO LAYERS, CONVECTIVE BOUNDARIES.

Most instruments designed for the measurement of the insulation properties of thin layers of material are based on the use of a heated metal plate on which the test sample is placed. For steady-state guarded hot-plate systems the properties of plate can effectively be ignored. For transient work however, the properties of the metal plate, in particular its thickness, thermal conductivity and thermal diffusivity, appear in even the most rudimentary calculation of the instrument's response. The system is best considered as a two layered arrangement with convective inner and outer boundaries and a convective interface between the two layers. The solution to Fourier's equation within each layer is the same as has already been discussed:

$$T_j(x,t) = g_j(x) + \sum F_{j,n}(x) \exp(-S_n^2 t) \quad 6.40$$

where $g_j(x) = C_j + D_j x = T_j(x, \infty)$ 6.41

$$\frac{\partial g_j(x)}{\partial x} = D_j \quad 6.42$$

$$F_{j,n}(x) = A_{j,n} \sin(Vx) + B_{j,n} \cos(Vx) \quad 6.43$$

$$\frac{\partial F_{j,n}(x)}{\partial x} = V (A_{j,n} \cos(Vx) - B_{j,n} \sin(Vx)) \quad 6.44$$

Subject to the boundary conditions:

$$h_1 (T_s - T_1) = -k_1 \left(\frac{\partial T_1}{\partial x} \right) \quad \text{at } x = 0 \quad 6.45$$

$$h_2 (T_1 - T_2) = -k_1 \left(\frac{\partial T_1}{\partial x} \right) \quad \text{at } x = d_1 \quad 6.46$$

$$k_1 \left(\frac{\partial T_1}{\partial x} \right) = k_2 \left(\frac{\partial T_2}{\partial x} \right) \quad \text{at } x = d_1 \quad 6.47$$

$$h_3 (T_2 - T_a) = -k_2 \left(\frac{\partial T_2}{\partial x} \right) \quad \text{at } x = d_1 + d_2 \quad 6.48$$

Where T_s and T_a are the temperatures external to the innermost and outermost faces respectively and the subscripts 1 and 2 refer to the two layers. Substitution of equation 6.40 into the equations for the boundary conditions (Eqs. 6.45-6.48) yields:

$$h_1 (T_s - F_1 - g_1) = -k_1 (F_1' + g_1') \quad \text{at } x = 0 \quad 6.49$$

$$h_2 (F_1 + g_1 - F_2 - g_2) = -k_1 (F_1' + g_1') \quad \text{at } x = d_1 \quad 6.50$$

$$k_1 (F_1' + g_1') = -k_2 (F_2' - g_2') \quad \text{at } x = d_1 \quad 6.51$$

$$h_3 (F_2 + g_2 - T_a) = -k_2 (F_2' + g_2') \quad \text{at } x = d_1 + d_2 \quad 6.52$$

The primes refer to differentiation with respect to x . As in the single layer case already described the terms involving the exponential can be separated to give two sets of four equations. If the terms not involving the exponential are considered then:

$$h_1 (T_s - g_1) = -k_1 g_1' \quad \text{at } x = 0 \quad 6.53$$

$$h_2 (g_1 - g_2) = -k_1 g_1' \quad \text{at } x = d_1 \quad 6.54$$

$$k_1 g_1' = k_2 g_2' \quad \text{at } x = d_1 \quad 6.55$$

$$h_3 (g_2 - T_a) = -k_2 g_2' \quad \text{at } x = d_1 + d_2 \quad 6.56$$

Substitution of the equation for g (Eq. 6.41) and solving for the coefficients C and D gives:

$$C_1 = T_s - \frac{(T_s - T_a)/h_1}{R} \quad 6.57$$

$$D_1 = - \frac{(T_s - T_a)/k_1}{R} \quad 6.58$$

$$C_2 = T_s - \frac{(T_s - T_a)(1/h_1 + d_1/k_1 + 1/h_2)}{R} \quad 6.59$$

$$D_2 = - \frac{(T_s - T_a)/k_2}{R} \quad 6.60$$

$$R = \frac{1}{h_1} + \frac{d_1}{k_1} + \frac{1}{h_2} + \frac{d_2}{k_2} + \frac{1}{h_3} \quad 6.61$$

These equations, as in the previous example, conform to the relationships developed in the study of steady-state heat transfer.

Equating the terms involving the exponential results in:

$$h_1 F_1 = k_1 F_1' \quad \text{at } x = 0 \quad 6.62$$

$$k_1 F_1' = k_2 F_2' \quad \text{at } x = d_1 \quad 6.63$$

$$h_2 (F_1 - F_2) = -k_1 F_1' \quad \text{at } x = d_1 \quad 6.64$$

$$h_3 F_2 = -k_2 F_2' \quad \text{at } x = d_1 + d_2 \quad 6.65$$

Substitution of the equation for F (Eq. 6.44) gives the following system of equations expressed in matrix format:

$$\begin{array}{cccccc} k_1 V_1 & , & -h_1 & , & 0 & , & 0 & A_{1,n} & 0 \\ k_1 V_1 \cos l & , & h_2 \cos l & , & -h_2 \sin 2 & , & -h_2 \cos 2 & B_{1,n} & 0 \\ +h_2 \sin l & , & -k_1 V_1 \sin l & & & & & = & \\ k_1 V_1 \cos l & , & -k_1 V_1 \sin l & , & -k_2 V_2 \cos 2 & , & k_2 V_2 \sin 2 & A_{2,n} & 0 \\ 0 & , & 0 & , & k_2 V_2 \cos 3 & , & h_3 \cos 3 & B_{2,n} & 0 \\ & & & & + h_3 \sin 3 & , & -k_2 V_2 \sin 3 & & \end{array}$$

Eq. 6.66

$$\text{where } V_1 = \frac{S_n}{a_1} d_1 \quad V_2 = \frac{S_n}{a_2} d_s = d_1 + d_2$$

$$\cos l = \cos(V_1 d_1) \quad \cos 2 = \cos(V_2 d_1) \quad \cos 3 = \cos(V_2 d_s)$$

$$\sin l = \sin(V_1 d_1) \quad \sin 2 = \sin(V_2 d_1) \quad \sin 3 = \sin(V_2 d_s)$$

These equations again form an homogeneous set which suggests that, for the solution to be non-trivial, the determinant of the matrix must be zero. This in turn means that the equations will not all be independent and that the solution for the A 's and B 's can only be

expressed in terms of ratios.

Setting the determinant of the matrix to zero is more complex than in the previous example. At this stage it is sufficient to say that a unique set of eigenvalues can be found for any particular set of parameters and boundary conditions. Details of how such calculations are carried out will be discussed in the following chapter.

One row of the matrix can be eliminated by expressing the A 's and B 's in terms of $A_{1,n}$ which in turn is set to unity. If the bottom row of the matrix is eliminated in this way the following expression results:

$$\begin{array}{ccc} -h_1 & , & 0 & , & 0 \\ h_2 \cos l - k_1 V_1 \sin l & , & -h_2 \sin 2 & , & -h_2 \cos 2 & X \\ -k_1 V_1 \sin l & , & -k_2 V_2 \cos 2 & , & k_2 V_2 \sin 2 \end{array}$$

$$\begin{array}{l} B_{1,n} = -k_1 V_1 \\ A_{2,n} = -k_1 V_1 \cos l - h_2 \sin l \\ B_{2,n} = -k_1 V_1 \cos l \end{array} \quad 6.67$$

This new system of equations can be solved by standard matrix methods (in this case by the application of Cramer's rule) to give a solution in terms of $A_{1,n}$:

$$\begin{array}{l} \frac{B_{1,n}}{A_{1,n}} = \frac{k_1 V_1}{h_1} \\ \frac{A_{2,n}}{A_{1,n}} = \frac{M(12)M(24)M(31) - M(12)M(21)M(34) - M(11)M(24)M(32) + M(11)M(22)M(34)}{\det M} \end{array} \quad 6.68$$

$$\frac{B_{2,n}}{A_{1,n}} = \frac{M(12)M(21)M(33) - M(12)M(23)M(31) - M(11)M(22)M(33) + M(11)M(23)M(32)}{\det M}$$

$$\det(M) = M(12)M(23)M(34) - M(12)M(24)M(33) \quad 6.71$$

Where $M(ij)$ refers to the i th row and j th column of equation 6.66

Which allows the equation for the general solution to be written as:

$$F_{j,n} = \frac{A_{j,n}}{A_{1,n}} \sin(V_j x) + \frac{B_{j,n}}{A_{1,n}} \cos(V_j x) \quad 6.72$$

With the values of $A_{1,n}$ used as constants external to the eigenfunctions.

The orthogonality relation, as already described (Eq. 6.27), can be extended and used to calculate the values of $A_{1,n}$ which are required to make the solution complete. The new orthogonality relation is given by:

$$\sum_{j=1}^k \int_a^j F_{j,m} F_{j,n} dx = \begin{cases} 0 & \text{for } m \neq n \\ N_n & \text{for } m = n \end{cases} \quad 6.73$$

Where N_n is again referred to as the norm.

The equation expressing the temperature distribution at time zero are given by:

$$T_j(x, 0) = T_j(x, \infty) + \sum A_{1,n} F_{j,n} \quad 6.74$$

If both sides of this equation are multiplied by the m th eigenfunction, the product integrated over the extent of the layer the sum taken over

both layers and the equation for the norm (Eq. 6.73) used then:

$$\sum_{j=1}^2 \frac{k_j}{a_j} \int T_j(x,0) F_{j,m} dx = A_{1,m} N_m + \sum_{j=1}^2 \frac{k_j}{a_j} \int T_j(x,\infty) F_{j,m} dx \quad 6.75$$

from which an expression for $A_{1,n}$ can readily be derived:

$$A_{1,n} = \sum_{j=1}^2 \frac{1}{N_n} \frac{k_j}{a_j} \int [T_j(x,0) - T_j(x,\infty)] F_{j,n} dx \quad 6.76$$

The value of the norm can be found by combining equations 6.72 and 6.73 and carrying out the integration which yields:

$$N_n = \sum_{j=1}^2 \left[\frac{k_j}{2a_j} \left\{ \left(\frac{B_{j,n}^2}{A_{1,n}^2} - 1 \right) \frac{1}{2V_j} \sin(2V_j(d_j+d_{j-1})) \right. \right. \\ \left. \left. + \frac{B_{j,n}}{A_{1,n}} \frac{1}{2V_j} (1 - \cos(2V_j(d_j+d_{j-1}))) + \left(1 + \frac{A_{j,n}^2}{B_{1,n}^2} (d_j+d_{j-1}) \right) \right\} \right] \quad 6.77$$

As in the single layer case it is probable that the initial temperature distribution will be a linear function of position within each layer and hence the difference between the initial and final distributions will also be a linear function of position. Such an assumption allows the integration of Equation 6.76 which gives a more complete expression for the coefficients $A_{1,n}$:

$$\begin{aligned}
 A_{1,n} = & \frac{1}{N_n} \sum_{j=1}^2 \frac{k_j}{a_j} \left[C_{d,j} \left(\frac{B_{j,n}}{A_{1,n}} \frac{1}{V_j} \sin(W_j) - \frac{1}{V_j} (\cos(W_j)-1) \right) \right. \\
 & + D_{d,j} \left(\frac{1}{V_j} \frac{1}{2} \sin(W_j) + \frac{B_{j,n}}{A_{1,n}} \frac{1}{V_j} \frac{1}{2} (\cos(W_j)-1) \right) \\
 & \left. - (d_j+d_{j-1}) \frac{1}{V_j} \cos(W_j) + (d_j+d_{j-1}) \frac{B_{j,n}}{A_{1,n}} \frac{1}{V_j} (\sin(W_j)) \right]
 \end{aligned}$$

where $C_{d,j} + D_{d,j}x = T_j(x,\infty) - T(x,0)$

$$W_j = V_j (d_j + d_{j-1})$$

$$d_0 = 0$$

Frequently in experimental studies the measured quantity will be the temperature at the base of the hot-plate. If a proportional temperature control system is used this temperature will be linearly related to the instantaneous heat flux being supplied to the plate. In terms of the equations developed in this chapter the temperature and the associated flux can be written as:

$$T_1(0,t) = C_1 + \sum B_{1,n} \exp(-S_n^2 t) \quad 6.79$$

$$q(t) = h_1 [T_s - T_1(0,t)] \quad 6.80$$

These equations will be applied to specific test conditions in the chapter that follows.

CHAPTER 7

MEASUREMENT OF TRANSIENT ENERGY EXCHANGE

7.1 ENERGY DEBT

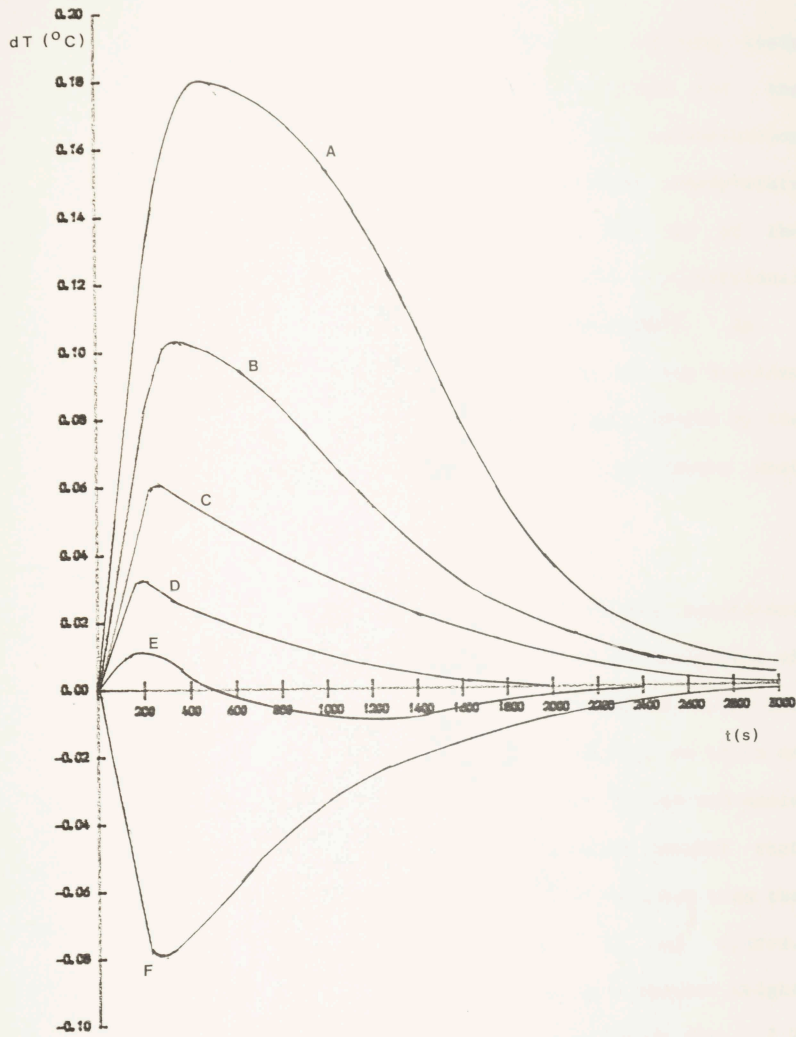
A large amount of information can be derived about fabric properties and in particular the role of water by considering the energy lost from or gained by the hot plate due to change from one fabric sample to another.

7.1.1 EXPERIMENTAL PROCEDURE AND RESULTS

In Chapter 2 it was noted that the hot plate control circuits could be monitored to give a plot of the temperature at the base of the plate. The proportional temperature control system meant that this temperature was always proportional to the heat supplied by the plate. If the initial and final temperatures of the plate were the same then the area under the curve caused when samples were changed could be related directly to the energy loss or gain associated with that change of samples.

The fabric samples were conditioned to a range of regains and the energy debt or gain for each sample was measured. The weight of each sample both before and after the test run was also measured.

A typical set of chart recordings are shown in Fig. 7.1 In this figure the temperature deviation is plotted against time for six samples pre-conditioned to different regains. The samples lost or gained



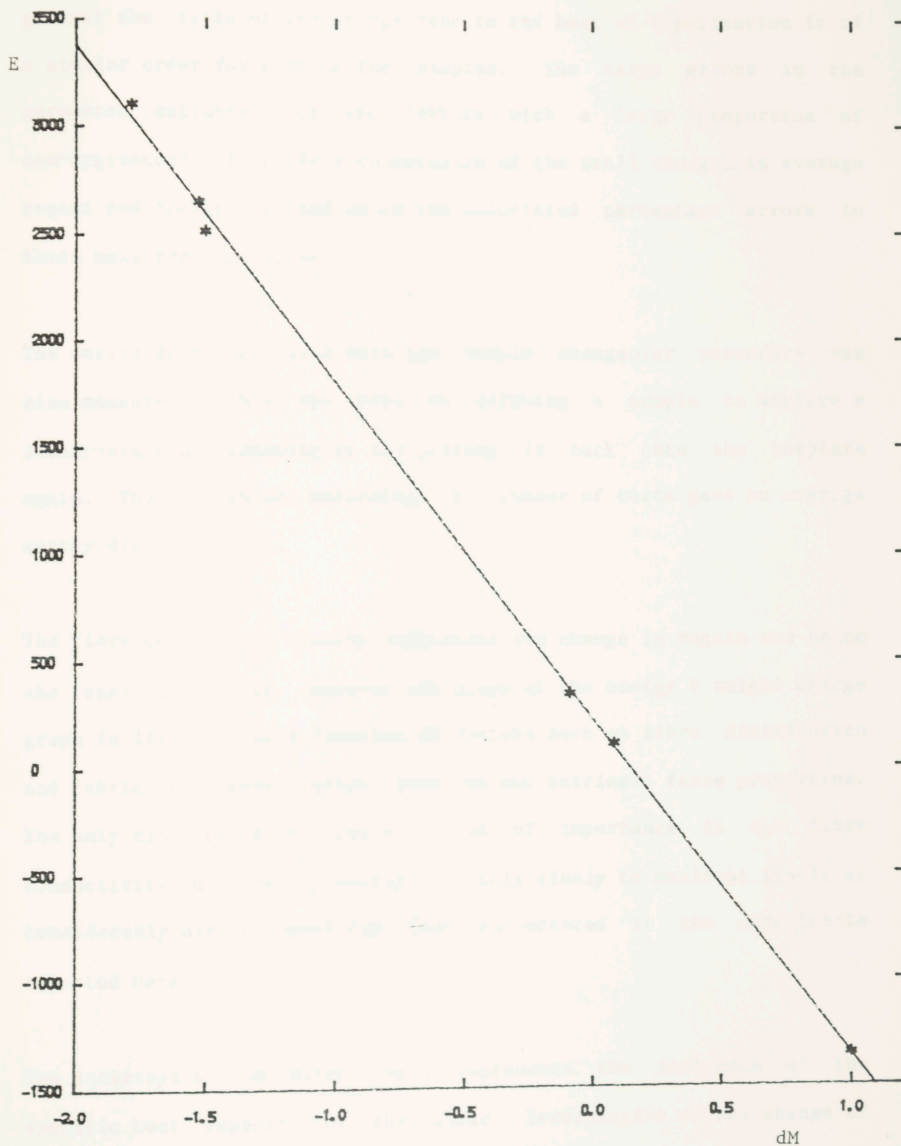
WEIGHT CHANGE (G)

A	- 2.0
B	- 1.0
C	- 0.5
D	0.0
E	+ 0.2
F	+ 1.0

RELATIONSHIP BETWEEN WEIGHT CHANGE AND TRANSIENT RESPONSE
 FIGURE 7.1

different masses of water to or from the atmosphere in reaching their final steady-state experimental regains. The baseline for the measurement of the temperature deviation and hence the instantaneous power deviation is taken as the plate temperature under steady-state heat flow as achieved as time approaches infinity. For all of the experimental results quoted in this chapter the proportional temperature control unit was set to 14W/degC (or 140W/degCm^2). As has already been mentioned the area between the curves and the baseline is therefore proportional to the energy loss or gain caused by the reconditioning of a fabric sample as compared to the steady-state heat loss through the same sample.

The example given in Fig. 7.1 demonstrated the very strong dependence of the energy debt incurred by a sample of fabric on the amount of water lost or gained by that fabric. The energy associated with the changing fabric regain can, as a first approximation, be taken as proportional to the change in the mass of water in the fibres and hence the change in the mass of the fabric. This approximation assumes that the latent heat of vaporization of water is far greater than the differential heat of absorption of liquid water by the fibres. According to this approximation a plot of energy debt against weight change should give a straight line. Such a plot is shown in Fig. 7.2 along with the slope and intercept and the standard deviation of those two quantities. As anticipated the plot does yield a straight line. The slope represents the energy per gramme of water vapour as seen by the heater supply circuitry. In this case the slope is 1.4 kJ/g which can be compared to the latent heat of vaporization of water which is 2.4 kJ/g . For this fabric, therefore, the energy debt associated with a change in regain was only about 60% of the total energy change of the fabric due to the latent heat of vaporization.



INTERCEPT = 223.8
 ERROR = 25.2
 SLOPE = -1576.8
 ERROR = 8.5

FIGURE 7.2

Relationship Between Energy Debt and Weight Loss for a Typical Sample

In Table 7.1 the results for all fabrics have been summarised. In general the ratio of the energy debt to the heat of vaporisation is of a similar order for most of the samples. The large errors in the parameter estimates for the fabrics with a large proportion of non-hygroscopic fibres is a consequence of the small changes in average regain and energy debt and hence the associated percentage errors in those measured quantities.

The energy debt associated with the sample changeover procedure was also measured. This was done by allowing a sample to achieve a steady-state and removing it and placing it back onto the hotplate again. The temperature recordings of a number of tests gave an average energy debt of 11 J.

The fibre composition clearly influences the change in regain and hence the total energy debt. However the slope of the energy V weight change graph is likely to be a function of factors such as fibre distribution and fabric thickness rather than on any intrinsic fibre properties. The only fibre property likely to be of importance is the fibre conductivity but that property is only likely to manifest itself at considerably higher densities than encountered in the experiments reported here.

The intercept on the energy axis represents the influence of the specific heat capacity of the fabric. Irrespective of the change of fabric regain there was always an increase in the average temperature of the fabric from room temperature to the temperature at steady-state plate conditions. The intercept represents the energy loss associated with this increase in temperature. The fibre specific heat capacity is likely to be of prime importance in determining the intercept. The

Sample	Intercept(J)	Slope(J/g)
6	175	1376
8	274	1557
9	271	1473
10	191	1500
12	148	1311
13	228	1443
15	390	1487
16	162	1325
17	146	1369
18	271	1451
19	69	1002
20	174	1195
21	167	1176
22	201	1255
23	82	1278
24	180	1186
25	193	1274
26	221	1386
27	235	1161
28	192	1246
29	124	1587
30	264	1476
31	323	1541
32	-57	1703
33	166	1423
34	107	1355
35	224	1577
36	240	1406
37	202	1459
38	168	1591
55	306	1292
61	125	1108
62	156	1219
66	109	887
68	154	926
39	169	895
71	236	1187
73	270	1072

Table 7.1

Coefficients of Linear Relationship Between Energy Debt
and Weight Loss

error in the estimate of the intercept are so large as to make any difference between fibre types difficult to evaluate.

7.2 ENERGY CONTENT CHANGES

The change in the energy content of a fabric sample can be found from the change in regain and temperature of that sample. The change in regain gives a change in energy content E_v due to the latent heat of vaporisation and E_w due to the heat of absorption of liquid water. The change in temperature gives a change in energy content E_h due to the heat capacity of the sample. These quantities can be calculated as follows:

$$E_v = M_o (r_f - r_i) H_v \quad 7.1$$

$$E_w = \int_0^d \int_{r_i}^{r_f} \frac{M_o}{d} Q_L dr dx \quad 7.2$$

$$E_h = (T_i - T_f) M_m C \quad 7.3$$

where M_o = the dry mass of the fabric

r = fabric regain

M_m = mean mass of the fabric

C = specific heat capacity

d = fabric thickness

Q_L = differential heat of absorption of liquid water

The equation for E_h assumes that the heat capacity of the fabric is independent of temperature over the range of temperatures likely to be encountered and that the effective mass of the fabric sample can be taken as the average of the initial and final regains. Both of these

approximations are not likely to cause significant error because of the relatively small percentage change in mass and the insensitivity of the heat capacity to temperature over a range of only about fifteen degrees Celsius.

In order to calculate the total energy debt or gain it is necessary to have expressions for the relationship between relative humidity and regain and the differential heat of absorption of liquid water and regain.

From the WIRA data book(42) the regain of wool and cotton fibres at different relative humidities can be estimated. The relationship between regain and R.H. can be seen to be nearly linear over the range 20 to 80% R.H. This particular relationship can thus be written as:

$$r = a + b H \quad 7.4$$

where the values for wool of a and b are 0.038 and 0.002 for desorption and 0.018 and 0.002 for absorption.

Also in the WIRA data book information concerning the differential heat of absorption of liquid water as a function of regain can be found. If the heat of absorption is plotted as a function of the natural log of regain a straight line results implying the relationship.

$$Q_L = A - B \ln (r) \quad 7.5$$

The values for A and B are -762 and 552 for wool.

The final piece of information that is required is the relationship between the saturation vapour pressure, P_{sat} of water and the temperature of the air. This relationship can be found in several sources and over the temperature range of interest here can be written as:

$$P_{\text{sat}} = 5.0479 \exp (0.061 T) \quad 7.6$$

which implies that the actual vapour pressure, for a relative humidity, H , will be given by:

$$P_v = H 5.0479 \exp (0.061 T) \quad 7.7$$

It is worth noting that under steady-state conditions the vapour pressure will be constant throughout the sample and equal to the ambient value.

The local relative humidity within the fabric can readily be obtained as the ratio of the actual vapour pressure to the local saturation vapour pressure.

$$H = H_a \exp [0.061 (T_a - T)] \quad 7.8$$

From the earlier chapter on dry heat transfer it is known that the temperature distribution through the fabric will be proportional to the distance perpendicular to the fabric surface here taken as being in the X direction. This implies that the temperature at the plane mid-way through the fabric will be at the average fabric temperature T_f .

The relative humidity at any point within the fabric can be found from the temperature at that point. If the total temperature drop across the fabric is known and the coordinate system shifted so that the plane halfway through the fabric represents $x=0$ then the local temperature will be given by:

$$T = T_f - \Delta T x/d \quad 7.9$$

The local relative humidity is therefore given by:

$$H = H_a \exp[0.061 (T_a - T_f)] \exp(0.061 \Delta T x/d) \quad 7.10$$

As the value of the temperature drop will not be greater than 4 degC for the samples under test then the right hand exponent will always be in the range between plus and minus 0.12. An approximation can therefore be made and the right hand exponential replaced to give:

$$H = H_a \exp[0.061 (T_a - T_f)] (1 + 0.061 \Delta T x/d) \quad 7.11$$

This approximation suggests that local relative humidity is a linear function of position within the fabric sample. It has already been shown that the local regain is similarly a linear function of relative humidity which establishes a linear relationship between regain and position. Such a linear relationship immediately gives the result that the average regain of the fabric is equal to the local regain for the plane midway through the fabric.

$$H = H_f (1 + 0.061 \Delta T x/d) \quad 7.12$$

$$r = a + b H_f (1 + 0.061 \Delta T x/d) \quad 7.13$$

It is now possible to evaluate the integral shown in Eq 7.2 as follows:

$$E_w = \int_0^d \int_{r_i}^r \frac{M_0}{d} [A - B \ln(r)] dr dx \quad 7.14$$

$$E_w = \int_0^d \frac{M_0}{d} [(A+B)(r-r_i) - Br(\ln(r_f)) + Br_i(\ln(r_i))] dx$$

$$- \int_0^d \frac{M_0}{d} B r \ln(r/r_f) dx \quad 7.15$$

Because r is linearly dependent on x the first integral can be replaced by the average value multiplied by the thickness to give:

$$E_w = M_0 [(A+B)(r_f-r_i) - B(r_f \ln(r_f) - r_i \ln(r_i))]$$

$$- \int_0^d \frac{M_0}{d} B r \ln(r/r_f) dx \quad 7.16$$

From the observations already made it can be assumed that the ratio of regains in the second integral can be taken as close to unity implying that the integral can be ignored.

The initial and final average regains can be written in terms of measured weights before and after testing to give:

$$r_f = M_f/M_0 - 1 \quad 7.17$$

$$r_i = M_i/M_0 - 1 \quad 7.18$$

The equations for the energy debt can now be written in a form that will allow easy calculation.

$$E_v = (M_f - M_i) H_v \quad 7.19$$

$$E_w = M_o [(A + B) (M_f - M_i) / M_o - B (\ln (M_f / M_o - 1) - \ln (M_i / M_o - 1))]$$

$$E_h = C (T_f - T_i) (M_f + M_i) / 2 \quad 7.21$$

$$E = E_v + E_w + E_h$$

A fairly typical experiment on a fabric sample of 25g would lead to a change of weight from 28.8 to 27.6g and a change in temperature from 20 to 31degC. These values when substituted into the equation for energy debt give:

$$E_v = - 2880 \text{ J}$$

$$E_w = - 450 \text{ J}$$

$$E_h = + 420 \text{ J}$$

$$E = - 2910 \text{ J}$$

Where large changes in moisture content are taking place it is clear that the term concerned with the condensation or evaporation of the water E_v will dominate the total value. For fabrics pre-conditioned to a state where a small amount of water only is absorbed or desorbed then the percentage contribution of the term relative to the temperature change E_h will increase even though its absolute value remains approximately constant.

It is the dominance of the latent heat of vaporisation term and the constancy of the heat capacity term that accounts for the linearity of the earlier plots of weight loss against energy debt.

A comparison can now be made between the energy change in the fabric and the energy debt or gain as measured by the hot-plate circuitry. By plotting the fabric energy change against the electrical energy debt it was found that the points for each sample fell on a straight line. The slope of the line indicating the efficiency of the insulating system in transmitting the energy change to the hot-plate surface.

A summary of the results is shown in Table 7.2 and a typical plot is shown in Fig. 7.3. For this sample the slope of 0.6 indicates that the energy change for the hot-plate is 60% of the total energy change.

The relationship between the slope and the physical properties of the fabric is difficult to evaluate from a theoretical approach without a complete solution to the coupled diffusion problem.

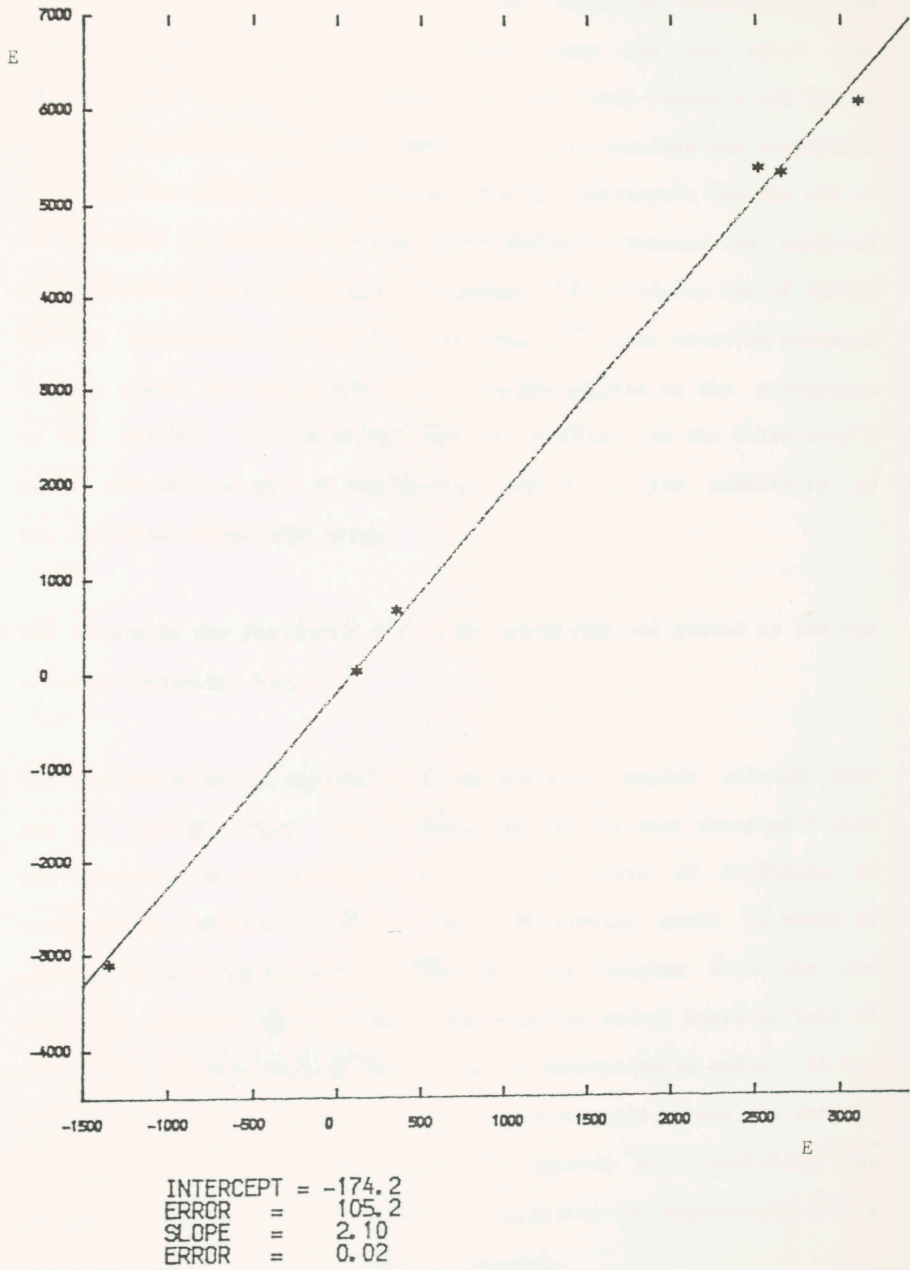
7.3 TRANSIENT CALCULATIONS

In the previous chapter a theoretical approach to the problem of transient conductions was described. The first of the two systems considered related to the removal of a layer of insulation from a hot-plate and the subsequent response of the hot-plate. A comparison of experimental results to the derived series solution should enable the relevant physical properties of the plate to be estimated. The second of the two arrangements considered was equivalent to a uniformly conditional sample of fabric replacing a fabric of the same thermal resistance on the hot-plate. In this case a comparison of theoretical and experimental results should give information about the physical properties of the fabric and its surfaces.

Sample	Intercept(J)	Slope
6	-183	2.4
8	-169	2.0
9	-138	2.1
13	- 52	2.1
14	38	2.1
15	-394	2.1
16	491	2.2
17	-131	2.3
19	37	3.2
20	- 28	2.6
21	-165	2.7
22	223	2.6
23	320	2.4
24	-154	2.6
25	- 98	2.5
26	- 93	2.2
27	-226	2.6
28	-262	2.6
29	46	2.0
30	-300	2.2
31	-427	2.1
32	408	1.8
33	20	2.2
34	291	2.2
35	-174	2.1
37	-135	2.2
38	-155	2.0
41	-816	2.1
47	-119	2.8
50	-166	2.3
66	- 61	3.7

Table 7.2

Coefficients of Linear Relationship Between Calculated
and Measured Values of Energy Debt



Relationship Between Calculated and Measured Values of Energy Debt

FIGURE 7.3

A direct inversion of the experimental results into sample or plate properties is not possible due to the number of variables and the complexity of the relationships between them and the final time dependence of the plate temperature. For this reason a sum square deviation minimisation approach was used. This involved the estimation of values and ranges for the unknown physical parameters and the use of an algorithm to minimise the sum square deviation between the measured and calculated plate temperature response. The resulting set of values for the parameters represented the best fit that could be achieved between theory and experiment for the ranges imposed on the properties of the system. The algorithm used was available on the University's Amdahl computer as part of the package supplied to the university by the Numerical Algorithms Group.

The errors in the parameters were then calculated and quoted to the one standard deviation level.

The derivation of the equations in the previous chapter allowed only for the specific heat of the fibres and not for heat associated with the adsorption or desorption of water. If the rate of diffusion of water vapour through a fabric was sufficiently great it would be possible to use the equations of the previous chapter with the new effective specific heat accounting for both the actual specific heat of the fibres and this heat of absorption and desorption of water. It has long been recognised however that for most applications the rate of diffusion is so low that it cannot be ignored in calculating the transient response of an assembly consisting of hygroscopic fibres where the regain of those fibres is changing.

The problems caused by the coupling of heat and vapour flow and the

dependence on the rate of diffusion of water vapour make it difficult to apply the relationships developed in the previous chapter.

Before the equations describing the flow of heat through a fabric from a hotplate can be assessed it is necessary to calibrate the plate properties. This was achieved by allowing the plate to come to a steady-state condition with a heavy insulator. The layer of insulation was then removed and the time dependent temperature was measured as the plate came to a new steady-state condition with no fabric covering.

Such a situation can be analysed using the formulae derived for transient heat flow in a single layer with convective boundaries. A least mean squares regression procedure was used to minimise the difference between calculated and measured temperatures by selecting the best set of plate parameters. The quantities calculated from the data were the conductivity and diffusivity, all other relevant properties being measured directly or derived from them. The resultant values with error estimates were 17.4 (0.6) W/mdegK for the conductivity and 5.0×10^{-6} (0.7) m^2/s for the diffusivity.

Using these values for the plate properties it was possible to calculate the energy debt associated with the changing temperature of a layer of fabric placed on the hotplate. The energy debt is calculated by integrating the time dependent part of Equation 6.80.

A set of sample properties and associated energy debts and total fabric energy changes are shown in Table 7.3. The values are based on a fabric conditioned to 20 degC and the hotplate set to 33 degC.

The values shown in the first row of Table 7.3 are based on a typical

	k	d	M	h2	h3	C
Case 1	0.045	0.002	200	160	10	1.3
Case 2	0.060	0.002	200	160	10	1.3
Case 3	0.045	0.003	200	160	10	1.3
Case 4	0.045	0.002	200	160	20	1.3
Case 5	0.045	0.002	200	160	10	2.0
Case 6	0.045	0.002	200	80	10	1.3

	E at plate	E total	ratio
Case 1	-1820	-2491	0.73
Case 2	-1898	-2549	0.74
Case 3	-1708	-2397	0.71
Case 4	-1332	-2107	0.63
Case 5	-2800	-3833	0.73
Case 6	-1209	-2032	0.59

Table 7.3

Sample Calculations of Energy Debt For Different
Fabric Properties and Test Conditions

set of results as found in Chapter 4 for most of the light to medium weight wool fabrics(samples 1 to 45). It can be seen that large changes are required in the fabric properties to cause a substantial change in the ratio of the hotplate energy debt to fabric energy change.

These results are based on the case of zero vapour transfer. However the close agreement with the measured values of the energy ratio suggest that the rate of vapour diffusion does not greatly affect the proportion of energy released or absorbed by the fabric transmitted to or from the notplate (or the body in the case of clothing in use).

CONCLUSION

The experimental work described here was divided into four main sections. The first section involved the measurement of fabric thickness under various loads. The construction of the instrument and the results are given in Chapter 3. The second section concerned the measurement of the dry heat transfer properties of the fabric samples. This work involved the development of a guarded hotplate as described in Chapter 2. Results were also obtained from the Togmeter and all of the results for dry heat transfer are described in Chapter 4. Using the same guarded hotplate the results for the third experimental section were found and are given in Chapter 5. In this chapter the combined flow of heat and vapour through knitted fabrics was considered. The final section concerned the transient response of knitted fabrics to changing conditions. Here the emphasis was placed on the importance of the absorption and desorption of water vapour. The results of this section are given in Chapter 7.

The instrument constructed for the measurement of fabric thickness was simple in both design and use. It consisted of a flat plate suspended through a coupling from a section of optical bench. The height of the plate could be measured to an accuracy of 0.02mm. The plate was held above an electronic balance fitted with a flat weighing table. The fabric was placed on the table and the load and thickness measurements readily made.

Using this instrument two sets of measurements were made. The first set compared the relationship between thickness and pressure for rapid and steady-state measurements. The second set considered only the rapid testing but was carried out over a much larger range of applied pressure. For all tests it was found that the fabric thickness was proportional to the logarithm of the pressure. For the test carried

out over a wide pressure range a discontinuity was found in the logarithmic relationship. Above a certain pressure the rate of change of thickness with the logarithm of pressure decreased quite markedly. The pressure at which the slope changed differed between samples and it was assumed that its value related to the surface characteristics of each sample.

The construction and use of an instrument to measure the simultaneous flow of heat and vapour through fabrics was central to the work carried out here. The instrument was designed to allow the separate assessment of the contribution from heat and vapour flow. In addition it could be used to measure dry heat transfer and the transient response of fabrics to changing conditions. Great care was taken to ensure the accuracy of measurement of the energy input to the hotplate and the maintenance of very stable test conditions for the steady-state work. The sensitivity of the control circuitry and the splitting of the power supply allowed for very precise measurements of the energy losses during a period of transient response which would not have been possible with more conventional heater supply systems.

For the measurement of dry heat transfer under steady-state conditions both the Togmeter and the guarded hotplate were used. Measurements on the Togmeter were made at a series of different plate separations for each sample. It was found that the relationship between thermal resistance and plate separation showed two distinct regions. The values at higher plate separations could be explained if it was assumed that the plate separations were larger than the uncompressed thickness of the fabric. From the known radiative and conductive losses between two nearly black surfaces the effective fabric thickness and thermal resistance could be found. These values of effective fabric thickness

were then compared to the thickness values associated with the transition between high and low pressure pressure as measured directly on the thickness apparatus. It was found that there was a very close agreement between the two sets of thickness values, with the togmeter results giving the slightly higher estimate. This difference was explained in terms of the the air gap between the fabric and the hotplate in the absence of an applied load.

The values of thermal resistance for fabrics under compression was also considered. For the wool fabrics tested it was found that, as a first approximation, the thermal resistivity was 2.15 Togs/cm. The relationship between volume fraction and thermal conductivity for the compressed fabrics was also considered. The decrease in thermal conductivity with increasing volume fraction suggested that the radiation term was the more important than the conduction term in determining the derivative of the effective thermal conductivity with respect to volume fraction. For the range of volume fraction considered here the fibre conductivity would play an almost negligible role. It is the contribution from radiation which explains the large difference between the thermal resistivity of 2.15 Tog/cm for a fabric and 4 Tog/cm for an equivalent layer of still air with no radiant exchange.

Thermal resistance measurements under steady-state conditions were also made on the guarded hotplate. The thermal resistance between the fabric surface and the environment was found to be considerably greater than the thermal resistance of the fabric itself. For this reason it was difficult to assess the difference between samples as measured using this technique. The relationship between the fabric thermal resistance as measured on the hotplate and that measured on the

togmeter was considered. It was found that an approximately linear relationship existed although the scatter of points was large. This relationship suggested a surface resistance of approximately one Tog and also that the thermal resistance of a fabric was lower on the hotplate than in the Togmeter. The establishment of air currents associated with natural convection and the penetration of those air currents into the fabric was suggested as a possible explanation.

The simultaneous flow of heat and vapour under steady-state conditions was investigated using the guarded hotplate. Different air gaps between the liquid and the fabric were used under conditions of natural convection at the top fabric surface. Under the conditions used it was found that the energy losses due to heat and vapour flow were approximately equal. Due to resistances at the upper fabric surface and between the liquid and the lower fabric surface it was found that the differences in heat and vapour flow for different samples was difficult to assess with certainty. For this reason a further series of measurements was carried out with a minimal resistance between the liquid and the fabric and with forced convection at the top surface. This arrangement led to far greater total energy flow, from about 180 W/sq.metre to around 500 W/sq.metre. Most of the increase in energy loss was due to increased vapour flow.

The response of a fabric to changing conditions was studied both theoretically and experimentally. The equations relating to the propagation of a temperature change for a hotplate and fabric system were derived. These equations were limited to cases where water vapour transfer was not occurring due to the dependence of the response on the rate of diffusion of vapour. The complete solution involving the coupled diffusion of heat and vapour was beyond the scope of this work.

The changing water content of the hygroscopic fabrics was found to be the major factor determining the energy debt incurred by the fabric as measured by the hotplate. The relationship between the energy debt and fabric weight change was found to be an approximately one with, typically, a slope of around 1400 J/g and an intercept of around 200 J.

From the known values of the heat of absorption of water vapour and the specific heat of the fibres it was possible to calculate the expected values of the total energy released or absorbed by the fabric during its change of condition. When this calculated total energy was compared to the measured energy debt it was found that, in general, just under half the energy involved in the transition was supplied by or to the plate.

The samples used for this work covered only a narrow range of the fabrics commonly used for clothing. Such a narrow range was used with the aim of studying particular aspects of the mechanisms of energy exchange. General features of the insulating properties of clothing have long been known. The increasing thermal resistance with fabric thickness is well documented although the mechanisms of heat transfer and the importance of different fibre and fabric properties are not clearly understood. In this work it was found that the most important fabric property, after thickness, was the fibre volume fraction. The importance of this property was related to the transfer of energy by radiation. The importance of radiation suggests that a fabric produced from finer fibres should have a higher thermal resistance than one produced from coarser fibres, all other things being equal. This could prove to be an important parameter in determining the thermal insulation of fabrics and thus a valuable area for future research.

Similarly, the local variations of fibre volume fraction should prove important in determining fabric performance. However, when the results for different fabric constructions were compared it was found that no definite patterns emerged. Further research in this area with samples specifically selected for structure and hence fibre distribution could prove worthwhile.

The results of this work suggest a need for caution in using experimental techniques and instruments such as the Togmeter. This instrument, which is accepted as a standard for the measurement of thermal resistance, proved very useful for the this research. However, if used strictly according to the standard method could produce misleading results. In particular the measurement of thermal resistance at only a single level of applied load may not truly reflect the fabric properties of relevance to end-use. This is due to the presence of air layers at the two fabric surfaces, the thicknesses of which are determined by the load supporting capacity of the surface fibres. Depending on the fabric application the protruding fibre layers may or may not contribute to the insulation. On the basis of the work carried out here, either a range of different pressures should be used on the togmeter or the thicknes as a function of pressure measured on a separate instrument and a suitable pressure or plate separation selected for the more time consuming measurements on the togmeter.

From the point of view of fabrics for clothing the results of the transient study were of considerable interest. The amounts of energy associated with changing moisture content of the hygroscopic fabrics were very considerable. For the wool fabrics preconditioned to 20 degC and 65% R.H. the energy needed to bring fabric to plate conditions was

about 30 KJ/sq.metre with most of this debt being incurred in the first thirty minutes. This suggests an average additional power loss of about 15 W/sq.metre with a peak of about 30 W/sq.metre. Considering that a person at rest loses about 45 W/sq.metre or when undertaking light exercise about 100 W/sq.metre then these transient losses or gains are clearly important.

Relating the hotplate data directly to the physiological influence of clothing is difficult. The actual mechanisms of bodily temperature control and the physical properties of the skin and tissue beneath would become important. In addition the distribution of clothing on the body and the separation of the skin and clothing would be important. However, the energies involved are sufficiently large that they should be considered in the choice of fibre type for different garments.

Clearly the advantages or otherwise of hygroscopic fibres will depend on the circumstances of the fabric's use. In moving from a hot, dry environment to a cold, damp environment the wearer would benefit from the release of energy. The opposite would be the case if the wearer moved from a hot, damp situation to a cold, dry one. In the case of the British climate with centrally heated offices and homes the first case is likely to be by far the more common one.

The duration of the transient behaviour being of the order of half an hour for hygroscopic fibres suggests that for most applications clothing is not likely to ever achieve a steady-state condition while being worn. This implies that the measurement of transient properties is likely to be of considerable importance for an understanding of clothing physiology.

The large numbers of variables and the complex psychological and physiological factors make the testing of of the comfort aspects of clothing extremely difficult. In this work the approach has been to choose a narrow range of fabrics and assess their properties with respect to very simple, well controlled experiments. The most important results relate to the close correlation between thickness measurements and dry heat flow and the amounts of energy transferred to or from the 'skin' associated with the changing condition of the fabric. With this information the techniques for the assessment of dry heat transfer could be reconsidered. Similarly, Physiological testing should take into account the nature of the fibrous content of clothing if work loads and such are to be properly assessed.

APPENDIX 1

SAMPLE	FIBRE	WEIGHT (g/sq.m)	STRUCTURE
1	W	289	2:2 RIB
2	W	255	2:2 RIB
3	W	234	2:2 RIB
4	W	317	2:2 RIB(TUCK)
5	W	274	" "
6	W	254	" "
7	W	264	" "
8	W	283	" "
9	W	322	" "
10	W	267	" "
11	W	258	" "
12	W	300	" "
13	W	253	1:1 RIB
14	W	236	1:1 RIB
15	W	320	INTERLOCK
16	W	328	" "
17	W	275	" "
18	C	236	" "
19	W	316	3xTUCK
20	W	308	" "
21	W	250	" "
22	W	240	TUCK FANCY
23	W	282	" "
24	W	276	" "
25	W	260	" "
26	W	256	" "
27	W	253	" "
28	W	232	RIB FANCY
29	W	289	" "
30	W	292	TUCK FANCY
31	W	304	THERMAL
32	W	278	MILANO RIB
33	W	295	PIQUE
34	W	320	" "
35	W	322	INTERLOCK
36	W/C 50:50	289	" "
37	W	336	" "
38	W	230	JERSEY EYELET
39	W	267	RIB EYELET
40	W	182	" "
41	W	181	2:2 RIB
42	W	224	JERSEY
43	W	252	" "
44	W	234	" "
45	W	146	LACE WARPKNIT
46	W	337	INTERLOCK
47	W	385	" "
48	W	265	" "
49	AC	295	" "

50	W	273	THERMAL
51	PVC	180	RIB FANCY
52	PVC	308	INTERLOCK
53	PP	293	INTERLOCK
54	PVC	180	RIB FANCY
55	C	373	INTERLOCK
56	C	273	" "
57	W	238	INTERLOCK BRUSHED
58	AC	480	INTERLOCK
59	V	338	1:1 RIB
60	AC	391	INTERLOCK
61	AC	153	1:1 RIB
62	V	323	INTERLOCK
63	PP	149	FANCY
64	W	182	RIB FANCY
65	W	225	" "
66	W	438	THERMAL
67	PP	402	"
68	W/PP 50/50	415	"
69	W/PP 50/50	439	"
70	W/PP 10/90	446	"
71	W/PP 10/90	434	"
72	PP	391	"
73	W/PP 25/75	467	"
74	W/PP 25/75	389	"
75	C	154	WOVEN
76	SILK	93	"
77	PE	210	"
78	C	191	"
79	PP	250	BRUSHED
80	W	314	1:1 RIB
81	C	304	" "
82	PP	120	" "

W	WOOL	C	COTTON
AC	ACRYLIC	PVC	POLYVINYL CHLORIDE
V	VISCOSE	PP	POLYPROPYLENE
PE	POLYESTER		

APPENDIX 2

SEMI-CONDUCTORS

IC1	Waveform Generator
IC2,15	LM 308 OP.AMP
IC3,16	LM 311 Comparator
IC4,5,7,8,11,17,19	Programmable Timer
IC6,9	74LS32 Inverter
IC10	74LS00 NAND Gate
IC12,13,14	Decade Counter
IC18	74LS04 OR Gate
Q1,2,4	BC108
Q3,5	MJ3001
D1,2,3,4,5	1N4001
D6,7	1N4002
LED1,2,3	Red Miniature
TH1,2,3	Glass Bead GL23
REG1	Prog. Regulator
BRI	7A Bridge Rectifier

CAPACITORS (MICROFARADS)

C1	0.2
C2	0.4
C3,29	1
C4	2
C5	4
C6	8
C7	16
C8	32
C9	64
C10,27	0.1
C11	0.15
C12,14,16,18	
20,22,23,25	0.001
C13,15,17,19	
21,24	0.047
C26	10000
C28	10

RESISTORS (OHMS)

R1,2	150 K
R3	18 K
R4	82 K
R5,6,7	2 K
R8	5 K
R9	1.2 M
R10	11 K
R11	50 K
R12	1 K
R13	1.6 M
R14	1.1 M
R15	760 K
R16	520 K
R17	360 K
R18	240 K
R19	160 K
R20	100 K
R21,22	40 K
R23,24	150 K
R25,26	150
R27	100 K
R28	175 K
R29	90 K
R30	75 K
R31	5 K
R32,33	25 K
R34,35	2 K
R36,37	200
R38	5 K
R39	11 K
R40	1.2 M
R41	50 K
R42	30 K
R43	450 K
R44	150
R45	240
VR1	100 K
VR2,3,4	1 K
VR5	1 M
VR6	10 K

References

- 1 O'Callaghan, P.W., Probert, S.D., *Applied Energy* 2, (1976), 269.
- 2 Ghosh, R.C., *Textile Trends*, 15, (1972), 51
or *Silk and Rayon Ind. India*, 15, (1972), 114.
- 3 Kerslake, D.Mc.K., *The Stress of Hot Environments*, 95.
- 4 Spencer-Smith, J.L., *Clothing Res. J.*, 5, (1977), 3.
- 5 Black, C.P., Matthew, T.A., *J.T.I.*, 25, (1934), T202.
- 6 Scheifer, S.M., *J. Res. Bur. Stand.*, 32, (1964), 261.
- 7 Rees, W.H., *J.T.I.*, 32, (1941), T149.
- 8 Naka, S., Kamata, Y., *T. Mech. Soc. Jap.*, 24, (1978), 33.
- 9 Spencer-Smith, J.L., *Clothing Res. J.*, 6, (1977), 82.
- 10 Whelan, M.E. et al., *Tex. Res. J.*, 25, (1955), 197.
- 11 Weiner, L.I., *Tex. Chem. Col.*, 2, (1970), 378.
- 12 Fourt, L., Harris, M., *Tex. Res. J.*, 17, (1947), 256.
- 13 Pierce, F.T. et al., *J.T.I.*, 30, (1945), T169.
- 14 Spencer-Smith, J.L., *Clothing Res. J.*, 5, (1977), 116.
- 15 Rees, W.H., 3rd Shirley Int. Seminar, (1971).
- 16 Rees, W.H. in Hearle and Peters *Moisture in Textiles*, Chap. 4.
- 17 Cassie, J.T.I., 31, (1940), T17.
- 18 David, H., *Tex. Res. J.*, 35, (1965), 820.
- 19 Spencer-Smith, J.L., *Tex. Res. J.*, 36, (1966), 855.
- ✓ 20 Vokac, Z., *Tex. Res. J.*, 43, (1973), 474.
- ✓ 21 Spencer-Smith, J.L., 3rd Shirley Int. Seminar, (1971).
- ✓ 22 Woodcock, A.H., *Tex. Res. J.*, 32, (1962), 628.
- 23 Mecheels, J., *Melliand Textilber.*, (1977), 58, 773.
Melliand Textilber., (1977), 58, 857.
Melliand Textilber., (1977), 58, 942.
- 24 Mecheels, J., Umbach, K.H., *Melliand Textilber.*, (1976), 57, 1029
Melliand Textilber., (1977), 58, 73.
- 25 Gilling, 3rd Shirley Int. Seminar, (1971).

- 26 Givani, B., Goldman, R.F., J. Appl. Physiology, 30, (1971), 429.
J. Appl. Physiology, 32, (1972), 812.
J. Appl. Physiology, 34, (1973), 201.
J. Appl. Physiology, 35, (1973), 875.
- 27 Larsen, R.E., U.S. Army Natick Labs. Tech. Rep., 69-31-CM
(AD 691144)
- 28 Peirce, F.T. et al., J.T.I., 36, (1945), T169.
- 29 Hoffman, R.M., Beste, L.F., Tex. Res. J., 21, (1951), 66.
- 30 Van Wyk, C.M., J. Tex. Inst., 37, (1946), T285.
- 31 Bogarty, H., et al., Tex. Res. J., 23, (1953), 730.
- 32 Larose, P., Tex. Res. J., 23, (1953), 730.
- 33 Fourt, L., Hollies, N.R.S., Clothing Comfort and Function, (1970)
- 34 Schumeister, H., Ber. K. Akad. Wein (Math-Natur. Klasse), 76,
(1877), 283.
- 35 Lees, C.H., Phil. Mag., 49, (1900), 221.
- 36 Baxter, S., Proc.Phys. Soc., 48, (1946), 48, 105.
- 37 Drummond, N.Z., J. Science, 4, (1971), 621.
- 38 Strong, H.M. et al., J. Appl. Phys., 38, (1960), 39.
- 39 Verschoor, J.D., Greebler, P., Trans. Am. Soc. Mech. Eng., 74,
(1952), 961.
- 40 Fishenden, M., Saunders, D.A., Heat Transfer, (1950).
- 41 Mak, S., Ph. D. Thesis, Leeds Univ., (1981).
- 42 W.I.R.A. Fibre Data Book
- 43 Spencer-Smith, J.L., Cl. Res. J., 5, (1977), 82.







